FIFTH GENERATION MOBILE COMMUNICATIONS

The effect of the built and natural environment on millimetric radio waves

For Department of Digital, Culture, Media and Sport
February 2018
Final Report

Responsibility for this document

Bart Chudas is responsible for the contents of this document.

Change History

Version	Date	Summary of change
1.0	February 2018	First Issue

Approval for issue

John Kimmance, Director Public Sector.

Trademarks

Document Structure

This document is one of three deliverables specified by DCMS under its contract of services: **Fifth generation mobile communications (5G) – Research for a network mapping / planning tool.**

This document includes details of research to understand the impact of geospatial features and weather on 5G mmWaves. Its conclusions have been used to inform a planning guide for a 5G planning suite; a separate contract deliverable.

This document:

- provides details of the research undertaken by Ordnance Survey, 5GIC and the Met Office
- defines a network planning tool based on the research
- draws conclusions relating to the impact of geospatial and weather factors in rolling out 5G in high-value geographies across the UK.

For the avoidance of doubt, the liability of OS, 5GIC and the Met Office to DCMS for any loss arising out of or in connection with this report is subject to all exclusions and limitations of liability set out in the Contract for Services pursuant to which this report was commissioned.

Contents

1

1 Executive Summary

This report sets out to address the following requirements:

1. Confirmation of which geospatial data are important to deciding on the best siting of infrastructure for 5G deployment at frequencies exceeding 6GHz. A detailed explanation of the work and results that led to these conclusions.
2. Setting out the learning gained from the project, including the scale of the challenge for 5G network deployment and evidence of the benefits the tool could deliver for operational 5G deployment.

This report informs a *Planning Guide for a 5G Planning Suite*, also developed under this project.

In the global 5G race, the government has a stated ambition for the UK to be a world leader[1]. The research undertaken in this project confirms that deployment of 5G mmWave solutions will need to take account of variables that do not apply to today's lower frequencies. The considerable densification of antennae necessary, especially in urban environments, and the significant impact on the performance of the network from obstructing physical objects and weather, are two very important differences. With so much engaging work being undertaken across all areas of 5G research, it is not surprising that the practical issues, supporting frameworks and standards relating to implementation of a 5G network have been overlooked to date.

This report highlights the significance of appropriate spatial planning to make 5G an affordable proposition for the UK, including high-resolution geospatial data integrated with a range of other information types (particularly meteorological data) served via a functionally-rich planning tool.

Today's essentially manual and fragmented methods of planning on-site deployment of networks are too costly to be scaled up to the considerable densification of antennae required to deploy 5G throughout urban areas of the UK, and run the additional risk of not being sufficiently accurate to account for the higher frequencies used by 5G technology. The requirement is therefore to model (from the desktop as far as possible to minimise on-site investigation) the impact of change in the physical environment on the performance of the network both in the initial network deployment and its subsequent management.

This research demonstrates the impact on performance of 5G networks from physical features not currently considered in network planning, including street furniture and vegetation, and the important role that weather conditions play. Having these data available and made easily accessible and usable through a planning tool has been shown as critical to a cost-effective 5G rollout. The solution recommended in this report (a combination of data and software) is an essential prerequisite to opening higher frequencies for 5G use – not just in the UK, but globally – meaning that the expertise developed here is exportable.

---

[1] Next Generation Mobile Technologies: A 5G strategy for the UK (https://www.gov.uk/government/publications/next-generation-mobile-technologies-a-5g-strategy-for-the-uk)

The geospatial data requirements described in this report are consistent with the evolving government agenda around Smart Cities and Building Information Modelling (Digital Built Britain[2]), Connected Autonomous Vehicles (for example illustrated within the Atlas project[3]) and a number of the aspirations laid out in the Industrial Strategy green paper[4]. Ordnance Survey is actively working across government to advise on the geospatial infrastructure required to support the delivery of government policy.

Specifying, acquiring, integrating and managing these types of data is complex, evidenced by the fact that we have incorporated over 30 datasets to create a single 3D view of Bournemouth, a typical high-value UK urban area. To scale this task to the whole urban geography of the UK will require a single authoritative, consistent set of data specifications and standards supported by integrated, maintained and secure datasets. An important benefit of this approach is that it will support a range of additional government policies and drivers and maximise return on investment for UK plc, built on a principle of 'capture once, use many times'.

The remainder of this report presents the detailed project work undertaken by a consortium of 5GIC (University of Surrey), the Met Office and Ordnance Survey.

[2] http://digital-built-britain.com/

[3] https://www.ordnancesurvey.co.uk/about/news/2016/uk-given-green-light-driverless-cars.html

[4] https://beisgovuk.citizenspace.com/strategy/industrial-strategy/supporting_documents/buildingourindustrialstrategygreenpaper.pdf

2

2 Project overview

The Department of Culture Media and Sport (DCMS) commissioned Ordnance Survey (OS), the University of Surrey's 5G Innovation Centre (5GIC) and the Met Office to undertake research into the enabling geospatial data and their associated granularity (level of detail) as well as weather data for use in cellular planning of 5G communication networks in spectrum bands above 6GHz.

Current communication networks operating below 6GHz are conventionally planned using simple block designs to represent buildings and large areas of vegetation over large cell areas. At mmWave frequencies, unlike lower frequencies, obstructions can have a significant impact on propagation. For these higher frequencies, base stations may typically be deployed close to ground level as they have a range of only a few hundred metres. These findings represent a key challenge for 5G deployment.

Because of this, 5G planners must have far more detailed data to plan their networks. Furthermore, weather considerations, and particularly rainfall, have significantly more impact on signal propagation above 6GHz. Understanding probable rates, timings and durations of rainfall is important to ensure reliable 5G coverage and capacity.

We undertook this research project using the town of Bournemouth as our case study, and working in close partnership with Bournemouth Borough Council (Bournemouth BC). The results of this study provide insight into the minimum size of physical objects and the weather conditions that impact coverage which we have demonstrated in a prototype 5G planning tool.

This report also aims to identify the scale of the 5G challenge and consider the benefits a 5G planning tool could offer. The work carried out included:

- Research into the availability and suitability of geospatial datasets from new capture and existing sources including Bournemouth BC;
- Generation of a 3D Digital Model of Bournemouth representing the built and natural environment;
- Research into radio propagation phenomena, the use of existing measurement data, and further practical measurements to inform how geospatial objects impact cellular coverage dependent on their size and specification;
- Simulation to analyse the behaviour of propagation in heavy rainfall conditions which cause limitations on the cellular range over which propagation can take place. Other effects such as gaseous absorption of radio and temperature effects on the system have been taken into consideration;
- Formulation of a signal propagation model based on measurement data that can be utilised in the planning tool to determine power received by a mobile device that is transmitted from a base station, enabling the impact of geospatial objects and weather to be included in or removed from the analysis;

- Development of a software-based mmWave demonstrator tool combining the Digital Model, weather data and the propagation model to demonstrate the impact of physical objects and weather on 5G signals. The tool shows the coverage range not only in terms of the signal power received from a particular base station, but also the interfering power that is received from neighbouring base stations which should be relatively lower;
- Simulations of the communication link, including signalling methods, intelligent antenna techniques and the coordinated scheduling of transmissions to mobile devices within a cell. The information obtained from these simulations enables the ability to determine what data rate in Gbits/s is delivered to the mobile from a base station and hence determine whether the planned cellular deployment will meet the communication requirements. To do this, the data must 'know' both the received power from the desired base station and the total interfering power from neighbouring base stations. This can subsequently enable the demonstrator tool to show locations where communication is insufficient due to the impact of geospatial objects;
- Compilation of this report, setting out key findings in respect of the geospatial and weather data required to enable 5G planning;
- Compilation of a planning guide for a 5G planning suite for national operational use.

This work has clearly identified that the natural and built environment has a significant impact on high-frequency signals above 6GHz which is as expected. However, this work has shown that the sensitivity of this impact is remarkable and has major implications for network operators, local authorities, infrastructure asset owners and policy makers. The supporting evidence is further outlined in the remainder of this document.

The scale of this sensitivity is illustrated in the heat map in Figure 2-1 below which shows two base stations indicated with white poles: one in the foreground and the other in the background. The heat map shows the capacity available at each pixel which is high when close to the base station but decreases with distance. Importantly, the street signs and lamp posts highlighted in black cause significant drops in capacity in their shadows. The demonstrator planning tool developed for this project illustrates this level of geospatial sensitivity as well as the impact of changes in frequency and weather conditions.

The demonstrator tool is distinct from commercially-available cell planning tools in that it can handle detailed geospatial information such as the type of façade of a building or the structure of a street-side object such as a road sign. This level of data, integrated with a suitable propagation model, enables the simulation of detailed phenomena such as surface roughness on a building's façade or the loss resulting from the shadow of a road sign.

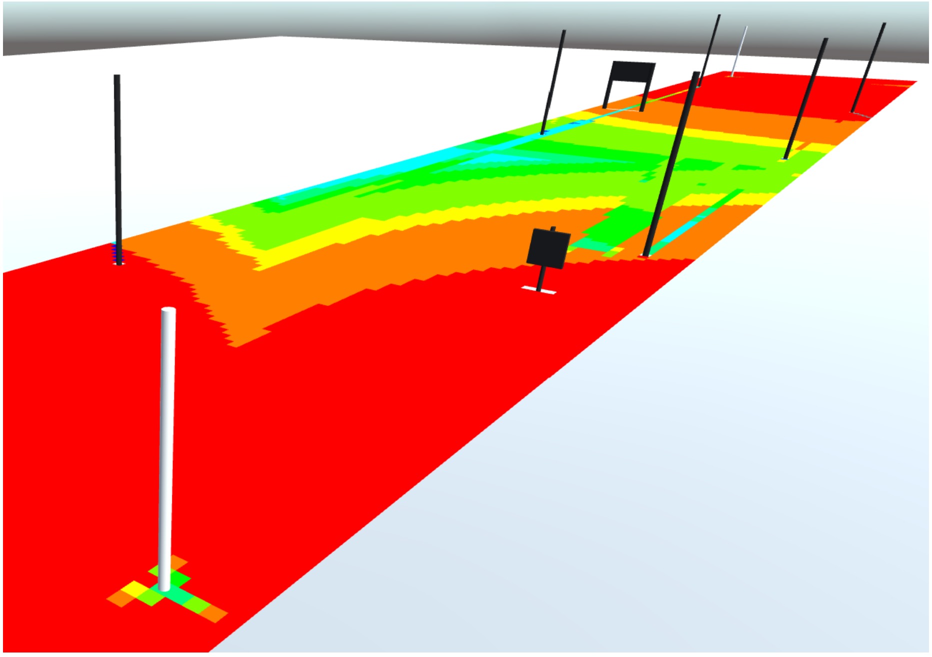

Figure 2-1: Heat map of 5G signal capacity

The impact of geospatial objects, weather and socio-economic factors is summarised in the following table, including an impact on propagation, data requirements and recommended further research.

Classification	Impact on Propagation or Communication Requirements	Data/Research Requirements
Weather	Extreme rainfall and sleet can have a real impact on the communication range and reach at the cell edge. Other meteorological factors including temperature, snow, gas, fog, or wind have negligible impact on the signal propagation.	Further research with the backing of measurement data is required to verify losses due to extreme rainfall and sleet conditions.
Vegetation	Vegetation causes substantial propagation problems, especially leaves. Measurements confirm that this impact is substantial for all tree types. However, certainty of the precise loss caused is highly dependent on the volume of foliage and can vary by season.	To obtain an estimate of the propagation loss through vegetation detailed datasets are required containing information not only about size and position of the plant but also type, i.e. coniferous or deciduous.
Street furniture	Street furniture has a significant impact on propagation. It can be categorised as: 1. Standing objects (e.g. road signs, pillars or lamp posts especially with sign attached). Any standing object with a width exceeding 10cm at 26GHz and 5cm at 90GHz on a street will have substantial impact on coverage. 2. Enclosed objects (e.g. bus shelters or telephone boxes). Propagation will be subject to penetration losses as well as loss due to reflections off the structure (known as scattering loss).	A database of street furniture is highly desirable including detailed characteristics such as accurate position, object dimensions, material, structure and information of other objects attached to it including advertising banners, signs or seasonal decoration like hanging baskets or Christmas lights. Information about street furniture will enable the accurate determination of signal loss caused due to obstruction or blocking of the line of sight as well as additional loss due to reflections known as scattering. Accurate location of street furniture objects is also of vital importance in terms of siting of base stations as is more cost-effective to place antennae on, for example, a lamp post than a building.
Building façades	Building surfaces e.g. brick, concrete, wood, tinted windows or metal vary substantially in terms of the material roughness which effects mmWave signal propagation. The importance of roughness increases with frequency since the rough edges	Substantial data is required to form a suitable set of groupings for different building façades, which have varying forms of material type and roughness. These groupings need to be identified such that a representative façade of a group

	become bigger compared to the signal wavelength (which gets smaller as frequency increases). This is particularly important where a mobile device does not have a line of sight link with a base station and the only way a link can be established is to rely on reflections from a building's façade.	type can be modelled onto a building front and give a reliable result of the expected reflections off that surface.
Fibre connection points	The position of fixed fibre network connection points has no direct impact on propagation. However, base stations without access to a connection point will need to be connected with fixed wireless links, and signal propagation will need to be modelled for these links.	Locations of fixed network connection points, though out of the scope of this work, will be required in the cell planning process and the tool will need to establish which base stations are connected to fibre and which are not.
Road and rail infrastructure	Infrastructure along the road and rail networks has no significant impact on the signal propagation. However, physical structures (bridges, road signs and gantries) can be used to mount equipment. Information about those structures will simplify and improve planning processes and help make small cells deployment along the networks more efficient.	Infrastructure information has been modelled for this within the Bournemouth Digital Model. There is scope for improvement if attribution is available from other sources.
Population statistics and footfall data	To help predict demand and improve network capacity, reliable population statistics and footfall data should be utilised to complement network planning processes. Information about how many people reside or work in any area of interest at different times will both improve the planning process and help to monitor small cells networks by locating 'hot spots' of high mobile usage.	Population and footfall data will help network operators ascertain the level of demand for data and calculate the expected revenue from deployment in a given location. Footfall data could be harvested directly from small cells locations as part of the 5G rollout, providing important access to the pool of information about user behaviour and demand helping shape a more comprehensive network.

Traffic flow	Traffic information is important because vehicles, as large metallic objects, have a substantial impact on 5G signals. Moreover, traffic information can be used to model demand along road/rail networks as traffic flows change over time.	Traffic density data are important, and information on the prevalence of large vehicles including buses and lorries, would enable their impact on propagation to be modelled. Traffic information would also help predict demand from autonomous vehicles using 5G network, IoT applications and mobile devices used by road users.
Property information	Development sites. No urban location remains static after a mobile network has been deployed. New developments will change the propagation landscape and any development structures can obstruct previously cleared lines of sight. Property type. Residential and commercial properties will have different levels and patterns of demand for data due to the different nature of users occupying them, i.e. residential vs commercial premises. Listed buildings. Many small cells will have to be attached to building façades. Obtaining permission to mount radio equipment on listed buildings is notoriously difficult, so these data will help exclude them from consideration.	Knowledge of building developments and the planning process must include consideration of their impact on a deployed network. This will enable 5G infrastructure adjustments to be made both for the construction phase and the resultant built environment. Detailed address data, including a classification of building function, will support initial demand analysis. Listed buildings datasets will improve the antenna deployment planning process at the desktop level.

Table 2-1: Summary of the impact of geospatial objects, weather and socio-economic factors, including an impact on propagation, data requirements and recommended further research.

The findings summarised above show that geospatial data requirements fit into two categories: dimensions and specifications. The scale of the challenge requires detailed knowledge of street objects in terms of their location, size and specification to reliably determine how they will impact propagation. Additionally, a classification of every building façade at street level is necessary to consider roughness effects on signals. At least ten times more geospatial detail is required for mmWave planning than for current cellular planning below 6GHz.

3

3 Introduction

3.1 Purpose of this project

This 5G project forms a deliverable commissioned by the Department for Culture, Media and Sport (DMCS) in 2016. A team led by Ordnance Survey and consisting of the University of Surrey's 5G Innovation Centre and the Met Office was appointed to undertake the project.

3.1.1 Objectives

The objectives of this report are:

1. to confirm the necessity of geospatial data in an outdoor built environment when siting infrastructure for 5G deployment at frequencies above 6GHz; and
2. to document the learning gained from the project to demonstrate how the usage of geospatial data is beneficial to use in the planning of an operational 5G deployment.

The report contains several technical terms. For definitions, please refer to the Glossary in Annex D.

3.1.2 Scope

The scope of the project is:

- to form a suitable path loss model specific to frequencies above 6GHz which is applicable to small cell deployment. The frequencies we have investigated are: 26GHz, 32GHz, 39GHz and 60GHz;
- to analyse the impact of geospatial objects on the coverage of 5G signals, evidenced through available measurements;
- to form a planning tool example that demonstrates the impact of frequency, geospatial objects and weather conditions on 5G coverage and capacity;
- to deliver a document describing the work done on the project (this document).

3.1.3 Study area

The study area was based around the town of Bournemouth on the UK's south coast, in close collaboration with Bournemouth BC. Within the overall study area we also defined three regions for detailed analysis. The study area and the three regions are illustrated in Figure 3-1.

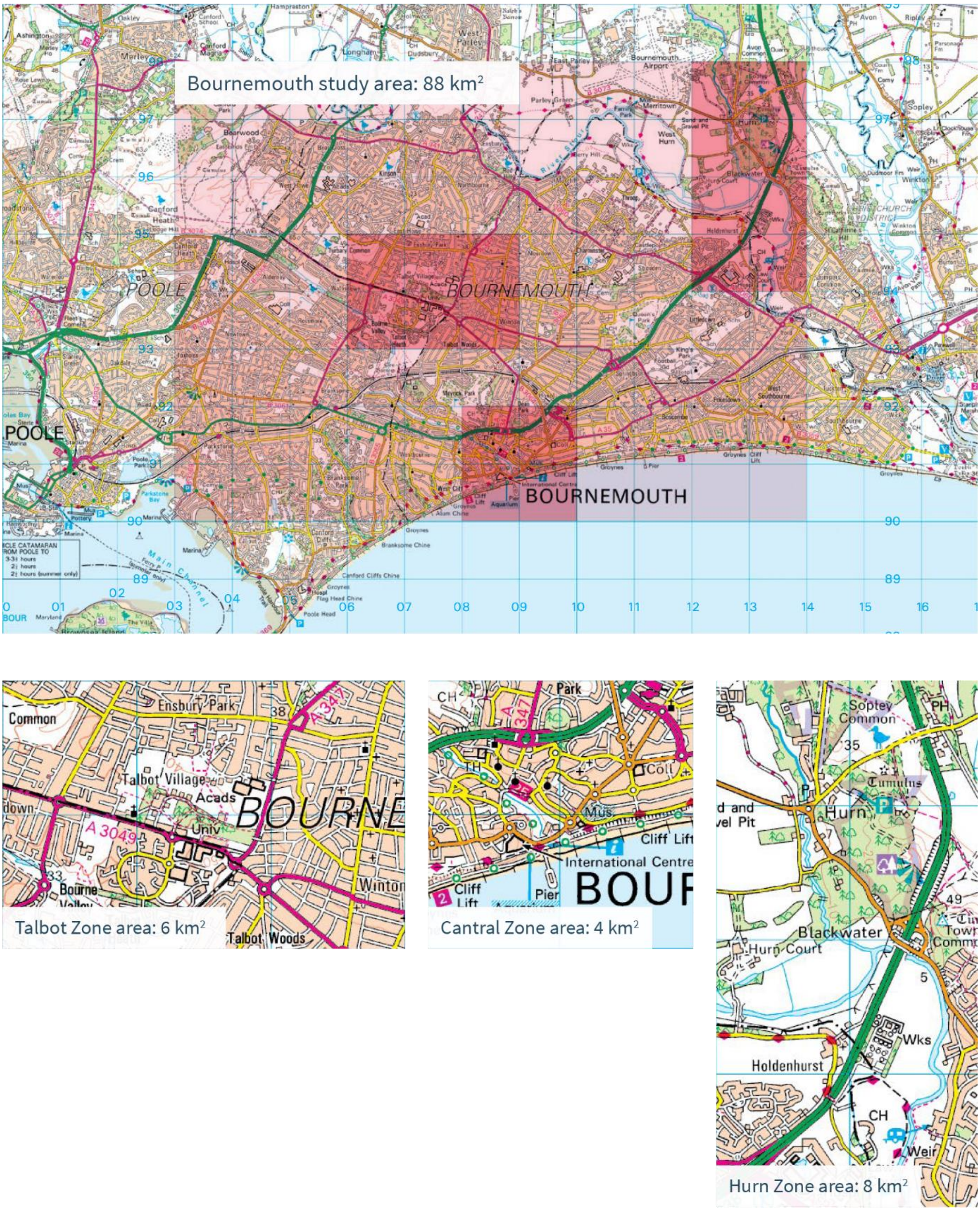

Figure 3-1: Bournemouth study area

The three selected regions contained a variety of local geographic characteristics as set out below.

Central Area (City centre)

- Shopping areas
- Public parks
- Many street furniture items
- Heavy traffic

- High movement of people at certain times of day

Talbot Heath (University)

- Dense residential areas
- Public areas
- High movement of people at certain times of day

Hurn (Outer city)

- Hospital
- Public areas
- High movement of people at certain times of day

3.1.4 Assumptions

The deployment of 5G mobile networks, due to the short-range nature of high-frequency signals and their vulnerability to the surrounding environment will be significantly more challenging than for previous generations of mobile networks. Based on the existing knowledge and experience within the project team, several starting assumptions were made about how high-frequency signals will behave in natural and man-made environments.

Impact of Vegetation

At high frequencies, coverage ranges are already limited by the laws of physics, and it becomes particularly important to understand and minimise all factors that might reduce ranges further.

We assumed that attenuation through vegetation, particularly trees and hedges, varies according to the following characteristics:

- Type of tree: there will be different levels of signal loss through coniferous and deciduous trees.
- Foliage: depending on the time of the year, foliage will have significant (April-October) or less disruptive (November-March) impact on signal propagation.
- Dimensions of the tree or plant: height and crown size will determine where best to place antennae to avoid or reduce blocking line of sight.

Although hedges do not obstruct signal propagation on a macro scale, we assumed that they will have a significant impact at street level along property boundaries, pedestrianised areas and parks.

Weather

At high frequencies, weather conditions have a noticeable impact on the signal propagation. We have assumed that heavy rain and melting snow (not uncommon in the UK) cause loss to the radio signals propagating through them and affect connectivity. Though other weather factors such as temperature, mist, fog and falling snow may affect signal propagation, we assumed that only liquid water in the air, such as rain and sleet, will have a significant impact on high-frequency signals.

Building façades

One of the key assumptions to investigate further was how different building frontage materials can markedly reduce the capability for high-frequency signals to 'travel'. This assumption is based on evidence in the available literature, which notably demonstrates how links can be impacted by reflection off a building's façade to a mobile device facing it. This has therefore been factored into the propagation analysis. For the purpose of this report, buildings were classified as follows:

1. Glass façade (glass in particular reflects infra-red)
2. Metallic façade
3. Brick façade
4. Façade based on a surface of wooden planks
5. Vegetation (for example a hedge at the front of a building)

It is important to compare these façades, not only because they are representative of the large majority of buildings, but also because they are significantly different in their degree of 'roughness'. Glass and metallic façades are typically smooth, while a façade of wooden planks or vegetation is rough compared to the wavelengths of high-frequency signals. A brick façade can be considered as rough or smooth depending on the frequency; if the grooves between bricks are large compared to a wavelength, then the surface can be considered to be rough. This is particularly the case at around 90GHz where a wavelength is just over 3mm.

Street furniture

As spectrum at higher frequencies has a much shorter range compared to current mobile bands in use, greater consideration must be given to clutter and its effect when planning wireless links. Because future network antennae will be deployed at street level, we assumed that street furniture including bus shelters, road signs, bollards, traffic lights, lamp posts and seasonal adornments (such Christmas decorations and hanging baskets) will reduce the capability of radio signals to travel.

Bus shelters will have a significant impact as they can cause penetration loss to signals, while reflected microwaves from points on a bus shelter in proximity to the mobile device will degrade data throughput.

3.1.5 Constraints

Because we are now exploring the use of the new high-frequency 5G spectrum, a wide range of unexpected constraints materialised and were overcome during the lifetime of this project, including:

Software availability and compatibility

We identified early in the project that there is currently no single commercially available software platform capable of ingesting the many and varied datasets required to deliver a comprehensive platform suitable for understanding mmWave propagation for 5G. The work that has been undertaken here makes it possible to consider the operational development of such an integrated software solution, to make it easier and cheaper to deploy in UK.

Image capture and image equipment availability

Due to the variability of the British weather, it was necessary to liaise with international image capture specialists to refine the quality of point cloud imagery (see Glossary Annex D) beyond what today would be regarded as state of the art. Further issues also arose regarding the availability of mobile mapping capability which is essential to deploy in certain areas, particularly where aerial imagery is unable to capture any data (e.g. under bridges or tree canopies). Moreover, seasonal factors, including the impact of Christmas decoration clutter and seasonal vegetation factors, required rapid mobilisation to capture information quickly.

Resources

The project team adopted an innovative approach that did not simply rely on traditional empirical path loss models. To deliver more cost-effective and more accurate results we needed to build a team of leading academic and industry experts from very different backgrounds. The resultant interdisciplinary group, whilst extremely effective, consisted of resources which in the UK are currently scarce.

Data issues

A very real constraint was the varying quality, availability and interoperability of existing datasets. This included, for example, the cost and complexity of obtaining reliable and accurate footfall data at an affordable price, the variable quality and accuracy of highly variable local authority data assets and the dearth of fixed network operator assets.

3.2 Our approach

The reality for mobile operators seeking to deploy additional network sites today is that they must go through a hugely expensive, complicated and time-consuming process. They require inputs from many different specialisms including radio planners, acquisition specialists, legal experts, build managers, link planners and data build technicians. The interactions required between people, process and systems to achieve successful network deployments is expensive. The kinds of activities involved begin with a review of coverage targets, engineering and planning rules and the distillation of these into some form of nominal plan which is used to compile a list of option sites, after which a multi-skilled site visit is necessary to validate these options. This is all before any considerations is given to planning approval, wayleaves, leases, link and power budgets, installation, commissioning and launch.

Nor is this the end of the story because this process only relates to radio assets. Further complexity arises when fixed network and other backhaul considerations are also factored in. Ofcom's recent consultation 'Wholesale Local Access Market Review'[5] sets out the kinds of complexity that can be involved when provisioning fixed link backhaul which is not owned in-house.

Therefore, our approach was not to begin by looking at spectrum propagation solutions alone, but by considering this problem in the round. Operators do not only wish to know about their infrastructure assets; they want a better understanding of the inter-relationships between their assets and those of other communications infrastructure providers to minimise cost and understand the revenue implications of their activities.

There is no current single approach which helps operators deliver the cheapest and fastest solution. In this project, we have identified and incorporated a variety of data sources and embedded them in a technical demonstrator with a user-friendly interface. We also recognise the importance of keeping information current. The UK has a dense and highly-populated geography which changes rapidly, and

[5] Available at https://www.ofcom.org.uk/consultations-and-statements/category-2/wholesale-local-access-market-review-proposals-PIA

this is significant for network operators, where they will require advanced planning tools to monitor the cell planning in a dynamically changing environment.

3.3 5G deployment challenges

5G communications will require highly densified networks with large numbers of mobile cells, which could cover only a few hundred metres depending on the frequency, substantially less than conventional 4G cell ranges. There are two reasons for this. First, the limited propagation range of the candidate frequencies above 6GHz, and second, the need to better exploit the available spectrum by distributing several cells over a large number of users in a dense environment as opposed to handling all users from a single base station.

3.3.1 Base station siting and deployment

The densification and reduction in size of mobile cells requires more locations for base stations. Suitable locations include lamp posts, bus shelters and other street furniture. Base stations need to be placed at street level to propagate through the shorter ranges, while conventional 3G and 4G macrocells propagate with ease over 1km or more. The landlord of suitable 5G base station locations is often a local authority, which can grant access to multiple sites. This substantially eases the siting of small-cell base stations in comparison to placing on buildings, where each site requires negotiation with the owner.

The need to deploy more base stations brings increased costs in acquisition and site rental, and carries more political obstacles. Information about the location and specification of potential sites (such as the height of lamp posts and what other objects, for instance road signs, are already attached to it) is becoming essential for cellular network planning.

3.3.2 Importance of fixed wireless links

In cellular network planning it is important to ensure a reliable link is maintained from the base station to a wireless device, and furthermore each base station must link to a ‘master’ base station from which a link to a cabinet can be readily obtained. This can be achieved by a fixed high-frequency signal link from one base station to another which is a simple and cost-effective method where fibre cannot be readily installed. The reliability of these links and the impact of both geospatial objects and weather data are as important as the link from the base station to wireless devices. These links are commonly known as backhaul.

3.3.3 Meeting the challenge for a planning tool

In forming a planning tool, there are two factors to consider. The first is to use suitable radio propagation models which will not only determine the power received by the antenna of a wireless device when the base station is transmitting towards it, but also the power from other base stations causing interference. This will determine the distances over which there is a minimum signal strength that is suitably higher than the interfering signals. The second factor is capacity; it is important to ensure that demand can be met in terms of bit rate of data throughput from the base station to the mobile which can only be achieved when the signal is suitably stronger than the interference.

3.3.4 Propagation models and coverage

To predict the received power at a distance from a transmitted source, the radio propagation needs to be accurately modelled. This is achieved by taking physical parameters such as frequency, distance, base station height and antenna characteristics to formulate the ratio of transmitted to received power, otherwise known as the path loss. Additionally, we need to understand not just how the received power decays over distance when there is a line of sight between the transmitter and receiver or how a signal penetrates through objects when there is no line of sight, but also how electromagnetic rays reflect off surrounding objects, as illustrated in Figure 3-2. These objects can also cause shadowing attenuation such as the propagation through vegetation illustrated by the dotted line in the figure. It is important to understand these characteristics as they not only affect the path loss but will also cause this path loss to become dependent on frequency, such that there will not be a constant path loss within a wide bandwidth used at frequencies above 6GHz. This phenomenon is known as frequency selective fading.

Figure 3-2: Illustration of reflection from surrounding objects

3.3.5 Deploying a cellular coverage plan

Currently no software exists to ingest the many datasets required by this project, so we identified the need for a bespoke proof-of-concept interface within which to test the 5G propagation model and investigate the effect that various environmental factors have on the planning of a 5G network.

We undertook a user-centred design process consisting of industry consultation workshops, user requirements specifications and interface design which led to a proof-of-concept build. The primary purpose of the proof-of-concept was to put the mathematical propagation model into a user-friendly environment to view its effectiveness and compare the model to real-world signal measurements. We also took the opportunity to gain insights into the value of the geospatial data and signal model, and how existing processes and practices within the network planning industry might be affected by a dense, small-cell network design.

3.3.5.1 Industry consultation

As part of the user-centred design process we consulted with manufacturers and telco providers including conducting two workshops with industry-expert network planners from Telefonica and Arqiva to understand their real-world processes and gain insight into how current macro-scale planning processes might be affected by small-cell network planning.

The workshops consisted of open discussion and the building of a process-flow describing the procedure used to plan and sign-off a network plan illustrated in Figure 3-3. Attendees were asked to think of the planning process from the point of view of planning a future 5G network and to consider the changes and adaptations that may result from planning the network with a greater density of cells and at higher frequencies.

Network planners placed considerable expectation on a future 5G planning tool to ensure that it would minimise any further work or tuning of the network beyond deployment. To quote directly from them:

‘For small-cell networks like 5G, the more we can get right in the office, as opposed to in the field, the better.’

The antenna density required for a functioning 5G network, and the sensitivity of antenna range and placement, means that the more accurate the picture created by an office-based planning tool, the more costs may be saved in physically checking and building the final network. Given the number of sites that will be needed, this cost saving could be significant.

The following all contribute to increasing the fidelity and reliability of any dense network plan, and therefore reduce the potential costs incurred during the planning stage:

- accuracy of geospatial environment information;
- accuracy of signal propagation model;
- a reliable and comprehensive understanding of the location of assets where antennae can or might be placed;
- a reliable and comprehensive understanding of location of assets that include backhaul or power connections;
- a cost estimate of each placement.

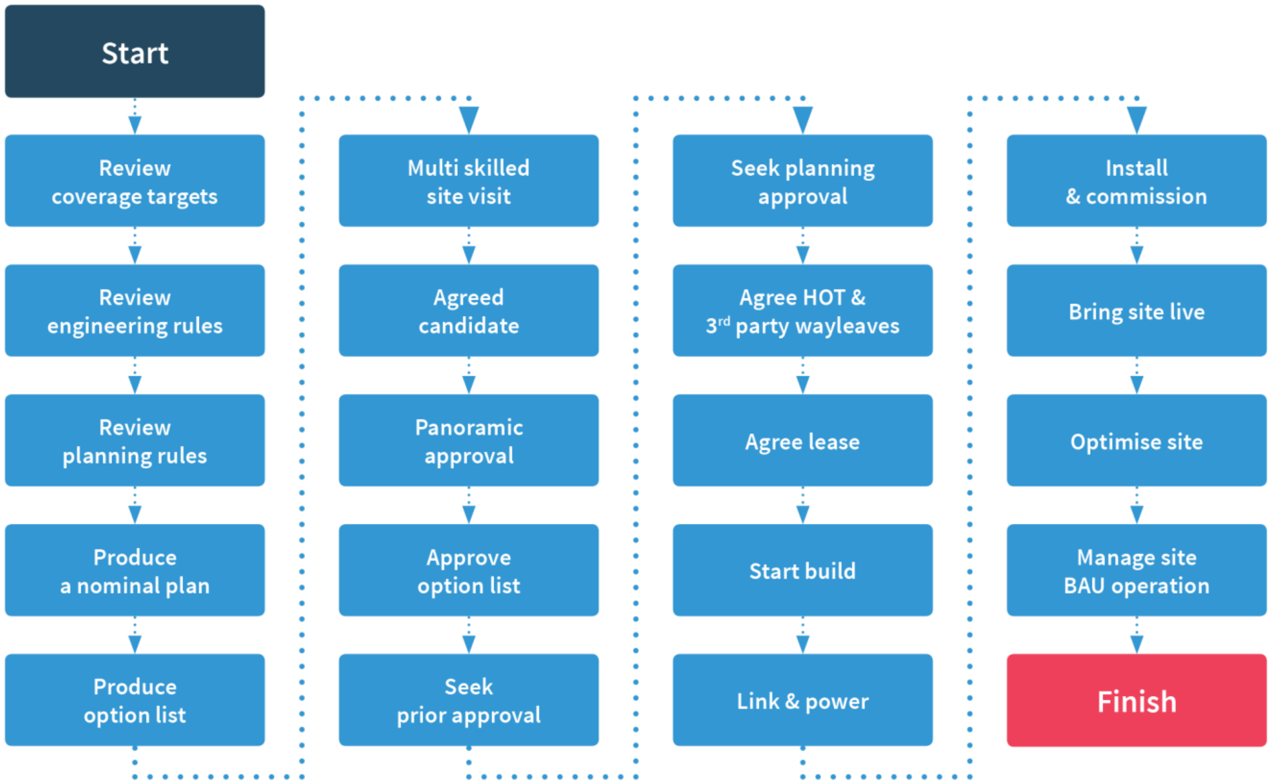

Figure 3-3: Lifecycle of a 5G coverage plan, derived from consultation with the mobile industry. See full diagram in Annex C.

3.3.5.2 Planning tool design

From the industry expertise gathered at the workshops we identified that the proof-of-concept should both show the fidelity of the data captured and demonstrate a 'thin slice' of functionality across several areas of planning. The aim of the proof-of-concept was not to design a fully-fledged piece of planning software, but rather to demonstrate how the data and signal model could be incorporated into future planning software.

The thin slice of functionality identified was:

- Setting up a project and project defaults, including allowing the planner to define what they deem to be an 'acceptable signal';
- Showing where network equipment could be located;
- Allowing the placement of network equipment;
- Displaying a 'quick view' of mmWave network signal propagation;
- Running a report to get a picture of detailed signal coverage;
- Visualising signal coverage which clearly defines the edges of acceptable signal strength;
- Understanding how bad weather might affect signal coverage;
- Showing how clutter including street furniture and vegetation can affect signal propagation;
- Providing an indication of cost of the proposed plan.

3.3.5.3 Use of 3D in the planning process

Larger-scale networks, where signal propagation is less sensitive to clutter, are often planned to an acceptable level of fidelity on a 2-dimensional stage. 5G networks, with their density and sensitivity requirements, benefit from a high-fidelity 3-dimensional view so that a planner can more easily understand the relationship between the signal and the environment. For example, switching to 3D helps a planner predict whether a small-scale object (such as a lamp post or pole) will cause a signal shadow.

3.3.5.4 Using an interface framework

Ordnance Survey's User Experience and Digital Design Teams are well versed in designing user-centric applications that utilise geospatial data which include map interactions and workflow functionality. They reviewed the results of the industry consultation workshops and designed initial versions of the mapping interface which they tested and reviewed with the wider team. Once it was clear that the designs were fulfilling the needs of the proof-of-concept, these initial designs were accepted for final design and build.

3.3.5.5 Future improvements to the network planning process

Several 'pain-points' and opportunities were identified during the industry consultation and proof-of-concept build process.

More accurate and comprehensive geospatial data reduce costs later in the planning process.

To have confidence that a proposed network plan can be implemented, one must have 'good' data, which in this context means they are accurate, comprehensive, detailed and recent. This will be explored further in this document. Existing network planning processes place the burden of accuracy later in the planning process by using site visits or further research.

In the industry consultation workshops, network planners were keen to understand how much data could be front-loaded into any future planning tool. For example, knowing at least some legal ownership information about a potential antenna site up-front would influence how confident the planner was that the proposed site could be used. The types of data for which they would like to see an increase in fidelity within a 5G network planning tool are:

- The location and type of assets where they know they can place their equipment cost-effectively – e.g. the assets they own, or someone they have a relationship with owns;
- Asset ownership details;
- Backhaul asset locations;
- The lay of the land; accurate surface and clutter modelling.

Knowing the future reduces cost

When planning a new network or monitoring an existing network, pre-warning of upcoming building developments, building works or other knowable changes to the built environment would highlight risks to the network before they occur.

Local authorities (and others) could be incentivised to provide reliable asset information

‘Assets’ are places where antenna equipment can be placed. Network planners highlighted that businesses often ask how much their assets are worth to a networking company. And network planners will need a greater number of asset options where antennae can be placed for compact 5G networks.

Proof of line of site is costly

Planners highlighted that ‘proof of line-of-sight’ between antennae and backhaul was costly and an on-site task. The addition of backhaul locations within a high-fidelity Digital Model of the landscape would enable microwave links for backhaul to be planned with greater confidence. To enable this, the location around backhaul sites should be included within the initial digital-twin survey.

Backhaul location data can be inaccurate

Network planners have low confidence in the accuracy and comprehensiveness of backhaul location data. In their experience, potential backhaul links can be inaccurate and difficult to obtain from companies that own the backhaul network. Again, considering the density of the antennae and backhaul links required to implement a 5G network, the cost of rollout can be reduced given better backhaul data to use during the planning process.

3.4 Tools

3.4.1 5GIC equipment

The 5GIC has previously undertaken measurements of path loss and frequency selective fading characteristics in small cell environments using transmitter and receiver equipment. State-of-the-art channel sounding equipment, illustrated in Figure 3-4, was used to characterise path loss and frequency selective fading at 26GHz, 32GHz, 39GHz and 60GHz, which were of interest when conducting the measurements at the time and provide a suitably wide frequency range with which to inform the accuracy of the path loss prediction models used in this study.

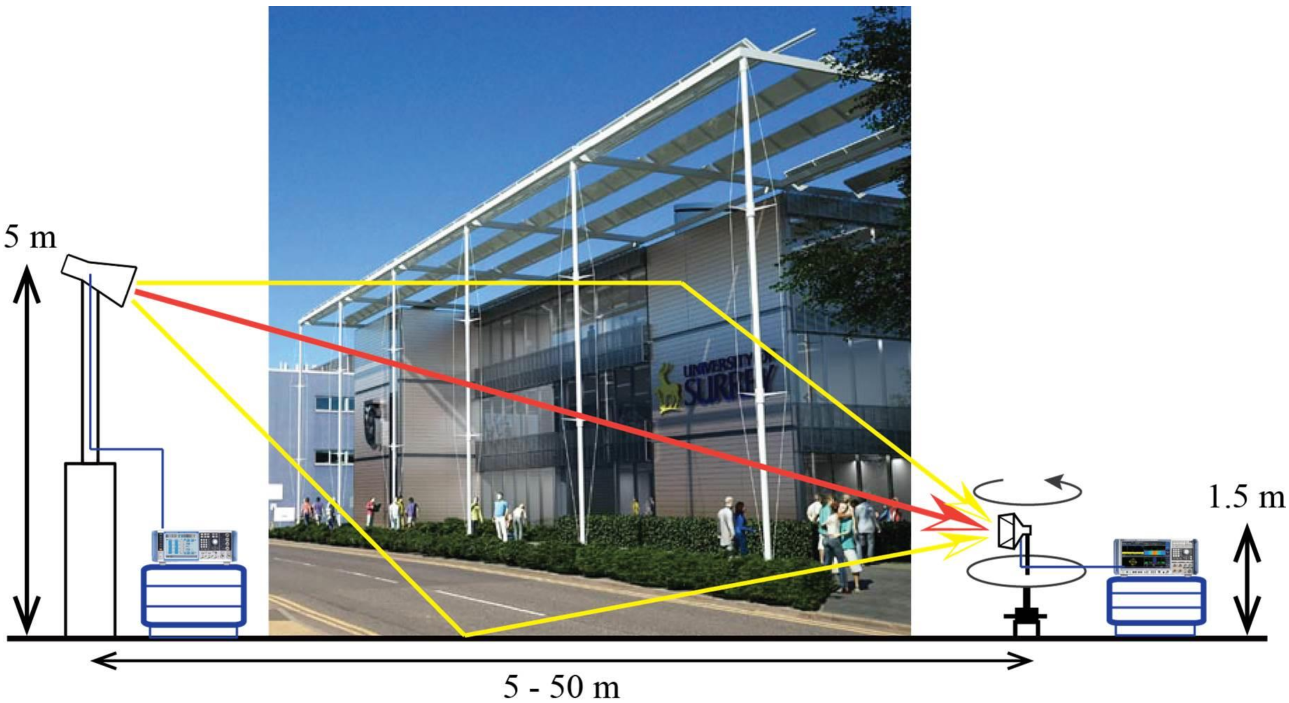

Figure 3-4: Illustration of channel sounding equipment used for path loss and frequency selective fading measurements

Measurements carried out using channel sounding were able to determine the path loss and frequency selective fading due to reflections off buildings and the ground. A vector network analyser was employed to measure the effect of geospatial objects such as lamp posts and bus shelters illustrated in Figure 3-5. These measurements were carried out to measure the extra path loss and frequency-selective fading that results from the presence of such objects.

Figure 3-5: Illustration of measurements carried out to measure extra path loss and frequency selective fading from geospatial objects such as lamp posts and bus shelters

3.4.2 Weather

The proposed mmWave frequency bands will have an increased vulnerability to signal degradation due to weather elements compared to previous generations of mobile networks. This is because, at these frequencies, the wavelength of the electromagnetic (EM) radiation is comparable with the dimensions of intervening raindrops and other atmospheric phenomena known as hydrometeors which results in the increased absorption and/or scattering of the EM wave.

The magnitude of this signal attenuation will increase with the path length of the signal and therefore the weather can be a limiting factor for the maximum separation of 5G assets, in particular in those areas where larger building separations may have otherwise allowed for a sparser network. A balance must be struck between reducing the frequency and severity of weather impacts on network performance and the significant cost of increasing network density to reduce this level of exposure.

A common approach to the assessment of environmental exposure of infrastructure is to estimate the return period of a high-impact weather event (e.g. a 1 in 50-year flooding event). It is premature to attempt this for 5G networks because the response of a wide cellular coverage area to rainfall which is spatially distributed over the network is unknown at this point. However, it is useful to:

1. understand the likely magnitude of the impact of weather elements on the different frequency bands;
2. prepare realistic representations of spatially varying weather and the associated signal attenuation to 'challenge' candidate network designs before they are built.

3.4.2.1 Outline methodology

As part of its role as the UK National Meteorological Service, the Met Office produces analyses of UK rainfall at a spatial resolution of 2km over the UK every 5 minutes. These are derived primarily from operational radar data, supplemented where necessary with satellite data. These data are archived allowing access to recent historical real weather events. The resolution of 2km is chosen for practical reasons as the effective resolution of the radar measurement varies as a function of distance from the radars themselves. The UK is served by 15 radars supplemented by others in Ireland and the Channel Islands as shown in Figure 3-6.

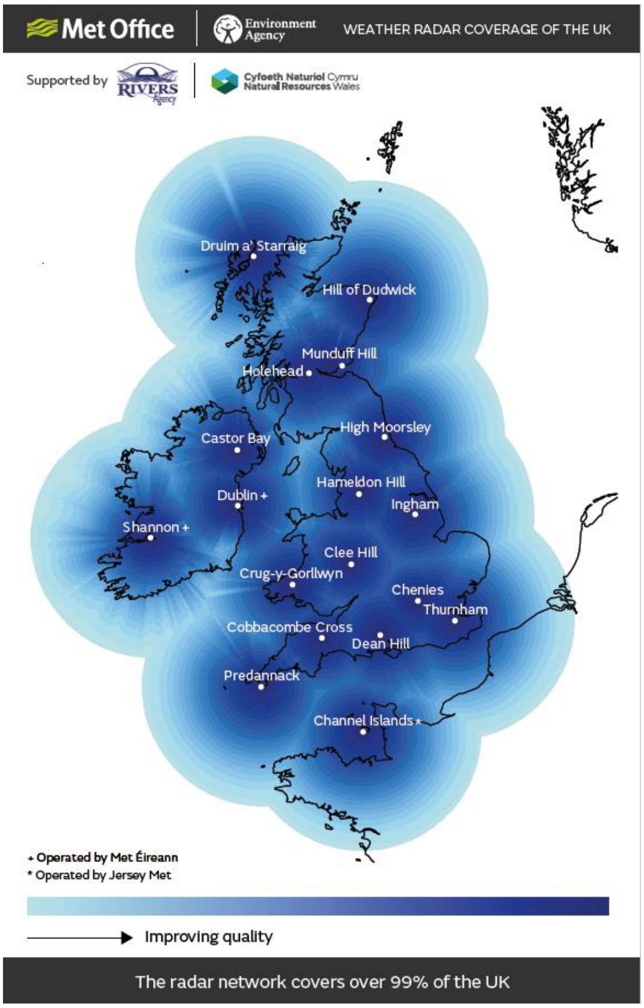

Figure 3-6: The weather radar network. Darker colours indicate higher quality, more granular observations.

As the 2km rainfall values represent average values over a relatively large area ($4km^2$), there will inevitably be sub-grid scale variability of rain rate at the smaller length scales associated with the expected separation of 5G antennae (10-100s of metres). A method to introduce this variability was identified and implemented, allowing the production of plausible 100m resolution rainfall datasets from the 2km archive.

Several recent case studies were identified where heavy rain was experienced in Bournemouth and Swindon. Each 100m rain rate 'pixel' was converted to free path attenuation values at each of the five proposed 5G frequency bands. The result was high resolution spatial datasets of meteorological parameters together with 5G attenuation values which were passed to project partners at 5GIC to be assimilated into detailed propagation models.

The project has therefore been successful in representing the impact of weather at the street scale required for the planning of 5G networks.

3.4.2.2 Identification of case studies

The primary weather challenge to 5G will be from rainfall. While cloud liquid water at ground level (i.e. mist/fog) will interact with EM radiation at these frequencies, its attenuation impact is lower than would be expected from more frequently-occurring moderate amounts of rainfall. For that reason, a network designed to operate in the presence of typical UK rainfall will be resilient with respect to cloud at the surface and therefore we excluded fog case studies from the project.

Rainfall in the UK can be categorised as 'stratiform' (with large horizontal extent and usually the result of large features such as low pressure systems and fronts) or 'convective' (more localised and showery due to local atmospheric instability caused by heating of the surface or the impact of local terrain features). The former tends to be more protracted in time and more common in the autumn and winter months, the latter more short-lived but often delivering more intense rainfall and more common in the spring and summer. In certain summer situations, convection may become more organised (into 'mesoscale convective systems' or MCSs), creating larger areas of more persistent and very heavy precipitation which may also result in flash surface flooding.

For this study, separate convective events were identified for the Bournemouth and Swindon study areas. For the stratiform case, 'Storm Angus' (19th November 2016) was used for both locations. For each case study, three time steps at hourly intervals were used to demonstrate how rainfall attenuation might change with time. In addition, a severe convective event over the SE of England from the early hours of 23rd June 2016 ('Referendum Day') was used to demonstrate the impact of a more organised convective event. Table 3-1 lists the dates and time steps used.

Location	Date	Times	Type
Bournemouth	2015/07/03	2100, 2200, 2300	Convective
London	2016/06/23	0100	Convective
Swindon	2016/06/24	1400, 1500, 1600	Convective
Bournemouth	2016/11/19	2100, 2200, 2300	Stratiform
Swindon	2016/11/19	2100, 2200, 2300	Stratiform

Table 3-1: Location, date and times for the selected weather cases

3.4.2.3 Generation of spatial rainfall datasets

The starting point for the generation of the 100m spatial rainfall dataset was the Met Office archive of 2km rain rate values. As these fields effectively represent mean rain rate values at this scale, we would expect that at the smaller scale of 100m both higher and lower rain rates will be found. To represent this variability, for each single 2km grid box, a more granular 20-by-20 grid (i.e. 400 elements) was produced, using the same 'downscaling' principles that apply to the estimation of small scale wind turbulence in larger scale wind flows.

Turbulent wind flow structures exist over a wide range of scales in the atmosphere, from the planetary ~10,000km scale to the 1km scale, and even down further to the millimetre scale. These fluctuations in wind velocity, when viewed as 'spectra' in the frequency domain, can usually be characterised by simple 'scaling laws'; typically, the wave power decreases as a power law with decreasing length scale, as described by the Kolmogorov[6] theory.

Rainfall intensity is a 'passive tracer of turbulence'; that is, it is affected by the turbulent motion of atmospheric eddies but has no effect on the turbulence itself. As a result, it can also have scaling behaviour, as demonstrated recently at scales down to ~1m by Lovejoy and Schertzer[7]. The scaling exponent for a given rain image (in our case a 2km rainfall rate analysis) was estimated empirically and extrapolated to 100m scales, enabling the blending-in of synthetic structure to achieve a 'downscaled' image with realistic variability; this is best demonstrated by Figure 3-7. We validated this downscaling approach against radar data from close to a radar installation where the radar pixels were of a typical size of 75m.

[6] Kolmogorov, A.N., 1941. The local structure of turbulence in incompressible viscous fluid for very large Reynolds numbers. In Dokl. Akad. Nauk SSSR, 30(4), pp. 301-305.

[7] Lovejoy, S. and Schertzer, D., 2008. Turbulence, raindrops and the l1/2 number density law. New Journal of Physics, 10(7), p.075017.

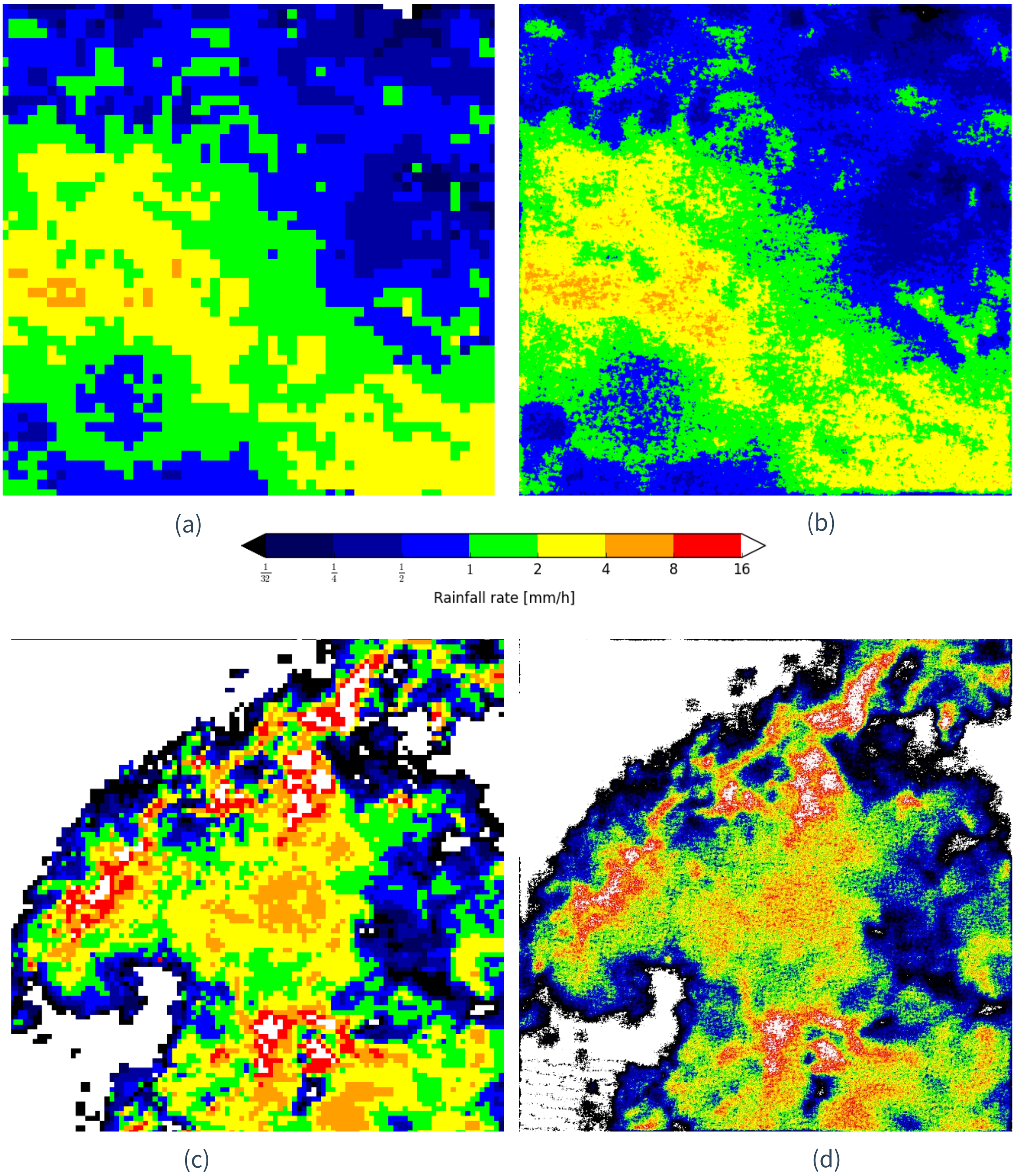

Figure 3-7: Creating a 100m rainfall map from a 2km analysis for the [top row] Storm Angus Bournemouth and [bottom row] London case study. The area shown is approximately 100km and 200km in each direction for each case respectively. Figures (a) and (c) show original 2km data; (b) and (d) demonstrate the impact of down scaling to 100m. Note that the >16mm/h colour band contains a small number of pixels >200mm/hr

In addition to the 100m rainfall values, associated values of temperature, humidity and wind speed (in both E-W and N-S directions) were also generated. For these additional parameters downscaling was not necessary. Instead, the 2km data were simply mapped onto their associated 100m pixels.

All the downscaled and remapped fields were prepared in fully self-described, geo-referenced netCDF format files.

3.4.2.4 Generation of associated attenuation parameters

As they traverse the atmosphere between antennae, radio frequency signals interact with both gaseous constituents (primarily oxygen and water vapour) and weather elements such as rain, snow and cloud liquid water. The strength of this interaction varies significantly across the range of potential 5G frequencies and it is essential to factor this in to any propagation model.

The attenuation problem becomes particularly complex at 5G wavelengths because the sizes of the hydrometeors are comparable to the EM signal waves themselves. In this instance, small changes in the sizes and internal composition of the individual hydrometeors may have a large impact on the efficiency with which they remove power from signal by absorption (where the signal energy is dissipated in the hydrometeor itself) and scattering (where the signal is redistributed in many directions, predominantly away from the receiving antenna). The sum of the absorption and scattering contributions is known as 'extinction'. The summation of extinction effects along the propagation path is the attenuation.

It is necessary to make simplifying assumptions to make the problem of estimating 5G attenuation tractable. These assumptions and their implications are summarised in Table 3-2.

Assumption	Impact
Hydrometeors are all liquid phase (i.e. no ice)	For the case studies in this study, this is a valid assumption. More generally, it is well understood that liquid hydrometeors will have a greater extinction efficiency than their fully frozen equivalents (hail or snow). Rainfall therefore offers a very useful worst-case to challenge the network. The key exception is in marginal near-freezing conditions when melting snowflakes (sleet) 'look like' very large rain drops at 5G frequencies as they become coated in water just prior to their collapse, which has the potential to significantly increase the amount of attenuation. The limitation of this assumption and its relevance to the conclusions of the study are discussed in Section 5.
All raindrops are spherical	Real raindrops become oblate (squashed in the vertical) as they fall, this being more apparent for larger raindrops associated with higher rain rates. The result is that the attenuation of horizontally polarised EM waves is greater than for vertical polarisations. The study does not capture this second order effect, rather it looks at the primary issue of the magnitude of signal attenuation. This does not affect the conclusion of the study given in Section 5.
The refractive index of water does <u>not</u> change with temperature	The refractive index of water is important because it determines the degree to which it refracts on interaction of the EM wave with the raindrop. For these case studies, we have chosen a representative value that is reasonable for all the case studies. The sensitivity to this assumption is discussed in Section 5.
The rain droplet size distribution (number density with size) can be described accurately by simple parameterisations with respect to rain rate	5G extinction efficiency is a very sensitive (and non-linear) function of the ratio of the wavelength of the EM wave to the rain droplet size. Therefore, the total extinction from a volume of air containing large numbers of hydrometeors is very strongly dependent on the assumed size distribution (and also the wavelength under consideration). The study has used two very different size distribution assumptions to understand the uncertainty in the results due to this. This is discussed in Section 5.

Table 3-2: Simplifying assumptions made in this study

Given these assumptions, we can convert any rain rate to an equivalent 5G attenuation value using well established models for single particle extinction and integrating the impacts over the assumed drop size distribution. In particular, the impact of a single spherical raindrop on an incident EM wave can be calculated accurately using Mie[8] theory, which has been coded by many researchers. It is, however, very inefficient to perform this calculation explicitly every time. For that reason, an existing Met Office capability – the Havemann-Taylor Fast Radiative Transfer Code (HT-FRTC) – was repurposed for this project.

HT-FTRC was originally developed to enable the rapid calculation of hyper-spectral infrared radiances from vertical profiles of temperature, humidity and cloud using a principal component analysis approach. (This was necessary to enable the exploitation of the new generation of satellite and airborne hyperspectral instruments used for atmospheric research and operational weather forecasting). The key feature of the capability is that it enables offline training of the model so that near real-time calculations may be done with high integrity, but many orders of magnitude faster than would otherwise be possible.

For the 5G project, HT-FRTC was trained using approximately 25,000 vertical profiles of weather parameters from numerical weather prediction models (further supplemented by cases of more extreme rainfall rates) so that extinction parameters at any arbitrary frequency across the 5G spectrum could be calculated for any rain rate. The result was that for any set of values of temperature, humidity and rain rate both the gaseous and rain-related extinctions could be calculated at the frequencies of interest.

The extinction parameters were calculated for each of the 5 frequency bands of interest, with each band represented by a low, middle and high frequency. These are given in Table 3-3.

	Low (GHz)	Middle (GHz)	High (GHz)
Band 1	24.25	25.75	27.25
Band 2	31.80	32.60	33.40
Band 3	40.50	42.00	43.50
Band 4	66.00	71.00	76.00
Band 5	81.00	83.50	86.00

Table 3-3: Frequencies for which extinction parameters were calculated

The calculated attenuation parameters were the extinction coefficient k_{ext}, and the absorption coefficient k_{abs} . k_{ext} may be understood as follows:

The amount of signal lost by extinction along a given path is proportional to the intensity of the signal itself and to the length of the path. The constant of proportionality is the extinction coefficient k_{ext} . So, if the extinction coefficient is k_{ext} =0.01 m^{-1} then, along a path of 1 metre, 1% of the initial radiation is lost. The absorption coefficient k_{abs} is simply the component of k_{ext} that is due to absorption loss (the remainder being due to scattering).

The values of k_{ext} and k_{abs} were also included in the netCDF files that contained the rainfall information.

[8] Mie, G. (1908), Beiträge zur Optik trüber Medien, speziell kolloidaler Metallösungen. Ann. Phys., 330: 377–445. doi:10.1002/andp.19083300302

Key results from the Met Office component of this report are presented in Section 5.

3.4.3 Software platforms

For this project Ordnance Survey built a 3D geospatial dataset, or Digital Model, of Bournemouth. A full market analysis of the wide range of software packages was out of scope for this project. The following commercially-available software packages were used in this work.

Skyline TerraExplorer Pro

The project required software that would enable us to attribute and move geospatial data within a 3D environment, including point clouds, mesh models, raster data and vector data, as well as enabling us to capture new data for telecom boxes, street furniture, lamp posts and bus shelters on the terrestrial point cloud and aerial mesh models.

We adopted Skyline software to build the Digital Model as it can integrate, display and analyse multiple data sources within an expansive 3D world model. It can integrate attribution information about feature data into a mesh model, allowing any 3D environment to be easily understood in a very intuitive way, providing a useful platform for assessing line-of-sight visibility for 5G antenna placement.

Safe Software FME

We used a variety of FME workbenches at various stages of the project, primarily to interrogate the data, attribute point clouds and create 3D objects. The primary benefit of using FME was to automate processes and create a replicable working environment.

Esri ArcMap, ArcScene and ArcPro

ArcMap software was used to capture, attribute, manipulate, process and visualise a broad variety of raster and vector geospatial datasets.

In addition, Esri ArcScene and ArcPro were used to view and analyse data in a 3D environment.

Global Mapper, QT Reader, Sure (nFrames) Trimble Trident and Trimble Realworks

These software packages were used to work within a point cloud environment, specifically for:

- accessing data within native survey formats;
- classifying mobile mapping point cloud data;
- classifying aerial point cloud data;
- extracting features from aerial point cloud data;
- generating and visualising.

ContextCapture

Software from Bentley, used for 3D mesh creation from imagery.

MapInfo, QGIS

We used MapInfo and QGIS software to evaluate and prepare data provided by Bournemouth BC in a variety of formats.

Further information about the use of these software packages is presented in Annexes A and B.

3.4.4 Unity

This software was used to build the 5G planning tool. Unity is a cross-platform 3D game engine and development environment. It is designed to enable rapid prototyping, but also sufficiently scalable to build production-ready software. Using a game engine provides much functionality relevant to the tool, including rendering of 3D environments, physics interactions and user interface development. The cross-platform feature is also advantageous as it allows the software to be targeted for a number of platforms including Windows, Mac and HTML5 which will enable the facility to run both through client software and web-based applications.

4

4 Geospatial data requirements

4.1 From 2D to 3D

2D mapping has proved adequate for planning networks at low frequencies where the geospatial landscape has limited impact on signals, but the new high frequency spectrum is particularly sensitive to small changes in geospatial features and requires a better understanding of the environment.

3D mapping is now coming of age. Since the advent of LiDAR and digital photogrammetry, the potential to generate rich 3D content modelling the real world has begun to be realised. These capabilities have matured over the last decade and are still evolving.

To generate a 3D environment suitable for 5G planning meant modelling the urban environment at new levels of granularity and this necessitated adopting new approaches to data extraction. To this end, research teams learned new techniques for automating the extraction of 3D data where possible and undertook manual extraction when automation was not viable.

The generation of the Digital Model of Bournemouth is the result: a 3D model which is rich in attribution and has a sufficient level of detail to represent objects that may interfere with mmWave 5G signals.

4.2 Data for building the Digital Model

4.2.1 Published data

Addressing data

Within the project we used **AddressBase Premium**, a comprehensive register of addresses in Great Britain. It contains data from multiple sources including local authorities, Ordnance Survey, Royal Mail and the Valuation Office Agency.

The data contain a hierarchical address classification, at the highest level distinguishing commercial and residential addresses, and also categorising commercial usage – an example is shown in Figure 4-1.

Attributes information	
DPA	Bournemouth International Centre, Exeter Road, Bournemouth, BH2 5BH
LPI	Bournemouth International Centre, Exeter Road, Bournemouth, BH2 5BH
CLASS_DESC	Bingo Hall/Cinema/ Conference/Exhibition Centre/ Theatre/Concert Hall
VOA_NDR_RE	3412625000
PRIMARY_DE	Miscellaneous
WARD_CODE	E05002129
OS_TOPO_TO	osgb1000012813265
LOCAL_CUST	1250
LOCAL_CU_1	Bournemouth
CALCULATED	11166.727396
IMB_VALUE	33.07
CAPACITY	10000
RATEABLE_ VALUE	11250

Figure 4-1: AddressBase Premium record of the Bournemouth International Centre; as an event venue, it represents periodic high demand for mobile services.

AddressBase Premium also contains non-postal address records, including electricity substations which may prove valuable when planning 5G infrastructure. Figure 4-2 below illustrates substation locations in a part of Bournemouth.

Figure 4-2: Overview of the location of existing mast infrastructure and electricity substations in central Bournemouth

Population data

We used the **National Population Database** from Health and Safety Laboratory. The Residential layer provides valuable information, referenced to AddressBase Premium, about statistically-estimated populations at their usual place of residence based on four different scenarios:

- Usual resident or night time population;
- Night time non-term time;
- Day time term time population;
- Day time non-term time population.

These data provide planners with intelligence to help model demand more accurately. Figure 4-3 illustrates the information available within the Residential layer.

Figure 4-3: The Digital Model attributed with AddressBase Premium and National Population Database Residential Layer

5G is a key enabling technology for a future smart digital economy. Mobile phones, tablets and smart home appliances, plus IoT devices, Connected Autonomous Vehicles and other pieces of smart infrastructure will all make extensive use of this technology.

Deploying 5G network capability where devices are not affordable to the majority of the population will not bring adequate return on investment to network operators. For this reason, we enhanced the demonstrator with the English **Indices of Deprivation** data published by the Office of National Statistics. Government will require data of this kind to assess where policy interventions may be needed to minimise social exclusion.

This dataset is based on 37 separate indicators, organised across seven distinct domains of deprivation which are combined, using appropriate weights, to calculate the Index of Multiple Deprivation.

Road data

OS MasterMap Highways Network was used for street information. It includes asset management information which identifies the authority responsible for maintaining a road, how a road should be restored following street works and whether there are any conditions that the local highway authority has associated to a road. It supports data sharing for compliance with the New Roads and Street Works Act, enabling mobile network operators to share information via the USRN (Unique Street Reference Number) with contractors and highways authorities to manage the impact of road closures from their desktop.

Flood zone data

As fixed assets will play an important role in 5G rollout, operational and maintenance costs must be minimised to maximise operational efficiency. Therefore, protecting and securing assets against physical damage will be highly important for network operators and local authorities. We used Flood Zone data from the Environmental Agency in the demonstrator. This enables network operators to reduce the risk of damage to their networks. The Flood Zone dataset, illustrated in Figure 4-4, depicts the extent of land at risk of flooding when flood defences are not considered.

Figure 4-4: Flood Zone polygons in central Bournemouth

Built and natural environment data

We used OS MasterMap Topography Layer; a detailed, maintained model of the built and natural landscape of Great Britain. It models the real world at metre-level resolution and includes height values for buildings. It is also used to reference the more detailed geography from point clouds and other data sources together.

In addition to Ordnance Survey and local authorities' content, we used the Listed Buildings dataset from Historic England to assist desktop-based network planning. When a building is recognised as being of special architectural or historic interest it is added to the statutory 'List'. Buildings on the List are given one of three grades which denote their level of importance, Grade I being the highest and Grade II the lowest. The listed buildings in central Bournemouth are illustrated in Figure 4-5.

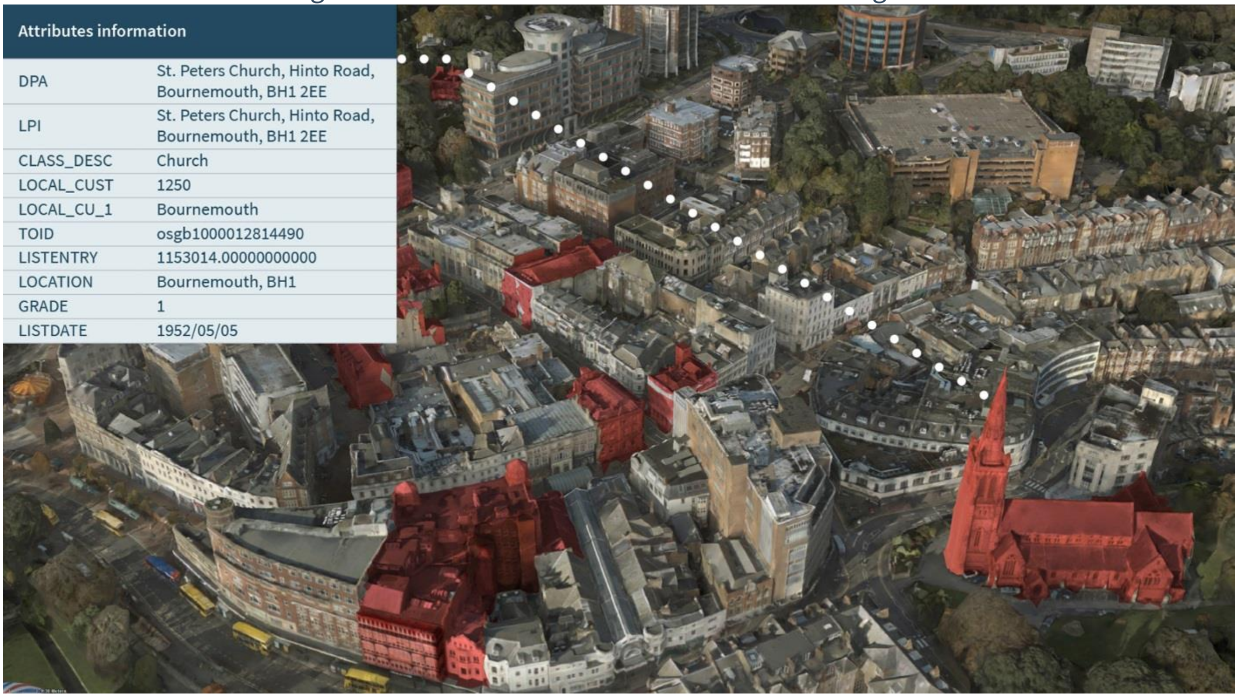

Figure 4-5: An example of listed buildings in central Bournemouth

This information is valuable for planning the placement of access points, many of which will have to be attached to the building façades. The process of applying for the permissions required is time-consuming and costly. Knowing where listed buildings are located will help network planners to estimate the probability of gaining approval at alternative site locations.

4.2.2 Bournemouth data preparation project

To meet the requirements for highly accurate 3D data within urban and suburban environments, OS undertook bespoke data capture in the Bournemouth study area.

During this project, some of the boundaries of aerial imagery exploitation have been explored. Image capture resolution is a limiting factor, as is the identification of features located in areas of deep shadow. An alternative solution is required, and in this regard mobile mapping technologies have shown significant potential.

Point clouds from aerial imagery are valuable for both 3D visualisation and data processing, notably for the classification of ground points, buildings, vegetation and particularly tree models, which has added considerable value to the overall 3D model.

Generating a 3D mesh model from imagery is a relatively new technique. It employs the principle of analysing many images of a scene taken from slightly different viewpoints and automatically detecting pixels corresponding to the same physical point.

The data preparation project was allocated into five activities split into Phase 1 and Phase 2, with the objectives listed below.

Phase 1 (Data Preparation):

- To prepare data in a known and consistent format for use in a 3D environment with all relevant attribution maintained from the available data;
- To extract highways asset information from Bournemouth BC;
- Create accurate geospatial datasets for each selected region, including metadata;
- To understand what different types of attribution characteristics we could extract successfully and what we cannot.

Phase 2 (Data Acquisition):

- To extract a point cloud and classify it using the Bournemouth BC data;
- To enhance the Bournemouth BC data by moving feature records into their correct position within the point cloud;
- To automate as many of the manual processes employed so they can be easily replicated in the future.

The overall project methodology is illustrated in Figure 4-6.

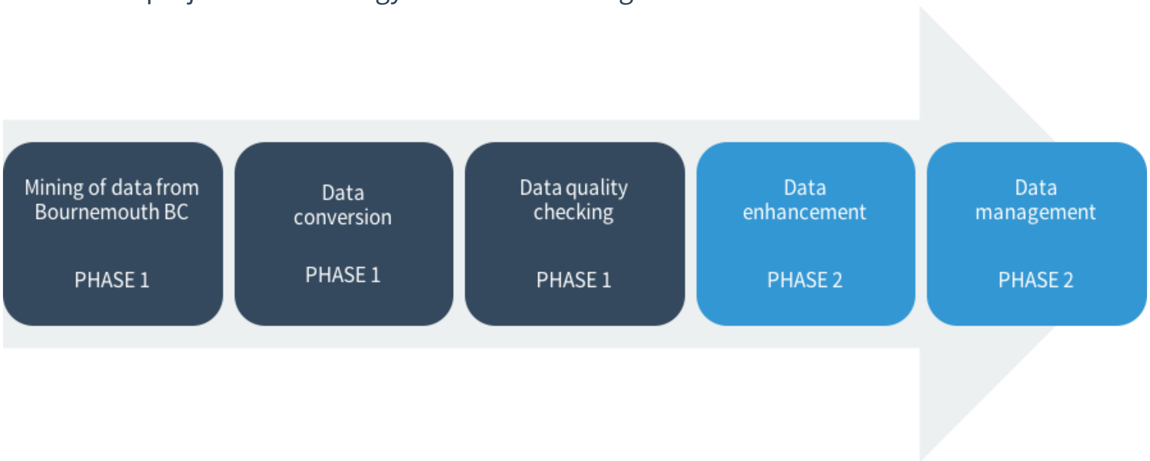

Figure 4-6: Bournemouth data capture project methodology

4.2.3 Bournemouth data

The characteristics of high-frequency radio, with its short range, will significantly affect the chosen location for access points and antennae. A small-cell infrastructure network has to be designed with greater resolution and accuracy, and many site options need to be available for network planners to assess for suitability before they can roll out or enhance a network. To reduce costs, existing infrastructure must be utilised as far as possible, and knowing in advance what is available around the deployment area will significantly improve that process by keeping planning costs to the minimum.

Objects captured were:

- lamp posts, telegraph poles and traffic lights where antennae could be installed to provide street level network coverage;
- telco cabinets, which indicate location of the fixed assets (dark fibre) in relation to street furniture used to locate small cells;
- CCTV infrastructure; in many cases this is connected with fibre optic cables, and moreover CCTV cameras can provide line of sight information which may help to deploy small cells more effectively;

- electricity network infrastructure to provide information on the nearest source of power.

As one of the requirements is to provide mobile coverage along major road and rail networks, we modelled physical road-side structures such as bridges, road signs and gantries (Figure 4-7). Accurate information about the location, size, shape and material of these structures will simplify and improve the planning process and furthermore help network operators to mount equipment on existing structures more efficiently and safely.

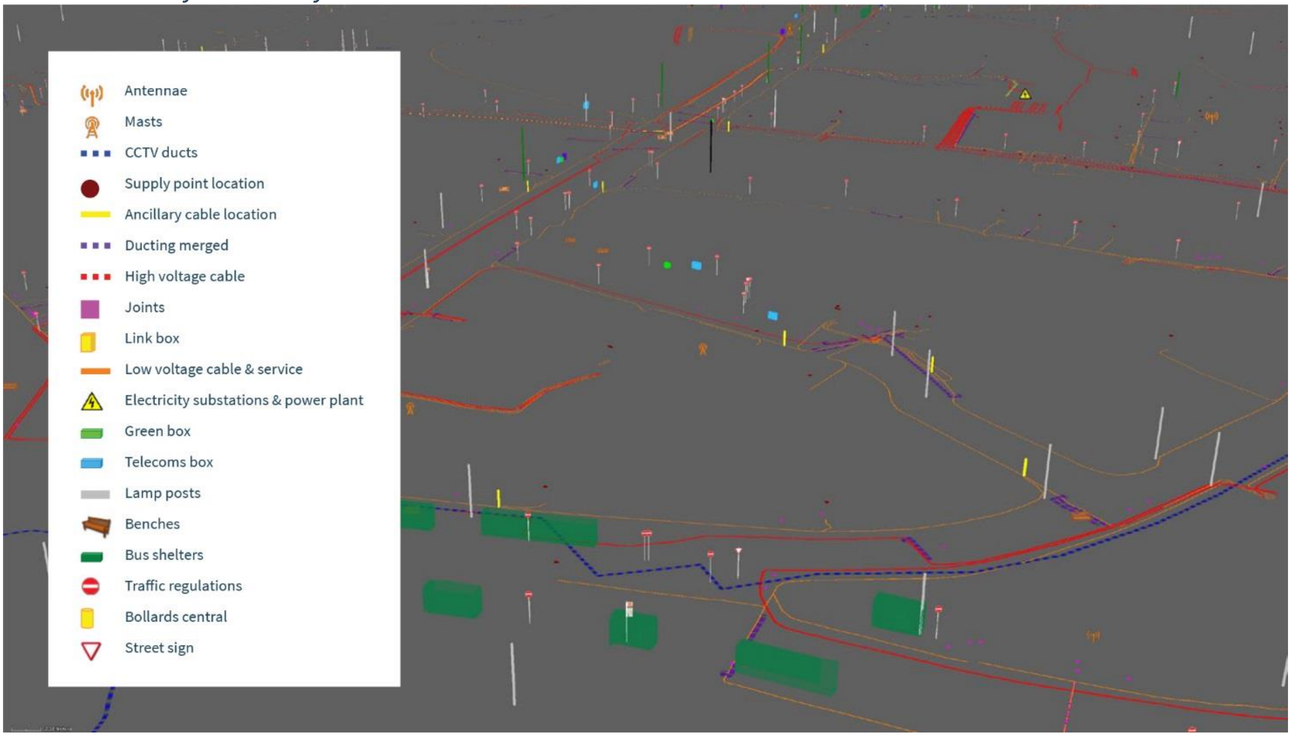

Figure 4-7: An example of network utilities and street furniture modelled within the Digital Model

Bournemouth BC provided further datasets to enhance the model and to enable quality checks against data captured during the survey. Specifically, the data included:

- traffic and parking regulations (traffic lights, street lighting, traffic signs);
- street furniture (bus stops, bus shelters, lamp posts, Christmas decorations);
- telecom boxes and infrastructure;
- electricity networks;
- tree preservation order data;
- walls;
- planning records relating to existing mobile and other transmission towers and masts, fences and CCTV cameras.

Further information on this subject is provided in Annex A.

4.3 How granular do the data need to be?

First, it is important to understand that aerial photography will offer a specific degree of resolution depending on flying height and how the imagery is captured, by NADIR or Oblique. Similarly, mobile mapping can be undertaken at different scan resolutions. Combining these two capture methods allows us to be build a 3D environment at a level of granularity suitable for implementing in the model. Selecting different levels of resolution for each method of capture will allow us to define acceptable granularity for analysis.

The data granularity, or detail, of a 3D model will have an impact on the modelled viewshed of a 5G signal depending on its frequency and associated propagation factors. For example, a simple 3D mesh model is only able to demonstrate a 'top down' result in a visibility analysis, whereas a terrestrial point cloud typically contains fine detail and can yield precise results. Other key parameters are the cost of acquisition and the ability to contain relevant attribution.

The following examples of viewshed analysis show how models built on various data sources perform for an antenna placed on a lamp post with a given 'look' direction, pitch, horizontal and vertical field of view.

1. OS MasterMap Topography Layer with building heights, street asset data, digital terrain model (DTM)

These datasets can only offer a simple assessment of the scene (Figure 4-8). The data do not include complex vegetation or street furniture and therefore may not be suitable for modelling the propagation of high frequency signals.

Figure 4-8: An example of viewshed analysis based on OSMM Topography Layer, digital terrain model and building height attributes. The red colour shows the area where line of sight is blocked by the objects. Green indicates clear line of sight.

2. Digital surface model (DSM)

A DSM will, according to its resolution, depict all above-ground features including buildings and vegetation, and is frequently viewed in conjunction with imagery or raster mapping (Figure 4-9). A DSM offers a 2.5D rather than 3D representation. As it is usually generated from NADIR aerial imagery, obscured features, for instance below canopies, are not represented.

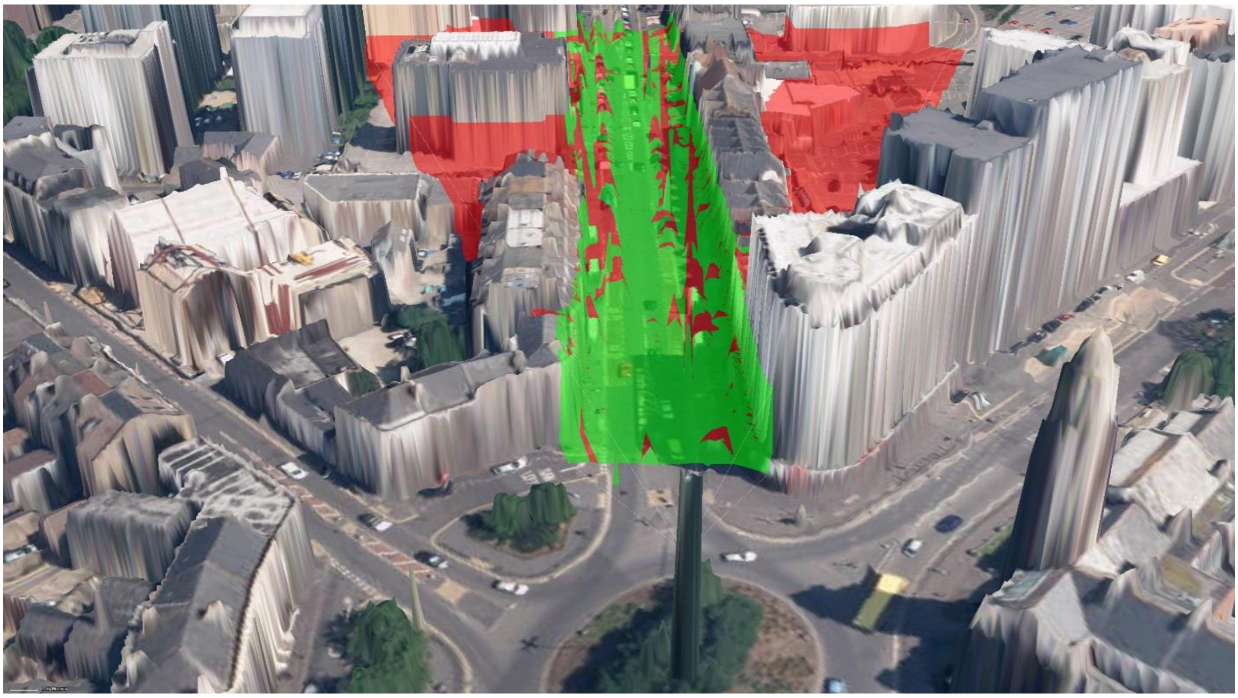

Figure 4-9: An example of viewshed analysis based on a digital surface model. The red colour shows the area where line of sight is blocked. Green indicates clear line of sight

3. Mesh model

Like the DSM, the mesh model shown here is generated from NADIR aerial imagery but can include minor overhangs as it is a 3D rather than a 2.5D model (Figure 4-10).

Figure 4-10: An example of viewshed analysis based on a mesh model. The red colour shows the area where line of sight is blocked. Green indicates clear line of sight.

4. Oblique mesh

A mesh model generated from oblique imagery has a wider effective field of view than NADIR imagery and therefore can generate a more consistent 3D model (Figure 4-11).

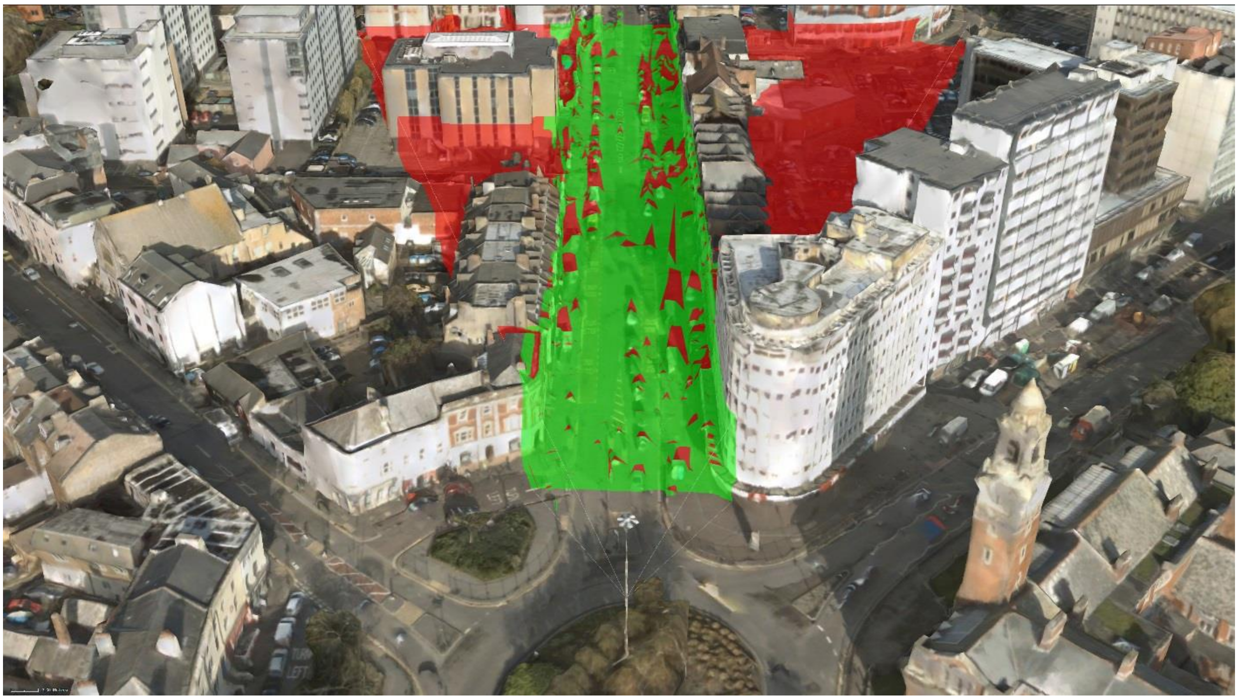

Figure 4-11: An example of viewshed analysis based on an oblique mesh model. The red colour shows the area where line of sight is blocked. Green indicates clear line of sight.

5. Point cloud

Using the same NADIR imagery as used in the DSM and mesh examples, a point cloud can be used to model a scene from a top-down perspective (Figure 4-12). The limitations here are common to all data generated from NADIR aerial imagery, although the visualisation result is not affected by the draping effect of the DSM or mesh where an elevated feature is connected to the ground surface.

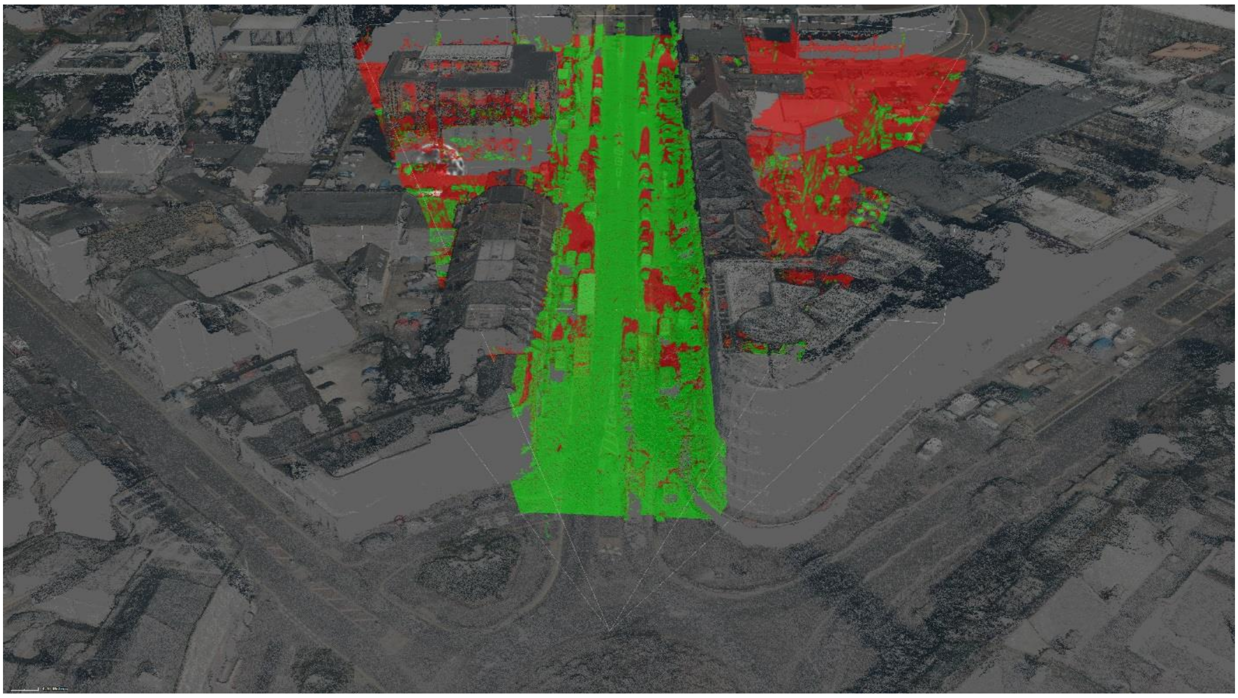

Figure 4-12: An example of viewshed analysis based on a point cloud model. The red colour shows the area where line of sight is blocked. Green indicates clear line of sight.

6. Terrestrial Point Cloud

Point cloud data based on mobile mapping provide a higher level of street-side detail. The scene is more granular as the data are captured close to ground level (Figure 4-13). They enable the analysis of additional features and allow consideration of impacts to a viewshed, for instance from street furniture and vegetation. However, the point will also represent other transient features, such as vehicles and pedestrians, which are not required.

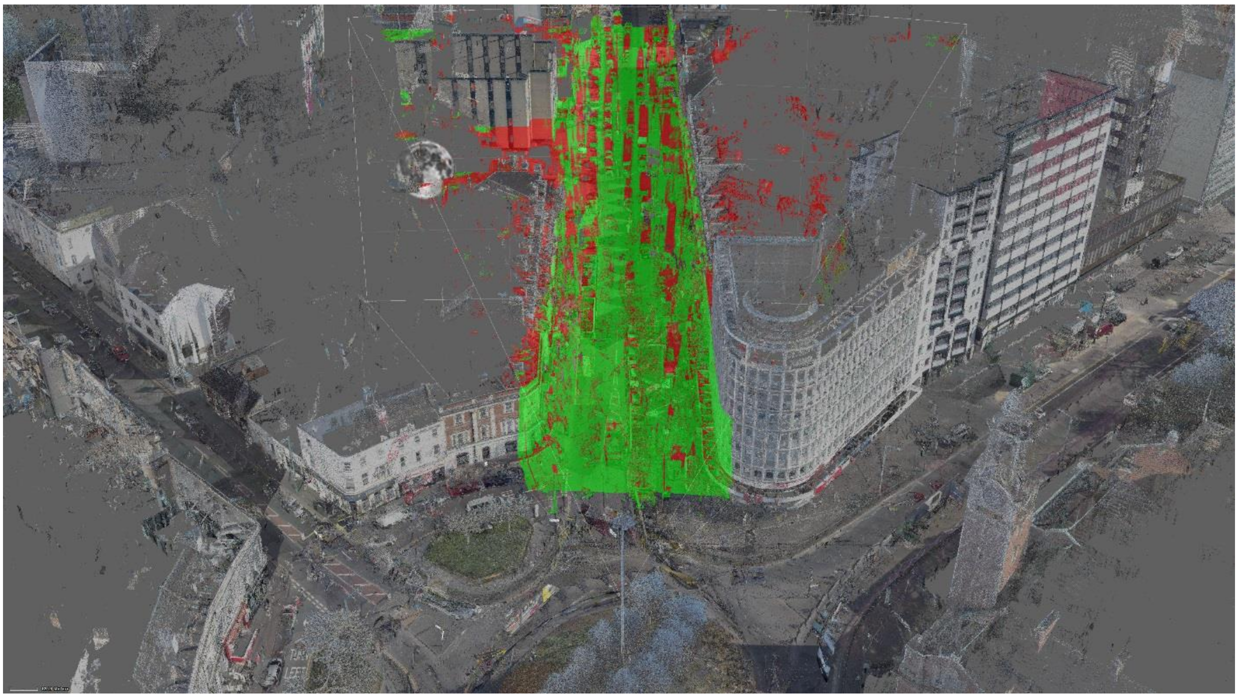

Figure 4-13: An example of viewshed analysis based on a terrestrial point cloud model. The red colour shows the area where line of sight is blocked. Green indicates clear line of sight.

4.4 Constraints and limitations

The software packages used in this process had various data format limitations. However, this did not prove to be a significant obstacle, and in all cases we were able to accept and produce data in the required format.

The data collection task demands a considerable amount of effort and planning, and the effort required to process raw collected data into a usable state can be substantial. This is especially true if the data are to be maintained for use beyond just 5G. The street asset data supplied by Bournemouth BC have been highly valuable, but we found that they contained many omissions and have some significant positional accuracy problems. For more information on this, see Annex A. In particular, the unavailability of telecoms infrastructure meant that new methods of data identification and capture were required.

As OS's conventional remote sensing processes are based on stereo aerial imagery, we quickly discovered that this posed limitations in developing a 3D model. Although stereo image capture methods are adequate for the extracting data to current OS data specifications, much of the data required for 5G planning require further levels of detail. It is nearly impossible to capture features under vegetation and building canopies or in areas of deep shadow. The 10cm resolution of the stereo imagery is such that features with dimensions of less than 30cm are difficult to accurately identify and extract. For this reason, it was decided to employ terrestrial mobile mapping data sources to assist the capture of street-side features.

Our mobile mapping data were collected using 3DLM's StreetMapper prototype, Leica Pegasus 2 and Trimble MX-8 systems.

The 3DLM StreetMapper survey was carried out in an extensive area both on and off the highway including some park and pedestrian areas. The data were processed in conjunction with ground control points, thoroughly tested for accuracy against independent instrumentally-controlled data and are considered good benchmarks for subsequent data capture in the Bournemouth area.

The Pegasus 2 and MX-8 surveys were restricted to the highways only, but both include associated imagery. The advantages are that the resultant point cloud data have imagery embedded and can be used as a 3D picture for easy identification of features. Both datasets are positioned via the on-board positioning/navigation systems and therefore offer a lower level of confidence in positional accuracy.

One factor which should be considered when employing mobile mapping data in understanding the street scene is that of unwanted 'clutter' such as people and vehicles. During this work, we have not had access to available software to achieve the removal of all clutter in the terrestrial point cloud.

4.5 Data processing methodology

During this project we have assessed many datasets from various sources for their value in building the Bournemouth Digital Model. We have sought novel approaches in using these data and developed new methods of data extraction. Data spanning aerial imagery, point clouds and highways inventory data have all been restructured into a single, coherent dataset.

We have assessed data extraction tasks for their potential to be automated, and those that could not be automated have been streamlined. Efficiencies in the use of new approaches to software and data have been considered throughout and in this section. In more detail in Annexes A and B, recommendations are made on where further research could improve processes and eliminate unnecessary procedures.

The results of the data capture, extraction and modelling processes show how the Digital Model has been generated, where issues have been encountered and in some cases solved to produce a 3D model that meets requirements. We have also reached conclusions on how planning processes for data capture can be improved and how future efficiencies might be realised.

ContextCapture software from Bentley utilises both a computer workstation's Central Processing Unit (CPU) as well as the Graphics Processing Unit (GPU) processing, exploiting the workstation's full capacity for extracting a 3D model from imagery. Processing the Bournemouth data block on a single-licence workstation with a suitable configuration took around 8 days. However, once the initial mesh model is created, output data for an entire block can be generated in a matter of hours, depending on the required densities and levels of detail.

The mobile mapping systems were chosen as being good examples of their type. Other systems are available that will generate both imagery and point clouds at a street level and technology in this field is progressing at a rapid rate.

The result is a dense 3D mesh model which represents surfaces with textures at a very high level of detail. Accuracy thresholds can be considered at factor of 3 times the original image pixel size; in this example, the measured point in the mesh is accurate to within 30cm of an independently measured control point, against a source image pixel size of 10cm. Figure 4-14 shows an example of a mesh model created from oblique imagery with oblique camera positions.

Figure 4-14: An example of photo centres for oblique camera positions used to generate 3D mesh model with ContextCapture

There are cloud-based software solutions available which can generate mesh data of similar quality. The benefit of cloud processing is speed. Where a block of imagery may take a week or more to process on a single workstation, the same process on cloud servers can be completed in a matter of hours. However, the process of uploading large images to the cloud may negate this benefit.

Image acquisition parameters have a crucial bearing on suitability for creating a 3D model. The available aerial imagery of Bournemouth was captured at a resolution of 10cm, comprising nearly 500 images and with high redundancy (overlap) both along the flight strip and between flight strips (see Figure 4-15). Redundancy is important factor in determining the value of imagery for extracting 3D data.

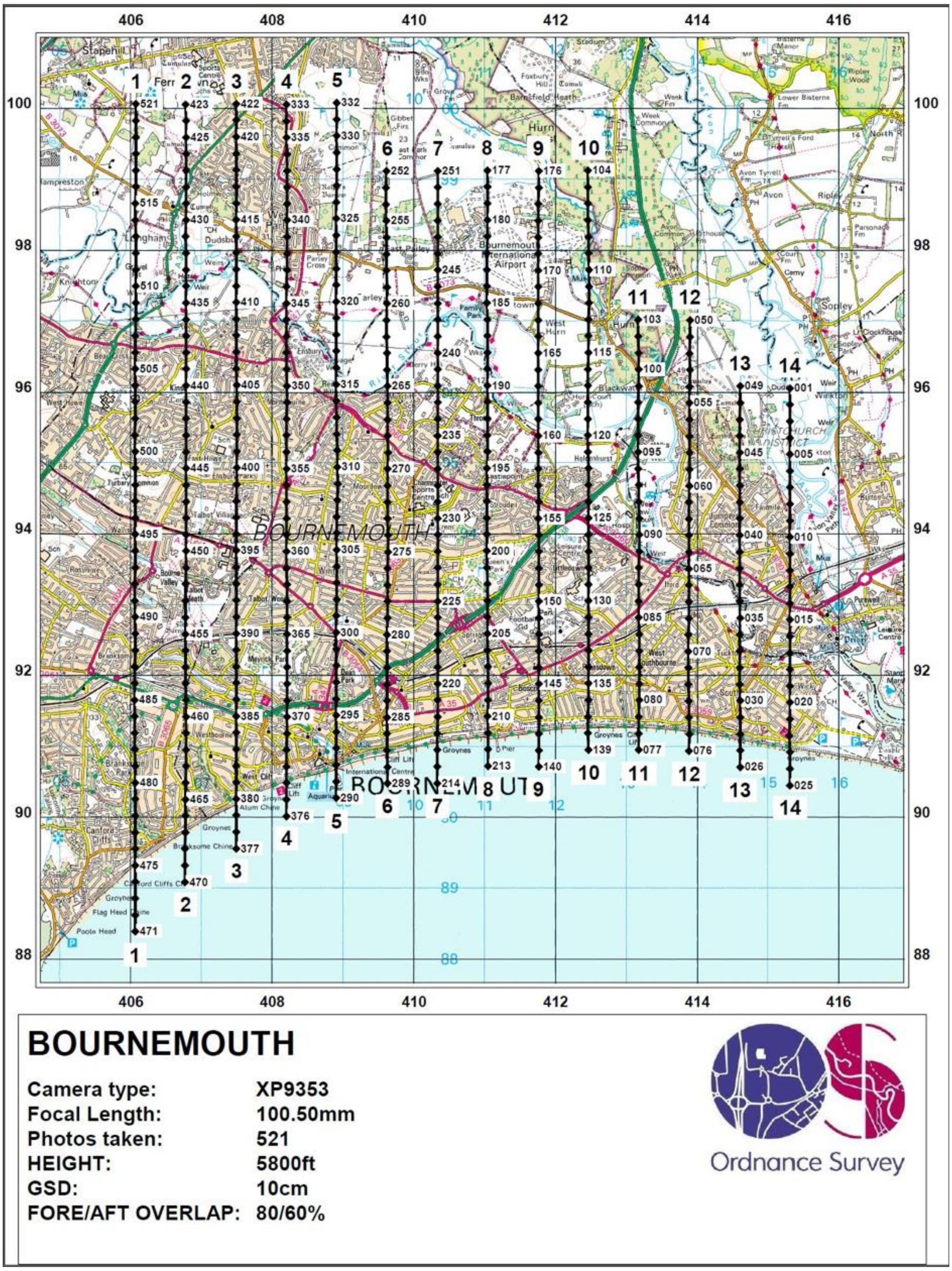

Figure 4-15: Flight plan for capture of Bournemouth aerial imagery

Figure 4-16 below sets out the overall data extraction process.

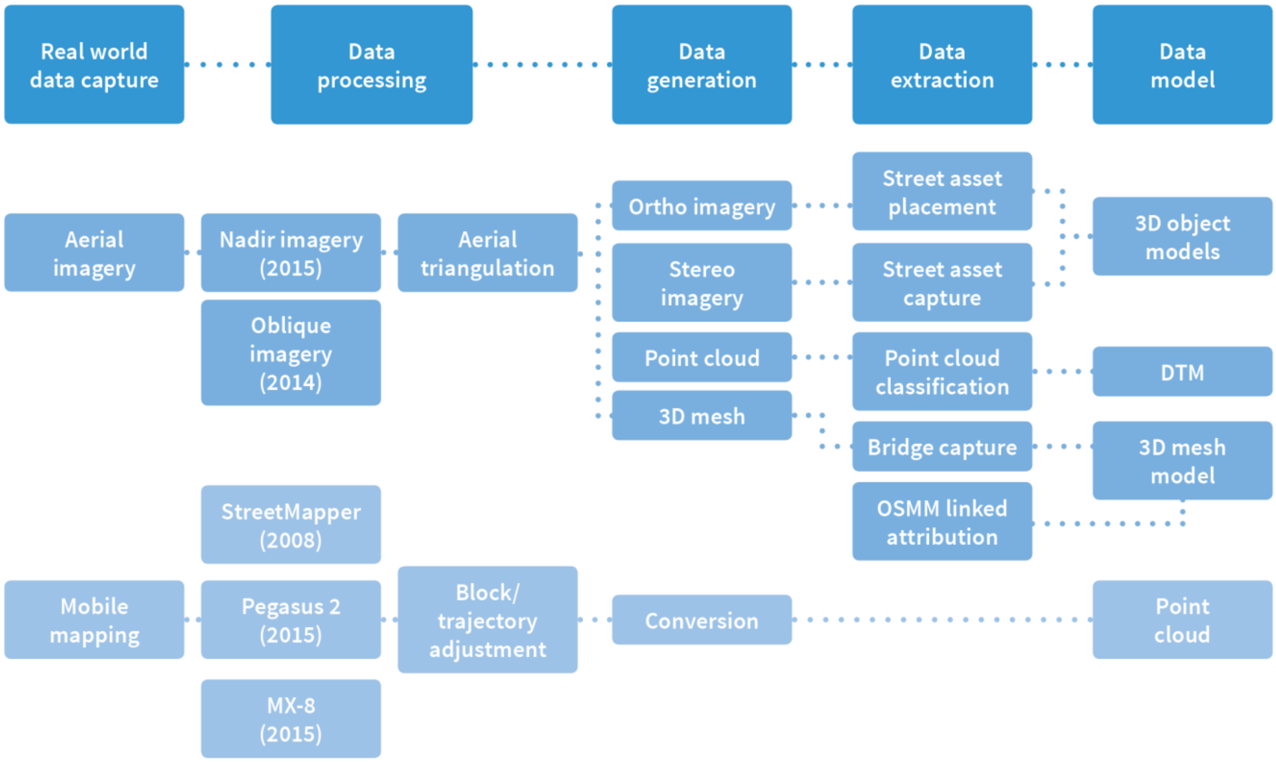

Figure 4-16: Data generation methods

4.6 Challenges experienced in the data capture process

- We experienced complications with data being broken up during conversion from TAB format; some of the data sets were split into several shapefiles, which was impractical.
- The positional accuracy and attribution of some datasets were incomplete and required manual rectification, a highly time-consuming process. For instance, all 4667 lamp post records needed to be repositioned, some by as much as six metres.
- Some Bournemouth BC datasets were incomplete and there was a lack of consistent attribution in the data provided. For instance, only 40% of the available data records for lamp posts contained attribution.
- A significant length of time was spent improving Bournemouth BC data accuracy.
- Mono imagery proved to be inadequate to identify street-side features; stereo imagery is required.
- 3D editing processing time can be lengthy when repositioning features in a point cloud environment and requires high-specification hardware.
- Automation was limited. Some of the data records from Bournemouth BC had random positional errors which made automation difficult and required manual intervention.

In summary, the development of the 3D Digital Model has proved very valuable in identifying which tools and techniques are best to apply and where there are opportunities to automate or seek out alternative solutions. It also brings to light the importance of sourcing reliable and consistent data which may prove challenging across the UK's local authorities.

We believe that automation of manual methods could today yield labour and processing cost savings of around 60%.

This has been taken into account in our calculations when forming the National Planning Guide.

5

5 Meteorological impact on signal propagation

The development of the meteorological component of the tool provided useful insights into the relative importance of different weather elements on future 5G networks. The nature of the interaction of electromagnetic (EM) radiation with atmospheric constituents at these frequencies is complex, primarily because the wavelengths involved are on the same scale as the sizes of the hydrometeors themselves. This means that there is a very strong sensitivity to the details of individual particle composition and shape as well as the assumptions made about the variation of hydrometeor number density with size.

Before drawing the key conclusions of the study on weather in the final part of this section, we found that rainfall is the only significant hydrometeor with any measurable impact on propagation for 5G small cells. Other mitigating factors due to weather are discussed first, namely gaseous absorptions from air and fog and the impact of extreme temperatures.

5.1 Temperature effects

Where there is extreme temperature in a radio communication system, the receiver will always be subject to receiving background noise. In fact, by the laws of physics there is natural background noise in the environment which corresponds to temperature. In warm weather conditions this background noise will therefore increase. The receiver will increase in temperature due to radiation from the sun. The receiver’s temperature will also cause it to add additional noise as well as the background noise that arrives at the receiver. Through studying the data sheets of amplifiers available in bands above 6GHz, the volume of noise added by the receiver does not change by a significant quantity as temperature changes.

Considering both changes in background noise and noise added by the receiver, either at the base station or the mobile device, the difference this makes to signal quality is not measurable. The main reason for this is that the interference that the device will receive from other base stations in neighbouring cells is substantially higher compared to the noise. Any changes in the noise, which are small in any case, are negligible in comparison to the interference which has a more substantial impact on signal quality and will be discussed in Section 6.

5.2 Gaseous absorption effects

The effect of gas and moisture absorptions at frequencies above 6GHz are known and information is widely available in the literature. Figure 5-1 shows the position of the central frequencies on a spectrum of gaseous attenuation, that is, with no cloud or precipitation present. At these frequencies, the primary sources of gaseous attenuation are water vapour and oxygen. The candidate 5G frequencies lie largely within ‘windows’ between these bands, although notably the 70GHz has the highest attenuation due to its position closer to the centre of the oxygen absorption maximum. In addition, Table 5-1 shows the percentage loss to gaseous absorption over different path lengths in each of the frequency bands where it is found that the percentage of power is less than 1% in the majority of frequencies and distances. In the worst-case at 66GHz, it does not rise beyond 10%. Therefore, any impact of absorption is negligible.

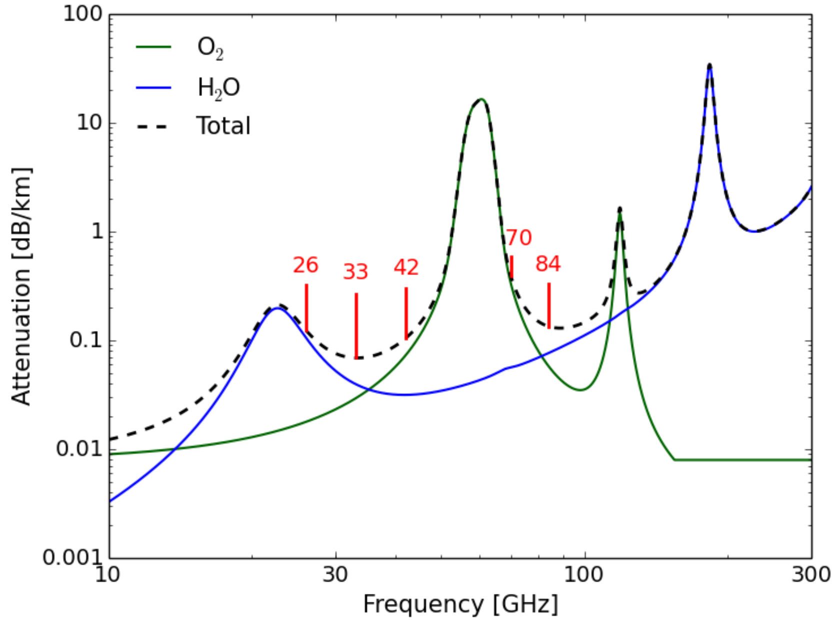

Figure 5-1: The position of the central frequencies of the 5G bands used in this study. The figure shows the attenuation due to the absorption of energy by gaseous water vapour (blue line) and oxygen (green), with the total also shown (dotted)[9]. The vertical axis uses a logarithmic scale representing the fact that the absorption varies with frequency over several orders of magnitude. The positioning of the 5G bands within 'atmospheric windows' (i.e. lower absorption) is clear.

Frequency (GHz)	Power lost at 50m range (%)	Power lost at 100m range (%)	Power lost at 200m range (%)
24.25	0.15	0.30	0.59
25.75	0.12	0.23	0.46
27.25	0.10	0.20	0.39
31.8	0.09	0.18	0.35
32.6	0.09	0.18	0.36
33.4	0.09	0.18	0.36
40.5	0.14	0.27	0.54
42.0	0.15	0.30	0.60
43.5	0.17	0.34	0.68

[9] C.C. Chen (1975), 'Attenuation of electromagnetic radiation by haze, fog, clouds, and rain', Report R-1694-PR for Rand Corporation, 41P.

Frequency (GHz)	Power lost at 50m range (%)	Power lost at 100m range (%)	Power lost at 200m range (%)
66.0	2.45	4.85	9.46
71.0	1.57	3.11	6.12
76.0	1.07	2.13	4.22
81.0	0.34	0.67	1.34
83.5	0.33	0.67	1.31
86.0	0.34	0.67	1.34

Table 5-1: The percentage loss due to the absorption by water vapour and the other atmospheric gases, predominantly oxygen, over three different paths of 50m, 100m and 200m. The values are for the US Standard Atmosphere[10].

5.3 Analysis of rainfall attenuation

This section provides the main conclusions of the study in which rainfall and sleet are found to be the sole contributing factors. Each conclusion is emphasised in bold followed by explanatory text. Before covering the conclusions, the concept of extinction of radio waves is explained and illustrated in Figure 5-2.

The extinction causes attenuation of radio waves with the result that they are weaker than they would propagate through free space where no rainfall is present. The attenuation takes place in two forms: the first due to absorption where the radio is attenuated due to losing energy as heat, and the second case due to attenuation from scattering where some radio waves are reflected or refracted in different directions. Either way, this results in attenuation.

[10] US Standard Atmosphere, 1976. US Government Printing Office, Washington DC.

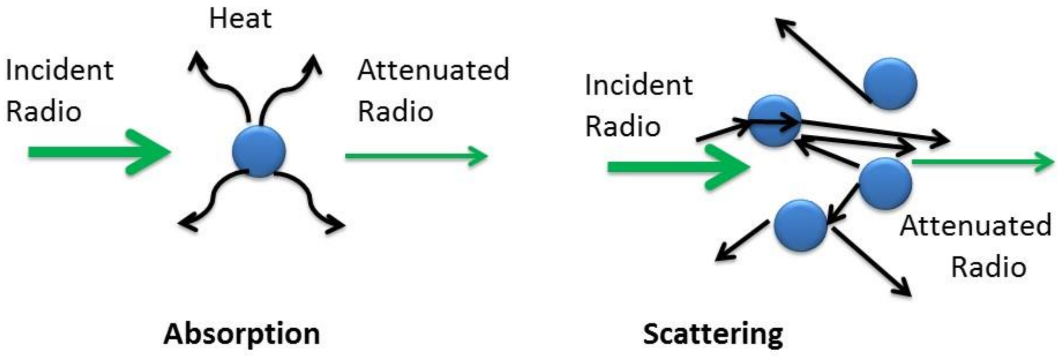

Figure 5-2: The extinction of radiation by rain droplets is due to two processes: absorption and scattering. On the left of the figure the process of the absorption by raindrops is depicted in which the radiation is turned into heat. Scattering by raindrops (on the right) also results in a loss of radiation from the incoming beam as the radiation is being redirected in other directions.

The occurrence of heavy rain in the UK has the potential to significantly attenuate 5G signal strength, even over the relatively short path lengths envisaged due to line-of-sight constraints. The impact is most severe at the higher frequencies (71 and 83GHz).

The primary parameter to describe attenuation is the extinction coefficient k_{ext}. For the purposes of presentation in this report, we have converted this into a more intuitive 'percentage power loss over a 100m path length'. Figure 5-3 shows the 100m loss for the lowest and highest frequency bands for the stratiform case (Storm Angus) and the more extreme London case.

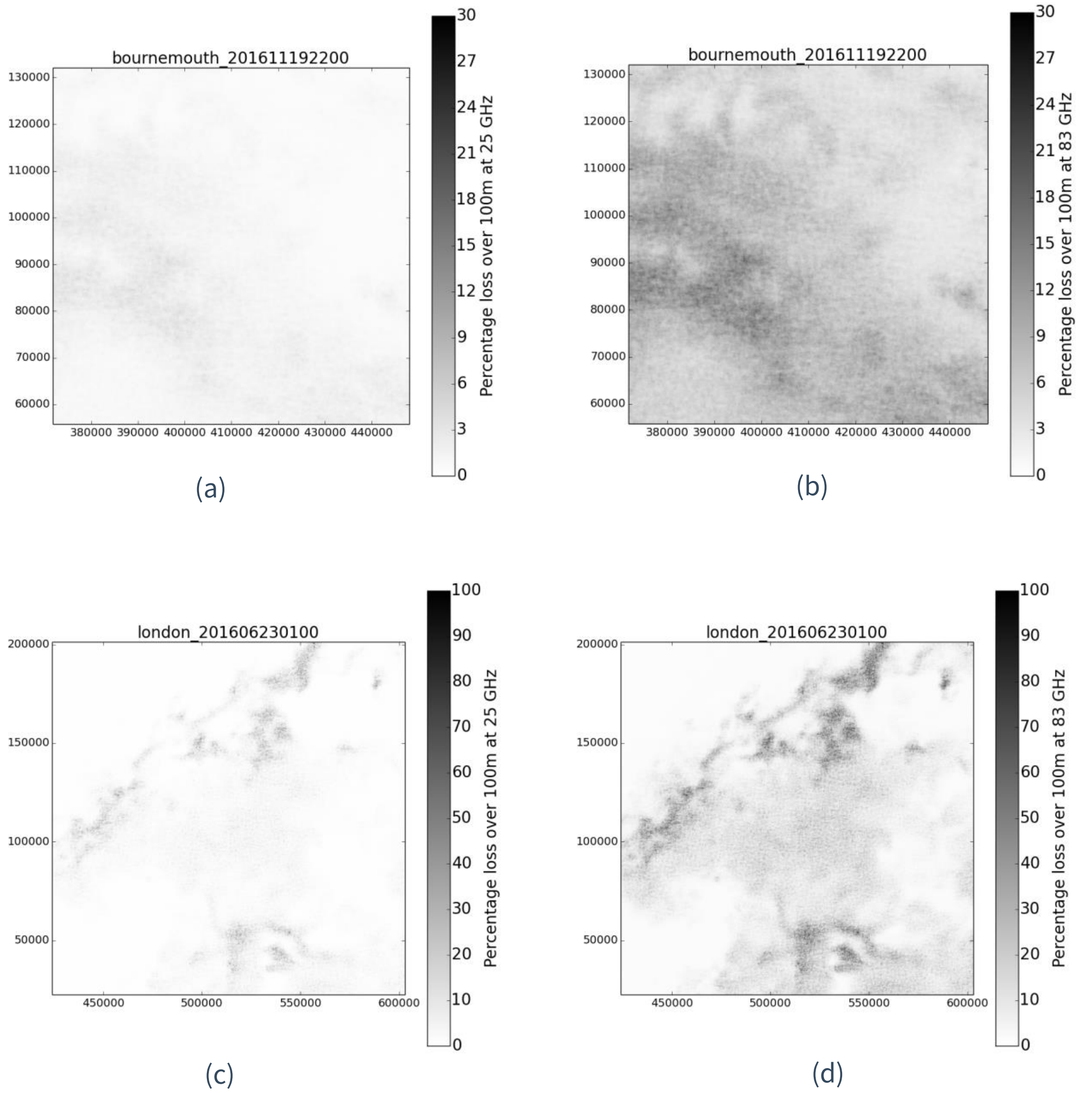

Figure 5-3: Percentage power loss over 100m for the [top Row] Bournemouth Storm Angus case at (a) 25GHz & (b) 83GHz and for [bottom Row] London case at (c) 25GHz & (d) 83GHz. These are the same cases as discussed earlier in this report. Note the physical dimensions of the London case (~200x200km) are twice that of the Bournemouth case (~100x100km) and the colour scale has been changed to accommodate the much larger areas of higher attenuation in the more severe London case.

An alternative representation of this uses cumulative distribution graphs. Figure 5-4 compares the percentage signal loss for the same cases as Figure 5-3 (one line for each plot).

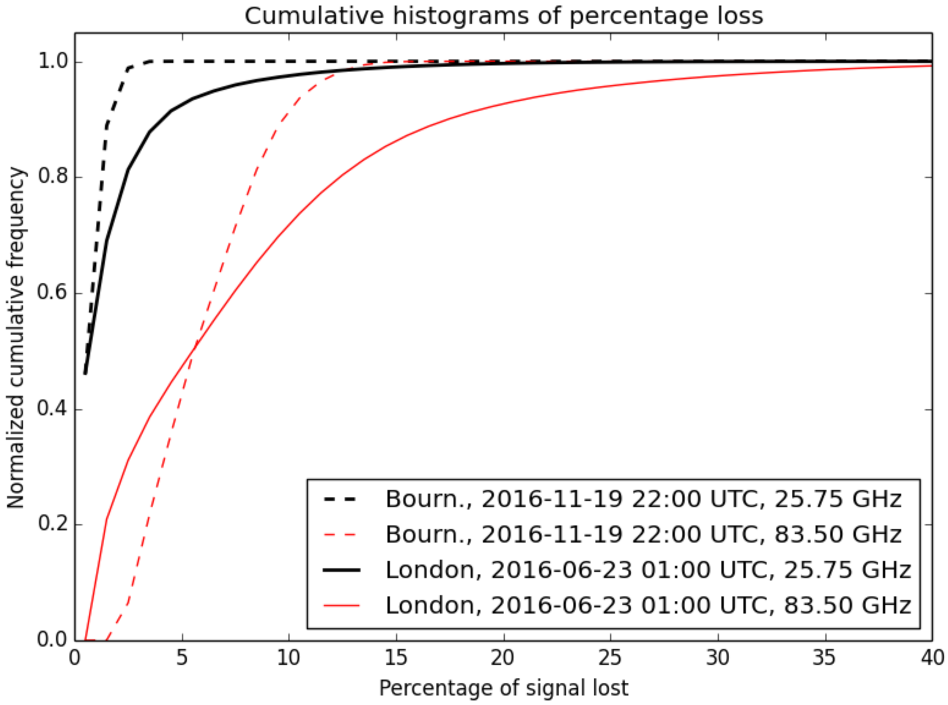

Figure 5-4: Cumulative distributions of percentage signal loss over 100m for the cases in Figure 4-3 above. Thicker black lines are 26GHz, thinner red lines are 83GHz. The plot shows that the more extreme rainfall of the London event produced much greater losses (in fact at 83GHz, some pixels significantly exceeded 40% signal loss). The plot also highlights the point that 83GHz is significantly more attenuating in rainfall than 26GHz.

To further explore the frequency dependency, Figure 5-5 shows the cumulative distribution plot for the London case only, but for all frequencies.

The net implication of these conclusions is that, while future 5G networks will be able to operate in the UK environment, the impact of weather must be factored in to the design to assure an all-weather service at an acceptable capacity, especially to inform the range over which a base station can propagate and that the cell edges will not be shortened in varying seasons.

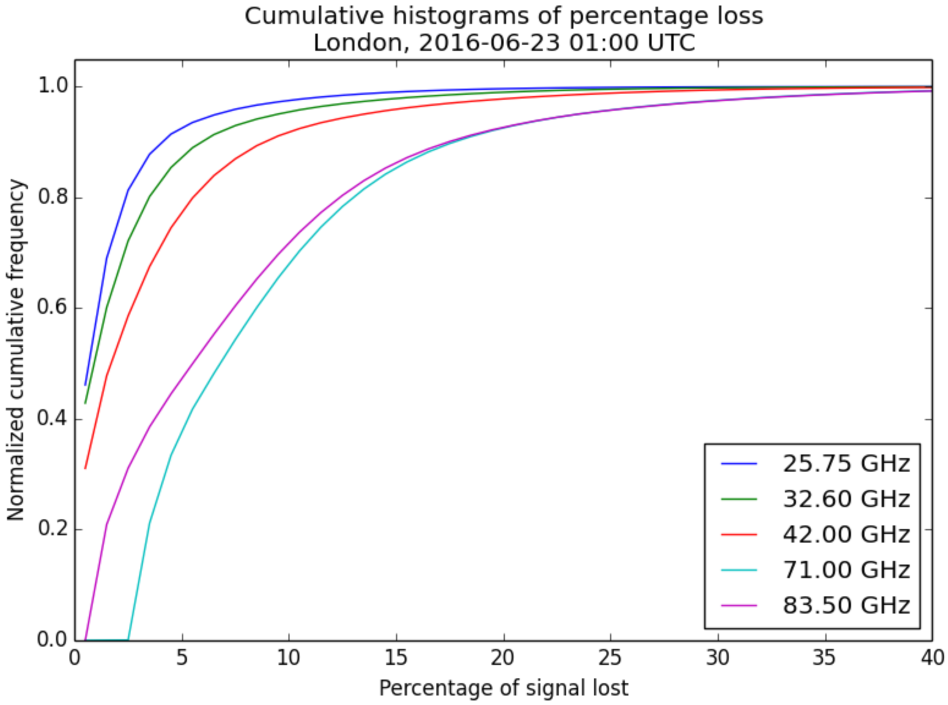

Figure 5-5: Cumulative distributions of percentage signal loss over 100m for the central frequencies of each of the 5G bands. The loss increases with frequency with the exception of 71GHz.

Referring to Figure 5-5, we can see that the 71GHz band undergoes such strong attenuation by molecular oxygen that only at the heaviest rain rates does the 83GHz attenuation become comparable.

It is possible to simulate plausible high resolution (5G-scale) fields of rainfall (and associated meteorological parameters) plus their resultant attenuation values for incorporation into a planning tool for each of the potential frequency bands.

A particular benefit of the work undertaken under the meteorology theme has not only been to demonstrate the magnitude of the potential impact of weather, but to provide spatially self-consistent ‘street-scale’ rainfall fields. These may be used to ‘challenge’ candidate networks in a manner that enables the response of a network to spatially distributed weather to be assessed. Furthermore, the nature of the fast extinction code makes it readily adaptable to any other candidate frequencies with little additional effort.

From a signal attenuation perspective, the weather conditions most likely to have a detrimental impact are (a) summer time severe convection and (b) winter time frontal precipitation in temperatures just above freezing (‘sleet’). Depending on the density of the network in place, the impact of these two phenomena will be markedly different for different 5G bands. In addition, the severity and frequency of occurrence of these phenomena has a strong geographical dependence. This must be factored in to future network design on a region-by-region basis.

The first case of summer time severe convection compared to stratiform rainfall has been demonstrated by the case studies above. Put simply, the atmospheric energy and humidity associated with severe summer time convection enables the generation of large numbers of highly attenuating rain drops, rendering this a sensible worst-case. The study did not attempt to find or define an absolute worst-case.

The second of these 'worst-cases' requires further explanation. The majority of winter time frontal rainfall is the result of large-scale atmospheric motion resulting in the formation of snow at higher altitudes which then falls, melts and reaches the ground as rain (the Storm Angus case). In conditions where the ground level air temperature is just above freezing, typically 0 to 3˚C, snow may be in the process of melting. At this point the melting snowflake (or aggregate, composed of a number of flakes) will be a complex mix of snow, ice and air, potentially with a coating of water around the outside. This makes it appear like a very large raindrop which can increase its extinction efficiency.

This effect is well documented in the radar literature where it is referred to as 'bright band' because, at the longer wavelengths used for rainfall radar, it is observed as a marked increase in radar return. At 5G frequencies the literature consistently notes that this bright band effect will result in an increase in extinction. However, as the wavelengths are comparable to the sizes of the melting particles the degree of enhancement is highly dependent on assumptions of size, shape and the distribution of water within the particle. Note that bright banding does not occur in active convective regions such as the heaviest rain areas in the London case.

From the limited exploration of this effect in this study the impact is understood to be as follows. At the lowest 5G frequency of 26GHz, the signal attenuation may increase by a factor of approximately 6 as rain turns to sleet. At 83GHz this increase drops to approximately a factor of 2. This lower value is because of the non-linear relationship between extinction efficiency and the relative size of the hydrometeor and the wavelength. This peaks near to a ratio of one; as particles get larger they move away from this region.

To make some sense of what that means in practical terms, reference can be made to Figure 5-4 which compares Storm Angus (stratiform) with the London case (severe convection). If we apply a notional doubling of attenuation to the 83GHz Angus case, the cumulative distribution would become comparable to the 83GHz London curve. For 26GHz, the impact is more marked; a factor 6 increase in attenuation would result in a distribution that implies the attenuation may be much more significant than the London case.

To understand the likely occurrence of significant bright band rainfall events (that is, moderate or heavy rainfall), statistics were extracted from Met Office observing sites near to Bournemouth, Swindon and Manchester (as an example of a more northerly city). These stations each provide more than 40 years of hourly temperature and rainfall accumulation. These statistics indicate that in Bournemouth approximately 2.0% of significant rainfall events might demonstrate attenuation enhancement, this figure rising to 3.3% for Swindon and 4.1% for Manchester. The lower figure for Bournemouth might be expected due to its warmer coastal nature.

A conclusion of this study is that it is necessary to explore the potential range of extinction enhancements due to bright banding further, especially with respect to the geographical variation of its frequency of occurrence.

There remains uncertainty in the quantitative relationship between precipitation rate and extinction at 5G wavelengths. This uncertainty must be better quantified if it is to inform network design in cases where the primary driver of network spacing is the weather. In practice, this is likely to apply to situations where typical line-of-sight separations are extended, increasing the length of path travelled through the atmosphere.

As described earlier, the attenuation caused by rainfall in the 5G bands is heavily dependent on the precise distribution of the total mass of the rain across the range of droplet sizes. The attenuation values used within the planning tool were derived using the commonly-adopted Marshall Palmer[11] (MP) distribution. In order to capture the uncertainty introduced by adopting any one distribution, an alternative size distribution assumption has recently been used in the Met Office's numerical weather prediction model (the 'Unified Model', UM). The results are given in Figure 5-6 and show that the choice of MP results in the largest attenuation, with this difference becoming more noticeable towards higher frequencies. A third distribution function, also employed in the UM, lies between these, but closer to the lower values.

All of the candidate schemes represent relatively simple parameterisations of size distribution and their ability to represent 'real rain' is unavoidably compromised as they are unable to represent explicitly the different mechanisms that lead to the formation of the raindrops. A tentative conclusion is that the attenuation values passed to the planning tool most likely represent a reasonable worst-case, with the difference between attenuation values broadly providing a good guide to the uncertainty in these values.

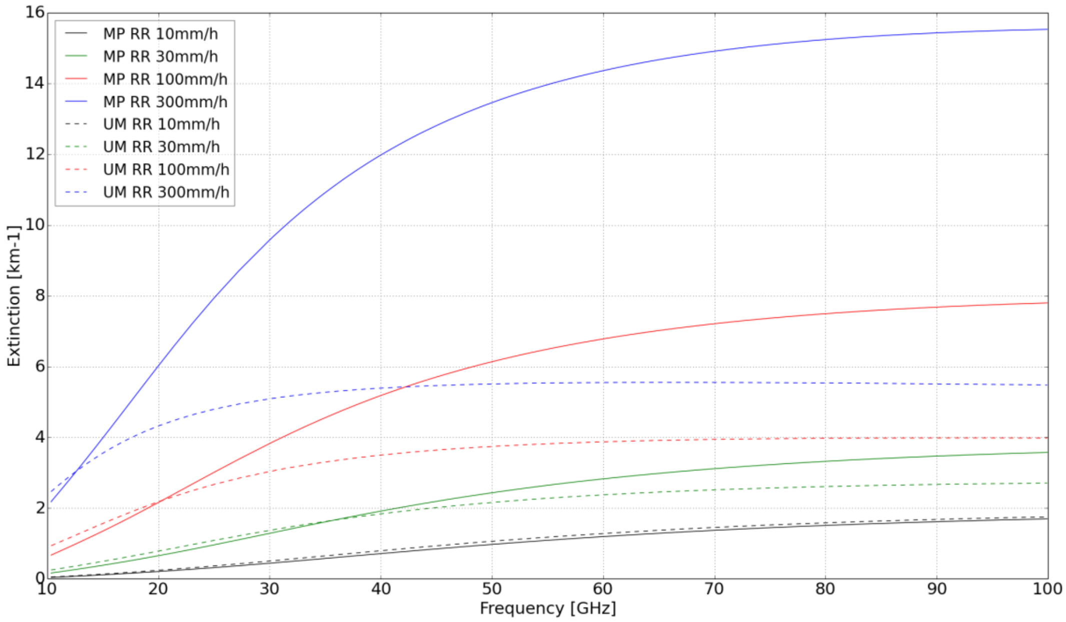

Figure 5-6: The variation of extinction coefficient with frequency for four different rainrates (shown by different line colours) using two different size distribution assumptions (solid=Marshall Palmer, dashed=Unified Model).

An additional source of uncertainty in the attenuation due to rainfall comes from the assumed refractive index of the water in the rain drops. This is a function of temperature. However, in the training of the FRTC a representative temperature of 20°C was used for simplicity. Figure 5-7 demonstrates that, compared to the uncertainty introduced by the assumed raindrop size distribution function, the impact of variable refractive index is relatively small.

[11] J.S. Marshall and W. M.C.K. Palmer (1948), 'The distrbution of raindrops with size', Journal of Meteorology, 165-166.

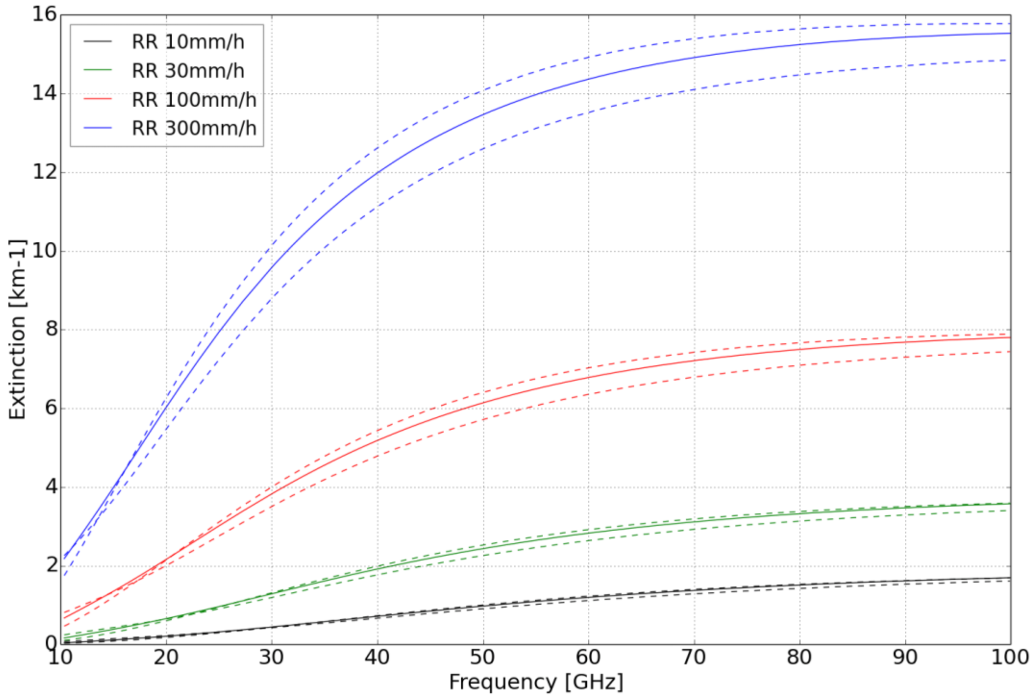

Figure 5-7: The extinction following the Marshall-Palmer distribution plotted for the four different rain rates from Figure 4-6. To demonstrate the sensitivity to temperature, two additional curves for 0 ˚C and 40 ˚C have been added (dashed) to the standard curve valid at 20 ˚C

The implications of these different sources of uncertainty are clear. If the network is to be designed to space assets as far apart as possible, leading to an increased vulnerability in performance due to attenuation by rain (i.e. performance becomes marginal with respect to the weather), it will be important to reflect the uncertainty in decisions regarding the level of investment. With that in mind, we recommend development of a framework to further minimise this uncertainty and then represent it quantitatively in a national 5G planning tool.

6

6 Propagation measurements, predictions and modelling

6.1 Introduction

We established in Section 3 that when a signal propagates from a transmitter to a receiver the electromagnetic waves radiated are subject to a path loss that increases with distance as the receiver moves away and hence the receiver receives a lower power.

Path loss increases at any fixed frequency and distance due to two factors:

- total or partial blockage caused by an object, such as vegetation and street furniture, obstructing the line of sight, known as shadowing loss;
- reflections off surrounding objects, known as scatterers, can cause frequency selective fading.

The propagation measurements carried out in this study are specifically aimed at learning more about how street objects cause loss due to shadowing and scattering at high frequencies. It is also necessary to use measurement data to justify the path loss model adopted in this study as a reliable prediction of the real path loss.

At high frequencies path loss increases rapidly with distance when compared to frequencies below 6GHz and this restricts the size of cellular coverage. However, at the same time, the extent of coverage is substantially increased by using directional radiation patterns illustrated in Figure 6-1. A directional base station is designed to radiate electromagnetic energy in a concentrated direction, in the same way that a torch concentrates light in a single direction, and by doing so it overcomes the path loss and enables more power to be received by the mobile device. This means the overall path loss is significantly less than if an antenna with omnidirectional radiation were used. At the mobile, it is more difficult to implement directional antennae but typically it is assumed to have be semi-directional which means it radiates or receives within a substantial part of a single hemisphere.

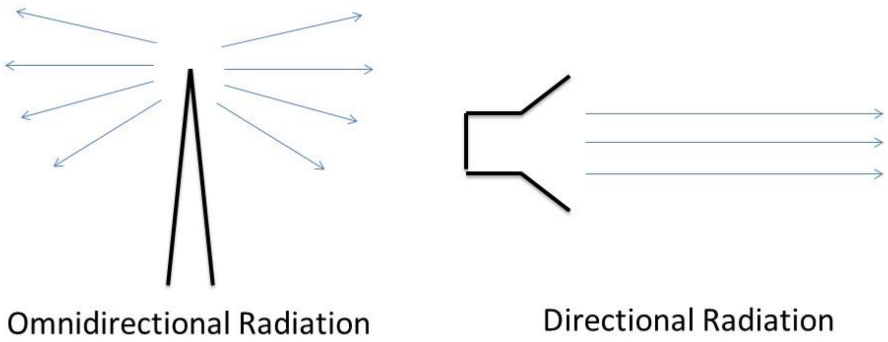

Figure 6-1: Illustration of an omnidirectional and directional antenna radiation

6.2 Assumptions

There are two important assumptions to make in this study when forming path loss models:

- that the cell size does not propagate further than 200m, an achievable range over which a base station can propagate when it has an assumed transmit power of 4W;
- that all propagation is taking place outdoors; the effect of any propagation through buildings or into buildings is omitted from the study. Therefore only the effects of the outside surface edges of buildings along with vegetation and street furniture are considered in terms of how they impact propagation.

6.3 Path loss modelling framework

There are broadly two ways of modelling path loss, outlined below.

The first is to use deterministic or physical modelling based upon physical parameters such as distance, height, antenna specifications and frequency. The path loss model is then applied as a mathematical formula which takes these physical parameters to form a path loss value. This method is reliable in that it can give clear indications of how path loss changes when a mobile moves from one point to another and it therefore achieves high accuracy. This can, however, come at the cost of complexity, particularly where reflections off walls, ground and street objects are considered. The deterministic model then needs to consider the angles and points at which the reflections happen and the material properties to determine how much power has been lost after the reflection has taken place. Therefore the greatest disadvantage of a deterministic model is the complexity and inevitably cost to obtain the appropriate data sets. However, the savings from having such accuracy in cell planning before going to site deployment and testing is highly beneficial.

The second method of determining path loss is to use an empirical model. In this instance, extensive measurements are carried out where data points are made of path loss at a given distance between the transmitter and receiver. By obtaining several samples of data, a line of best fit can be formed within the data to form a simple linear equation to describe the path loss. It is described as empirically reliable if it is based upon results from extensive measurements. An empirical approach for this study is not appropriate because such extensive results are not possible to form within the scope of the project, nor are sufficient results available to date. More importantly, the change in path loss from one point to another over a distance of less than 10m is not reliably predicted.

This study therefore takes a deterministic model approach. The model is simplified so as to not have to model the precise reflections off every object. A simplified approach is taken which sufficiently demonstrates how objects in an open street will impact the propagation and coverage of a small cell.

If we assume perfect free space conditions between the transmitter and receiver (i.e. no buildings, no ground, no street objects) then by the laws of physics, the received power would decay proportional to $1/r^2$, where r is the distance between the transmitter and receiver. As frequency increases, since the power decays more rapidly (as the path loss increases more rapidly) over distance, the proportionality constant will decrease with an increase in frequency. An alternate way to consider this is that the path loss is proportional to r^2 since the received power decreases as the path loss increases. Based on this proportionality, a simple mathematical equation can be derived to obtain the path loss for any distance and frequency.

In practical scenarios, there are no perfect free space conditions. It is therefore necessary to consider reflections off the ground and off the edges of buildings that can cause the received power to be higher than would be the case in free space, while at other times it can be substantially lower. This is entirely dependent on the position of the transmitter and receiver in relation to the buildings and ground.

In our case, we will assume that the mobile receiver is typically positioned inside a street and that there are buildings either side, as illustrated in Figure 6-2. The three electromagnetic waves and the line of sight (which is not shown for the purpose of clarity) will superimpose on each other and, depending on the position, they could add together constructively because the maxima and minima points of all the waves are closely aligned (this is known as 'in phase'). On the other hand, the maxima of two waves could be aligned with the minima points of the other two waves causing them to add together deconstructively (known as 'in anti-phase'). Where waves add constructively, the received power will be greater than that of free space, while in the deconstructive case the received power will be substantially less, possibly even zero, though this would rarely be the case.

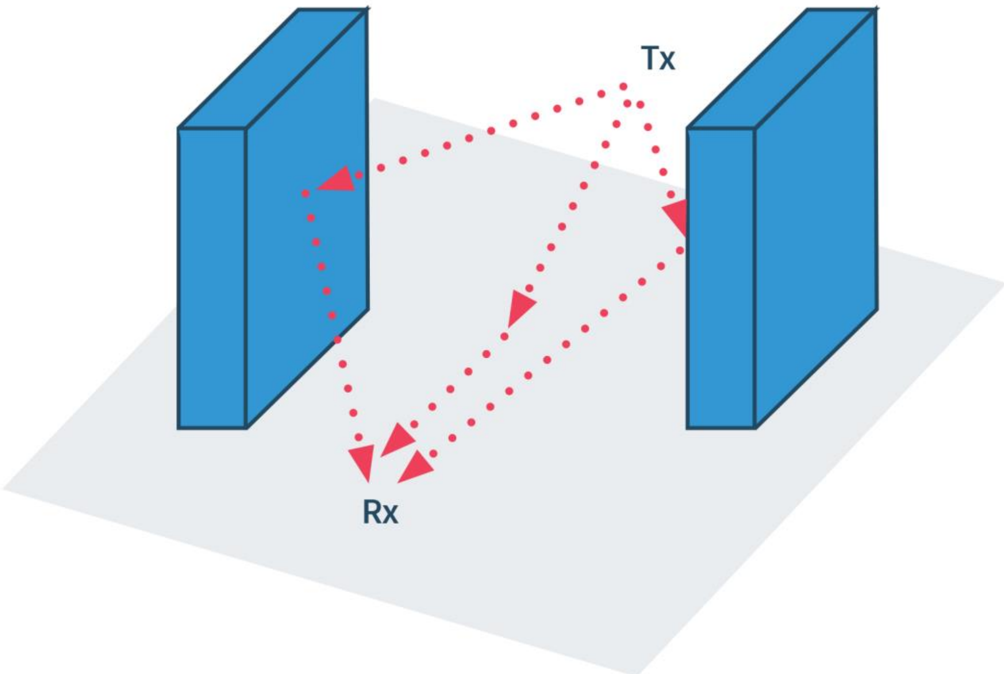

Figure 6-2: Illustration of a four-path model from the transmitter (Tx) to the receiver (Rx) where there is a direct line of sight (not shown) and three other reflected paths off the ground and two side buildings

Modelling the four paths for every mobile position as a fully deterministic approach is complex and not desirable to implement. For our purposes it is important to know how much lower the received power could be in most cases. We define 90% of cases as the threshold. As such, it is important to determine the maximum possible path loss, and extensive simulations were carried out to determine this. The instantaneous path loss is dependent on the position of the mobile in relation to the ground and buildings and whether there are two buildings, just one building, or no buildings. Furthermore, the material type of the buildings and the roughness of the surface of the buildings would affect the reflected paths. In this study, measurement data were analysed which used directional measurement antennae on a rotating turntable to verify that where no street objects are present, these four paths are a suitable basis on which to model the path loss when the antennae at the transmitter (Tx) and receiver (Rx) in

Figure 6-2 are assumed to be omni-directional. The effect of the antenna patterns at the Tx and Rx are added at a later stage.

From undertaking extensive simulations of the path loss for different Tx and Rx positions, as well as different material types for the building and ground, and considering whether buildings are present or not, we found that by setting the precedent for 90% of cases, the path loss can be up to 40% greater than that of free space path loss. The received power is therefore computed based on the model used for free space, but it is made 40% greater since it is more appropriate to overestimate the path loss by an acceptable margin than to underestimate it. This amount of uncertainty is acceptable to analyse the impact of objects in the built environment on propagation which is the purpose of this study and it does not impact the ability to deliver the minimum required data rate over 200m.

It should also be noted that the propagation from the Tx to Rx is reciprocal. In a communication system, it will be necessary for the mobile to transmit information back from the Rx to the Tx. The path loss from the Rx to the Tx is exactly the same as from the Tx to the Rx. Therefore, the propagation is reciprocal and it is only arbitrary that the base station is considered as the Tx while the mobile is the Rx.

Now that a base path loss model has been established, the extra loss due to street objects obstructing the line of sight and causing scattering and frequency selective fading is analysed from the measurements documented in the subsequent sections.

6.4 Diffraction and penetration loss of geospatial objects

The presence of street furniture will cause obstruction or possibly blockage to the line of sight at high frequencies depending on its size. Such obstructions or blockages will either substantially attenuate the signal such that it cannot meet the necessary bit rate requirements for communication or prevent any communication at all. Examples of street objects are shown in Figure 6-3. Their width or diameter will have different impacts on the propagation of a signal where the line of sight is obstructed. Note that the obstruction from tree trunks is different to the loss due to foliage. This is discussed in the next section. It is necessary to ascertain how large objects must be to cause a substantial impact on the propagation at 5G frequencies. The impact on propagation of such objects to signals below 6GHz is small and ignored. The lack of existing knowledge for 5G frequencies spurs detailed analysis of the effect of obstruction size.

Figure 6-3: Photographic examples of street objects which cause obstruction or blockage

The loss through glass such as in bus shelters illustrated in Figure 6-3, will be subject to a penetration loss which will depend on the material properties of the glass in the bus shelter, or the bill board mounts installed within it. To ascertain a general expected penetration loss in a bus shelter, it is found empirically by carrying out measurements where the transmit antenna is placed at a distance from a bus shelter radiating over its façade, while the receive antenna is first placed in front of the bus shelter to take a reference measurement and then placed inside the bus shelter, as illustrated in Figure 6-4, to evaluate the extra loss that results from doing so.

Performing the measurement in this way enables the possibility of evaluating the loss when the line of sight is incident on the bus shelter at any angle determined by the height of the base station. Measurements were taken at several points in the bus shelter to ascertain the variation in loss at different positions, particularly where a billboard is installed as shown in Figure 6-4.

Several measurements were taken in a bus shelter at the 24.25-27.50GHz, 31.80-33.40GHz and the 55.00-60.00GHz bands, through which the expected penetration loss could be extrapolated to the 66.00-76.00GHz, 40.50-43.50GHz and 81.00-86.00GHz bands. In both sets of measurements, an antenna with semi-directional radiation within half a hemisphere was used inside the bus shelter. This is necessary to reflect the expected radiation pattern at the mobile terminal and its susceptibility to several rays reflected off the metallic structures in the bus shelter. Hence the overall loss will be the result of both the penetration through the glass in the bus shelter and also the scattering loss.

Figure 6-4: Propagation loss measurement through a bus shelter

Measurements show that the overall loss is highly dependent on the point at which the line of sight propagates through the bus shelter. An example of two distinct cases is shown in Figure 6-5 where at point A, the line of sight propagates through the glass and the loss is lower. On the other hand, the propagation loss at point B is blocked by a metallic billboard structure which will substantially increase the loss. It should additionally be noted that measurements observed similar loss for other small blind spots in the bus shelter where the line of sight was blocked by the metallic skeleton structure shown in blue in Figure 6-4. Where a base station is high enough such that a line of sight could penetrate through the roof of the bus shelter, the same signal blockage effect would occur as found with the billboard blockage in case B. However, not all bus shelters are constructed in this way and may have a transparent ceiling.

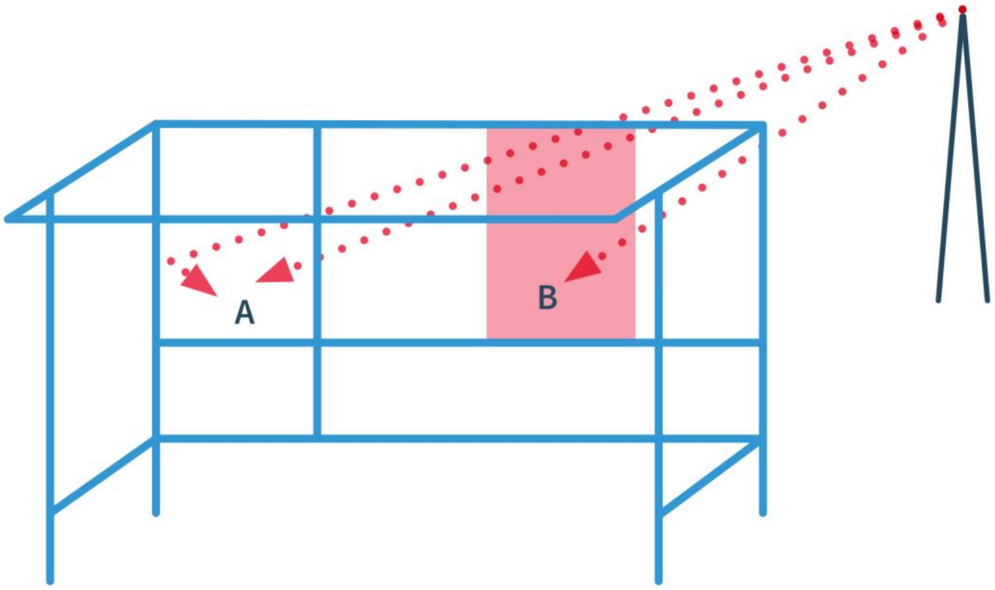

Figure 6-5: Propagation loss scenarios in a bus shelter. Scenario A: penetrating through glass with some scattering. Scenario B: blockage from a large metallic object in the bus shelter.

Table 6-1 shows the average percentage loss measured at the bands of interest where results have been distributed into scenario A and B as shown in Figure 6-5. Clearly, the impact of the metallic blockages causes in scenario B a loss of power exceeding 90%, which would require alternate base stations without a line of sight obstructed in this way to allow a communication link. This would be the case regardless of frequency. In scenario A, the loss is not as severe to the extent that it could harm a communication link but it is frequency dependent from which it is expected that the power lost could range from 75% at 24GHz though to 90% at 86GHz. From these results, it is evident that there is a requirement to know the structural form of the bus shelter to ascertain where obstructing items such as billboards or metallic planes would cause additional losses.

Frequency Range (GHz)	Scenario A (%)	Scenario B (%)
24.25-27.50	76	96
31.80-33.40	76	96
55.00-60.00	84	99

Table 6-1: Percentage of power lost due to penetration losses in a bus shelter in scenarios A and B

Other street objects illustrated in Figure 6-3, which are considered as vertically orientated cylindrical or planar structures, will be subject to a propagation phenomenon known as diffraction. The concept of diffraction is illustrated in Figure 6-6. Traditionally, communication systems have been subject to what is known as knife edge diffraction. Where electromagnetic waves propagate towards a knife edge, which could be the roof of a building or a hill top, the remaining waves above the lip of the edge will continue to propagate but they will change direction. This allows some propagation into the shadow region, albeit with substantial loss, since the waves below the lip will not propagate through. Knife edge diffraction can also be applied to electromagnetic waves propagating around a building when reorientated.

Knife edge diffraction occurs where the diffracting object is so large that it can be assumed the diffraction only occurs around one edge such that the diffraction around the other edge is negligible or non-existent, as shown on the left-hand side of Figure 6-6. A new concept formed in this work, defined as shield edge diffraction and shown on the right hand side of Figure 6-6, occurs where the diffracting object such as a lamp post or tree trunk is narrow enough that comparable diffraction will take place around both sides of the object. It is of course assumed here that the diffracting object is so tall that there will be no knife edge diffraction over the top of it. For frequencies below 6GHz, such diffraction has been unnecessary to model since the effect is not measurable, but in the case of high-frequency signal propagation, a new shield edge diffraction model has been derived and validated by measurement in this study. An example measurement of the shield edge diffraction is shown in the case of a lamp post in Figure 6-7.

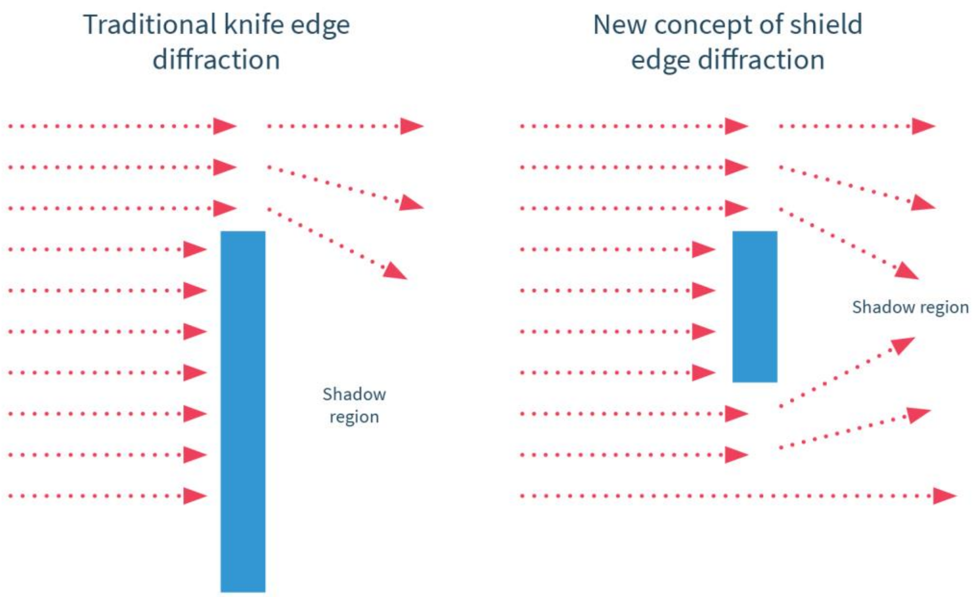

Figure 6-6: Illustration of the concept of the traditional knife edge diffraction and the new concept of shield edge diffraction

Figure 6-7: Example measurement of shield edge diffraction from a lamp post

Measurements were carried out at 11-17GHz and 22-33GHz to validate the shield edge diffraction model derived in this study. Good agreement was found for both these frequency bands; it proves the model to be valid for all frequency bands of interest. Subsequently, it is possible to use the model to derive the minimum width at which a diffracting object will have a significant impact on the path loss. The effect is illustrated in Figure 6-8 where the percentage of extra power lost (in addition to the path loss) is plotted against the width of the shield diffracting object. It should be noted that there are two important assumptions set in terms of the results generated here.

First, the diffracting object is 10m away from the source, while the receiving mobile is 90m away from the source. This is considered as a suitable worst-case scenario which could be further worsened if the mobile extended to 200m from the base station but the change is negligible. Therefore, a more typical cell size of 100m radius is assumed in this scenario where a diffracting object is assumed to be at least 10m from the source and the impact would be greatest in proximity to it.

Second, it is also assumed the source antenna is directive. This means that due to the directive radiation, the diffracting waves become weaker than if the antenna were less directive or omni-directional. It is therefore important to include the effects of a directive antenna in the model to account for the extra loss caused.

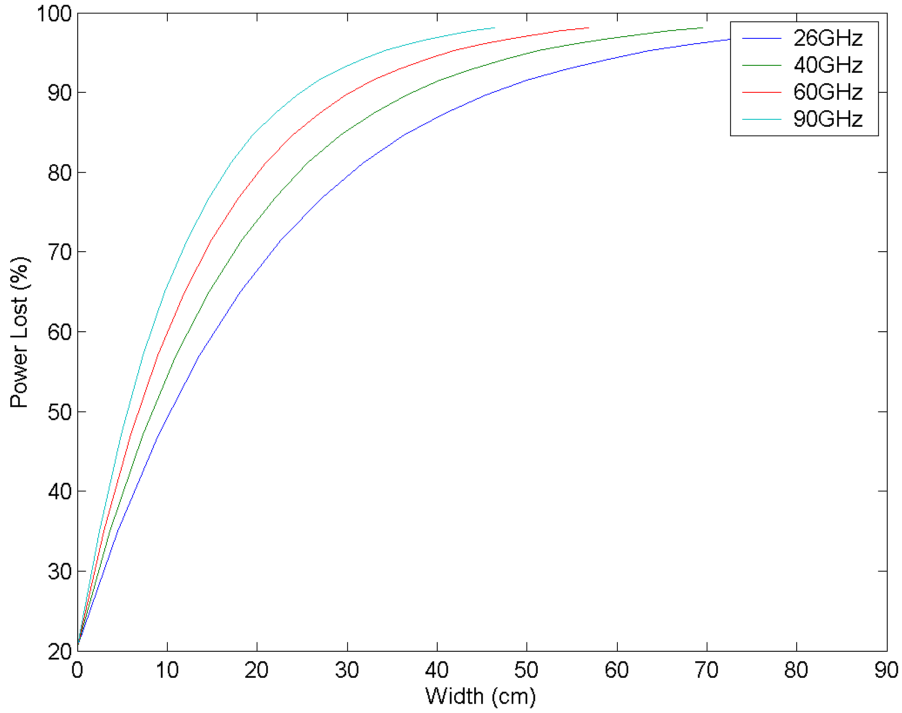

Figure 6-8: Plot showing the effect of the width of street furniture on the percentage of power lost due to shield edge diffraction for fixed frequencies

By taking figures from the plot in Figure 6-8, Table 6-2 shows the minimum width in cm that is required to cause additional power loss of 36%, 50% and 90% at the four frequencies. Where 36% of power is lost, it would be expected to have a small impact causing loss of data throughput from the base station to the mobile of less than 0.5Gbits/s based on the signalling schemes used in this study and assuming there would be a strong signal delivering over 1Gbits/s without the obstruction. With 50% or more power loss the impact would be more severe at which point the data rate is at risk of falling below 1Gbits/s. A 90% loss would lead to signal blockage in the majority of instances.

Frequency (GHz)	36% Loss Minimum Width (cm)	50% Loss Minimum Width (cm)	90% Loss Minimum Width (cm)
26	4.55	9.64	45.59
40	3.67	7.77	36.76
60	2.99	6.34	30.01
90	2.44	5.18	24.51

Table 6-2: Comparison of the minimum width that would cause power losses of 36%, 50% and 90% due to shield edge diffraction in a severe case scenario where the diffracting object is 10m from the base station and the mobile is 100m from the base station

On the basis of using 50% power loss as the threshold, geospatial objects in excess of 9.64cm (approximately 10cm) width are going to be of concern at 26GHz, while this reduces to just 5.18cm (approximately 5cm) at 90GHz. Though the typical width of a lamp post may be less than 10cm for 26GHz, this does not mean that knowledge of lamp posts as geospatial objects can be ignored at this frequency. On the contrary, many lamp posts would contain other objects on them such as road signs and bus timetable information which would exceed such widths. It is therefore of paramount importance not only to know the location of lamp posts but the specification of what is attached to them in terms of their width, orientation and at what height they are positioned. Their actual impact can then be analysed. This problem is exacerbated at higher frequencies where the width requirements reduce.

6.5 Vegetation loss

Traditionally loss from vegetation has been concerned with large trees which can cause substantial loss to satellite communications. Their effect at frequencies above 6GHz has been studied in detail. Further measurements have also been carried out in the terrestrial case at high frequencies to account for the loss through trees with varying levels of foliage. For small cells, many streets and open areas will have small items of vegetation such as hanging baskets and street plants and hence measurements were carried out on samples illustrated in Figure 6-9 to compare plants with and without different foliage.

Bay Tree Ficus Willow Conifer Bamboo

Figure 6-9: Photograph of the five sample items of vegetation used in the study

The measurement setup, undertaken in an anechoic chamber, is illustrated in Figure 6-10. The setup involved placing the item of vegetation to be tested between a transmit and receive horn to measure the loss directly. The measurement for each sample was repeated several times by partially rotating the vegetation under test to see how the loss changed as the position of the leaves and branches would inevitably change randomly as vegetation was rotated.

From this an average loss could be determined and evaluated against the chosen vegetation loss model, which was found to be sufficient for smaller items of vegetation. The bay tree and ficus plants were found to have higher losses as they have dense foliage while the willow has low loss with no foliage. The conifer and bamboo cases, on the other hand, were found to be similarly low loss to the willow due to the fact they have a low foliage and their leaves have considerably lower water content and smaller size, which makes a significant impact on the propagation through them. Therefore, a model for vegetation with high and low foliage is necessary as a best fit against several measured results. The chosen model[12] in this case that was used is shown in Figure 6-11 where it was found that the measured data was in line with the line of best fit that is plotted for both leaf and no leaf cases.

[12] The model selected was the COST 235 Vegetation Loss Model suited for above 9GHz.

Measurements were carried out for validation from 22-40GHz as well as 50-67GHz to verify that the chosen model was suitable for small items of vegetation in a street environment. It should be noted that for the no leaf case the graph shows that there is less power lost when the frequency increases. This does not necessarily reflect the reality in the physical case where a line of best fit has been used. However, the loss is not very concerning in this case as less than 30% of the power is lost. For the case where there is foliage, the loss is consistently at 90% across the frequency range.

Figure 6-10: Photograph of a bamboo plant under test for vegetation loss

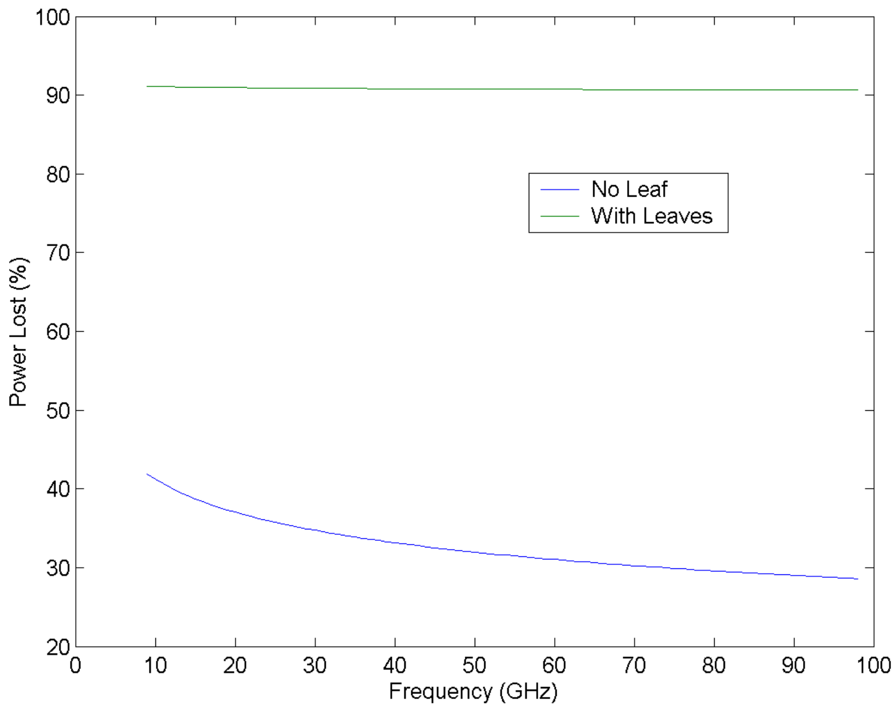

Figure 6-11: Plot of percentage of power lost vs frequency for the vegetation loss model with and without leaves for a width of 0.3m

It is clear from results presented that regardless of the season, small items of vegetation greater than a width of 12cm with substantial foliage will cause disruption to propagation above 6GHz consistent with the findings for shield edge diffraction. The difficulty with using vegetation is that the loss for a given width of foliage is never consistent due to the random position of the leaves. It is therefore the case that planning with vegetation will be down to crude predictions of their effect especially where small items of vegetation are present and the system will require some margin to accommodate errors.

6.6 Scattering loss from building surfaces

In the scope of this work we have assumed that there are no base stations installed inside buildings. Even in the case that there are, the penetration through windows and walls would be sufficiently great that any mobile device near to a wall would have to rely on an outdoor base station. In the worst-case scenario, the mobile antenna with semi-directivity may not be facing the base station but the building in which case the communication link must rely on the reflections from the surface of that building.

With the small wavelengths above 6GHz, there are different kinds of surface roughness that will cause significantly different scattering. The scattering concerned is known as diffuse scattering and illustrated in Figure 6-12 where on the left-hand side a smooth surface makes a single reflection, while in the rough diffuse case, there are several reflections. This has an impact on the reflected ray and the roughness of the surface is more significant at higher frequencies where the wavelength is lower and hence the rough edges of walls have a more substantial effect.

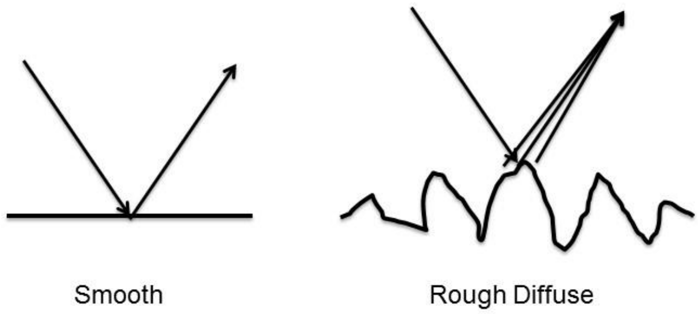

Figure 6-12: Illustration of a comparison between smooth and rough diffuse reflection

To ascertain the effect of different building surfaces and to identify any significant differences in diffuse scattering which would result in different path loss effects, five surfaces were tested for their roughness effects for 22-40GHz and 50-67GHz as illustrated in Figure 6-13. The surfaces were a brick surface, wood (as a set of planks with gaps), hedge (represented by plants for ease of measurement), glass (infra-red reflector glass typically used for building façades) and metal (using a recycling bin for ease of measurement).

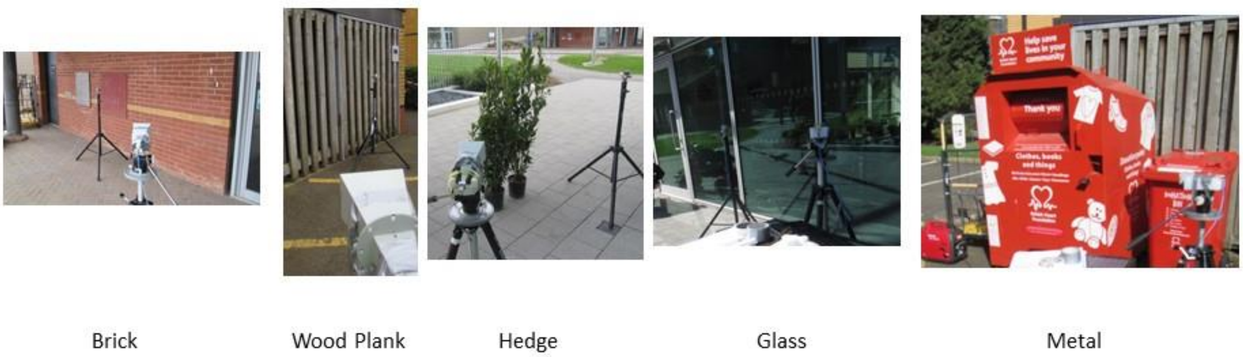

Figure 6-13: Photographs of the different building surfaces used in the study of roughness effects

The average loss (additional to the path loss) due to reflection from the buildings, compared with when the receiver antenna is pointing to the line of sight is shown for three frequency bands, 26GHz, 33GHz and 60GHz and plotted in Figure 6-14. Note that in each measurement the receive antenna was placed close to the wall, which had a semi-directional radiation, so it was therefore susceptible to picking up all the diffuse scattering that reflects off the surface when turned around towards the wall. The average loss is calculated over the number of measurements taken and also the whole bandwidth greater than 2GHz at which the measurements were made at each frequency.

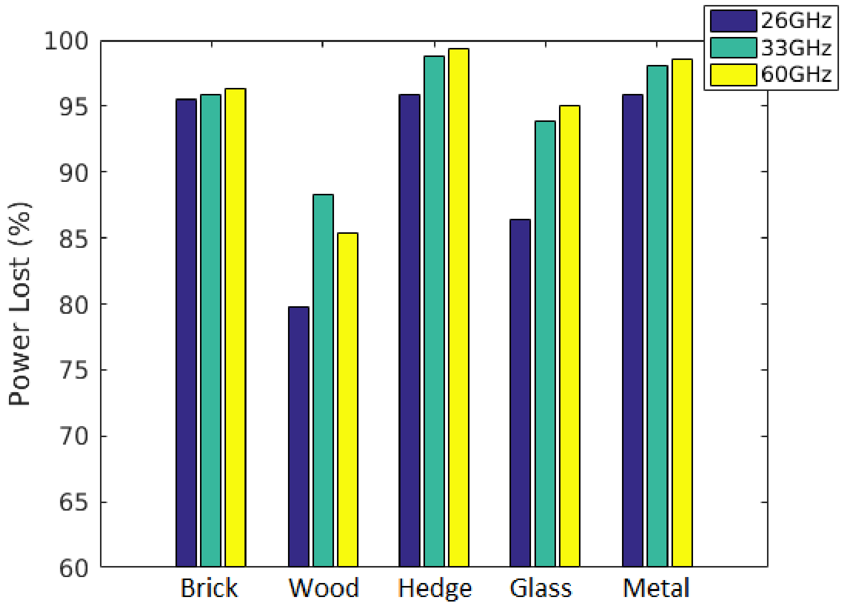

Figure 6-14: Comparison of the average power lost by the different building surfaces

Results show that when comparing the three frequencies, there is noticeable consistency for the different frequencies. For the brick, wood and hedge cases the loss is the highest (in excess of 95% of the power is lost) which is expected as all three materials are poor reflectors and their roughness is substantially greater than that of glass and metal. For glass and metal, it is marginally better with the power lost being below 95% but above 80%. The requirement here holds that there is a need for the material type to be known.

6.7 Wideband channel frequency selective fading

So far in the present report, the impact of roadside objects has been analysed with regard to the extra path loss they cause. However, we established in Section 3.3.4 that in addition to path loss itself, it is important to understand how path loss is also dependent on frequency within the wide contiguous bandwidths used in propagation channels above 6GHz. This phenomenon is known as frequency selective fading.

The simplest understanding of this is found by considering the line of sight propagation channel shown in Figure 6-15 where there is a direct line of sight path from the transmitter to the receiver but also a reflected path off a scatterer. Both paths will have a physical distance and for a given frequency it will correspond to a wavelength by knowing the speed of light as a physical constant. Therefore, any distance can be determined by the number of wavelengths when the physical distance is divided by the wavelength. In the case on the left, the frequency is set such that the reflected path has N whole wavelengths, while the direct path has M whole wavelengths. In this case, the electromagnetic fields from the two paths will add together in phase and the total signal will be twice the signal that would be obtained when there is no scatterer present. It is assumed in this case that the distance of the scatterer away from the midpoint of the line of sight is small compared to the distance between the transmitter and receiver. The diagram in Figure 6-15 is not drawn to scale for the purpose of clarity.

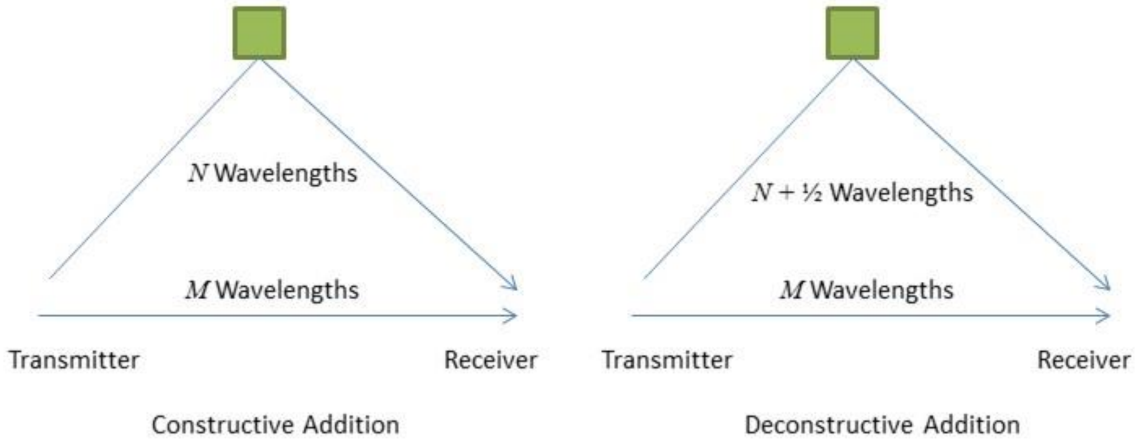

Figure 6-15: Illustration of a propagation channel with constructive and deconstructive addition due to frequency selective fading

At another frequency, as shown on the right-hand side of Figure 6-15, it is possible that the distance from the transmitter to the receiver is M wavelengths long while the reflected path is N + ½ wavelengths long. In this case, the two received electromagnetic waves are inversely correlated (out of phase) such that they cancel each other out and no power is received.

For example, where the transmitter to receiver distance is known (50m) and the distance of the scatterer from the line of sight is known (10m), the variation in signal versus frequency can be plotted for the 24.25GHz to 27.25GHz bands as an arbitrary 3GHz band in Figure 6-16. Clearly there are ten frequencies where there is no electromagnetic wave signal received at all and thus the ratio is 0% when compared with what would be received from a single line of sight in free space. These are all frequencies where there is a deconstructive addition. There are eleven frequencies where there is a constructive addition, and therefore the ratio of the resultant electromagnetic wave signal received at these points when compared to a single line of sight in free space is 200%. In between the frequencies for constructive and deconstructive addition, there is only partial constructive addition.

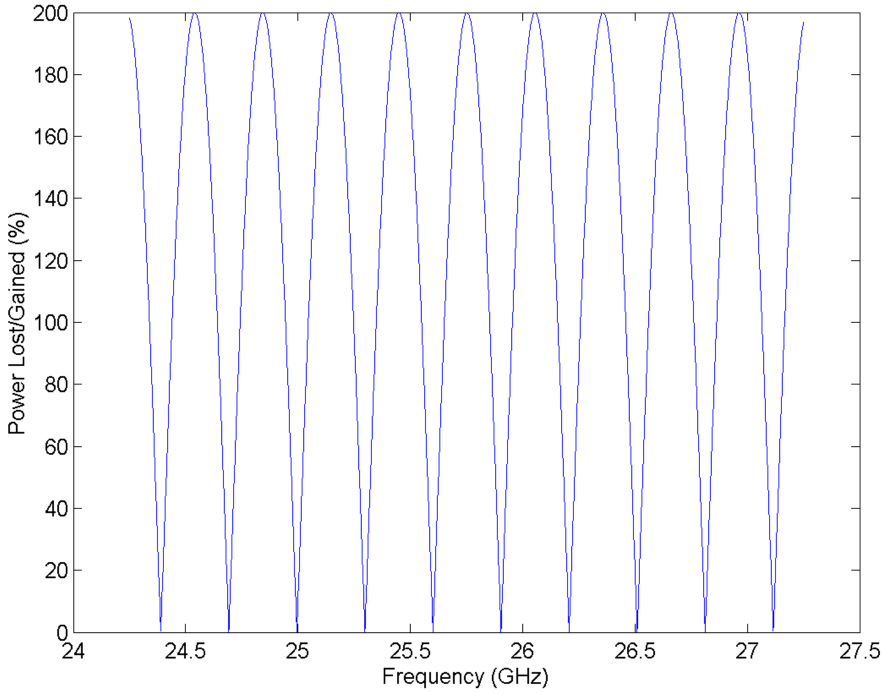

Figure 6-16: Plot of the ratio of the received signal relative to a single line of sight signal in free space vs frequency with a single scatterer causing frequency selective fading

In the example case shown here, there is frequency selective fading shown for just a single scatterer such that at certain frequencies, the received signal will minimise or go into a 'deep fade'. In a practical scenario, there is more than one scatterer present and so it is important to know the position of the scatterers and their material specification to determine how the electromagnetic waves will add together at the receiver and output a resultant wave signal as they will similarly cause deep fades at frequencies where there is deconstructive addition. This will enable cell planning using a ray tracing model which is beyond the scope and purpose of this report. A simple ray tracing solution is shown in Figure 6-15 where there is a single scatterer forming two rays, the reflected and line of sight rays. Additional scatterers will form additional rays. The geospatial data requirements identified in this work will be used in ray tracing models in the following ways:

Building surface roughness effects

Near to walls and building edges where a mobile device antenna is radiating towards the wall or building it is necessary for the wireless link to rely on the reflection from the surface it is close to unless smaller sub base stations are installed at several points along a building which would be costly and unlikely to be practical. Knowledge of building surfaces is therefore essential not only to determine the additional path loss but also to build knowledge of the roughness characteristics that can be incorporated into a ray tracing tool. It would not be necessary for an exact replica of the wall surface to be modelled, though a suitably comparable rough surface would need to be simulated that would yield a similar number of rays that would be scattered from the rough surface to determine the nature of the frequency selective fading. This will be highly dependent on the position of the mobile device in relation to the surface.

Scattering through vegetation

As has been established, the loss through vegetation is significantly higher where there is a high density of foliage with a significant water content. In cases where there is low or no foliage, there may be several branches present in the vegetation that the signal is propagating through and as such frequency selective fading would result. Modelling the exact geometry of the vegetation is complex and unnecessary, but it would be necessary to form a model of such vegetation derived through extensive measurements which would show the number of rays and their characteristics such as the length of the path and the angles at which they arrive at the receiver when transmitted from a certain angle. Such models for vegetation can then be incorporated.

Scattering within enclosures

As has been shown in Figure 6-5, the bus shelter is used as an example of an enclosure where the signal propagates in and has scattered. In such structures, it has been seen that the nature of scattering changes substantially in different positions within the enclosure and as such it is necessary to have a full specification of the structure, which would be less complex to achieve compared to building surfaces or vegetation. This would enable a full ray tracing based model to be formed to resolve the frequency selective fading at all points within a bus shelter.

For all three cases above, it should be noted that the scattering characteristics will be highly dependent on frequency as the distribution of the rays will depend on how well they reflect off the scatterers within the structure. Extensive studies will be required for different frequency bands.

6.8 Summary

Measurements have been presented in this section which show the principle by which the basic path loss of a high-frequency signal is modelled as four paths, consisting of a line of sight and three reflected paths off the ground and two adjacent buildings. The additional path loss caused by street-side objects is identified by three principal propagation phenomena. The first is penetration loss through materials including street furniture enclosures such as bus shelters, but also through vegetation. Second, a new concept of propagation known as shield edge diffraction is formed, which will determine the loss caused by tall narrow objects such as lamp posts and tree trunks. Finally, the impact of surface roughness where a mobile device has to rely on reflections off buildings to maintain a communication link is considered. Different rough surfaces are analysed by measurement to compare the impact they have on propagation.

7

7 Evaluating capacity and coverage maps

7.1 Introduction

After establishing the path loss due to the effect of buildings, weather, vegetation and street furniture, it is necessary to densify the cells to determine whether the communication requirements have been met. Once the path loss and frequency selective fading characteristics are known through the use of propagation models, we need to ascertain whether under such conditions the communication requirements of the wireless link between two points are met. This will depend at first not only on the signal power received but also the noise and interference received. Noise will be present because, according to the laws of physics, wherever there is heat present there will be thermal noise at the receiver which can be formed into a power quantity. It is essential that the received signal is substantially higher than this noise power to achieve communication. So the path loss must not be too great or the transmit power must be sufficiently high across the whole band and hence the frequency selective fading must also be considered.

Another matter of concern is the fact that more than one user will be in a cell or neighbouring cells at any one time using the same frequency band. Where two or more simultaneous links are operating at the same time they will create interference with each other. The interfering power will have to be known and will normally be less than the signal power of the desired link because the path losses from the interfering sources to the device will be greater than the link from the transmitter to the receiver. This therefore means that when the interfering power is added to the noise power, a signal to interference and noise ratio (SINR) can be defined as follows:

$$\text{SINR} = \frac{\text{Signal Power}}{\text{Total Interfering Power} + \text{Noise Power}}$$

The higher the SINR, the higher the data rate that can be achieved. It will be necessary to know this as well as using information about the frequency selective fading to evaluate the data rate. This requires simulations to be undertaken in which the signalling used in the communication system is also incorporated. The data rate due to SINR can then be ascertained.

As established in the previous section, at high frequencies the received power decays quickly with a rapidly increasing path loss over distance and this loss can be overcome by highly directional antennae. Achieving this concept is possible by a system known as beamforming which is illustrated in Figure 7-1. On the left-hand side is a single element which has a semi-directional radiation by virtue of the antenna's design. By taking multiple copies of this antenna and arranging them in a square array, as illustrated on the right-hand side of Figure 7-1, the radiation from each of the elements superimposes on the others and causes the resultant radiation to be highly directional.

The more elements are added, the more directional the radiation will result and this will therefore further overcome the extensive path loss at mmWave frequencies. Consequently, the SINR will increase substantially and with it the bit rates that can be delivered. It should be also noted that beamforming enables the radiation to dynamically steer in the direction of a user. The same can be achieved when the antenna is in receive mode on the basis of reciprocity.

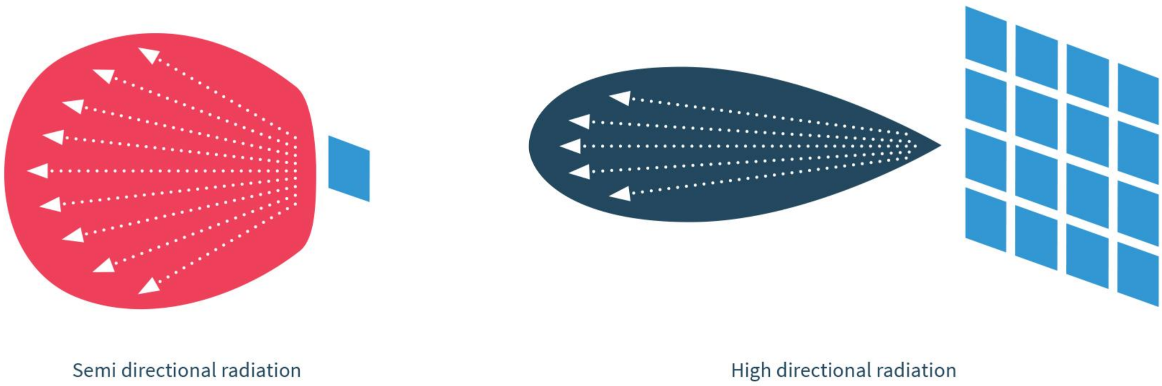

Figure 7-1: Illustration of the concept of beamforming

To comply with state-of-the-art communication systems, many parameters used in this work are based on the third-generation partnership project (3GPP) assumptions for 5G evaluation, which define the antenna design and array topology by which beamforming is undertaken. Such documentation is the latest available information in terms of setting standards that would be required for cell planning tools. There are two key sub-procedures to go through for a planning tool when evaluating the system level performance, which are summarised in the next two sections.

7.2 Resolving the received power

Having established the concept of path loss in Section 4 and the concept of antenna beamforming in this section to improve directional radiation, it is worth noting how the received power between a transmitter and receiver is calculated. The power received at a mobile from the power transmitted by a base station $P_{Transmit}$, can be summarised in a simplified form by the following equation:

$$\text{Power Received} = P_{\text{Transmit}} + P_{\text{Additional}} - P_{\text{Path Loss}} - P_{\text{GeospatialScattering}} - P_{\text{Weather}}$$

In the first instance, the transmit and receive antennae will have directional radiation. This will mean that the transmit antenna is able to transmit more electromagnetic energy in a given direction than an ideal antenna that radiates uniformly in all directions. This means that the electromagnetic energy transmitted by an antenna in a given direction is equivalent to an ideal antenna transmitting in every direction but with a larger source power, thus giving the same result in that direction. Similarly, it is possible at the receiver that the antenna will be able to focus on a given direction and be capable of receiving a larger quantity of power than an ideal antenna. To account for the effective extra transmitted power and the effective increase in receive power, this difference should be denoted as additional power, $P_{Additional}$. It is therefore desirable that the antennae are as directional as possible so as to increase this additional received power, which will in turn improve the propagation range. It is also shown in Section 5.2 based on the inverse square relation, that power will be lost due to path loss, which is given as $P_{Path\ Loss}$. Geospatial scattering will cause a further power loss, $P_{Geospatial}$, which includes diffraction loss from street furniture, reflections from buildings and penetration loss through vegetation and other objects. Finally, there is additional loss due to the weather, in particular rainfall and sleet, $P_{Weather}$. The sum of these three powers must be less than the transmitted power, though the difference could be small due to the fact that frequencies above 6GHz decay rapidly with distance.

7.3 Network initialisation

In forming a cell planning tool, it is necessary to form a mesh of square pixels to evaluate the coverage area. In this study, a pixel size of 10x10cm has been established to provide a deep resolution in order to identify the impact of the diffraction and scattering of small geospatial objects described in Section 6. With knowledge of the base station (BS) positions, the path loss to each pixel can be mapped using the modelling methodology described in Section 6 which will also consider the radiation characteristics of the antennae used.

Additionally, the serving area of each Base Station is divided into three equal sectors of 120o so that directional antennae are allocated to each sector and they radiate out to that sector directionally. Initially, they will radiate without beamforming and with a semi-directional radiation like that illustrated in Figure 7-1. Pixels are assigned to communicate with a BS that maximises the signal to interference and noise ratio (SINR) at the pixel under consideration. It should be noted that when considering the effects of geospatial clutter, the nearest base station sector to the pixel may not have the highest SINR due to blockage from geospatial objects. It should also be noted that where a mobile is very close to a base station (such that it may be almost directly underneath it) then it is not possible for the beamforming to radiate towards the mobile and therefore a mobile would not be served by a base station so close, but another one. In this regard, it is necessary to ensure that the path loss is not so small that it is less than a defined minimum coupling loss (MCL), which will subsequently prevent a mobile communicating with a base station it is too close to. This establishes what the Base Station serving area is in the initialisation phase.

7.4 Simulation and dynamic evaluation

After initialising the network and forming the SINR, it is then necessary for the link level simulation to determine a channel quality indicator (CQI) value which will subsequently correspond to a modulation scheme that the system will adopt resulting in a cell efficiency. This term can then be translated into a capacity value. The link level simulation has to use a suitable granularity of transmission time interval (TTI). This allows the BSs to schedule a user at a pixel randomly chosen in each cell and assign full transmission resources (which will enable maximum bit rate delivery) in the link transmitting from the base station to the mobile. Based on the CQI value of the user, this will determine the modulation/coding scheme to be used. By use of a lookup table, the CQI value will then correspond to a cell efficiency, which will determine the bit rate after applying beamforming to that pixel which will correspond to a capacity value. This procedure is repeated in each cell by randomly selecting another pixel (excluding the previously covered ones), and then continues until all pixels in all the cells are covered/evaluated. This will generate a coverage map.

7.5 Cell planning flow process

The target is to position enough base stations so that there is a data rate delivery of 2100 Gb/s/km^2. Note that this target figure includes the areas occupied by buildings over a square kilometre so this number can be proportionally scaled to a smaller area such as a street, park or pedestrianised zone. The locations of the BSs are randomly chosen under a minimum BS-to-BS distance constraint of 50m which falls within the range specified by 3GPP standards. The following steps summarise the procedure for deploying the BSs using the procedure shown in the flow chart in Figure 7-2:

1. Position an initial set of BSs in suitable locations (e.g. on lamp post, on top of building);
2. Evaluate the throughput/coverage achieved under this deployment by going through the steps in the flow chart;
3. If the achieved throughput/coverage is below the chosen target of 2100Gb/s/km^2 (or the derived value if scaled down to a smaller area), then it is necessary to deploy additional BSs. The extra BSs must be positioned within pixels that have a minimum distance of 50m from the locations of the existing BSs. Therefore, suitable geospatial locations (e.g. lamp posts and building fronts) that meet this criterion should be chosen;
4. Repeat steps 2 and 3 until the target throughput/coverage is achieved. This is also shown by the loop in Figure 7-2.

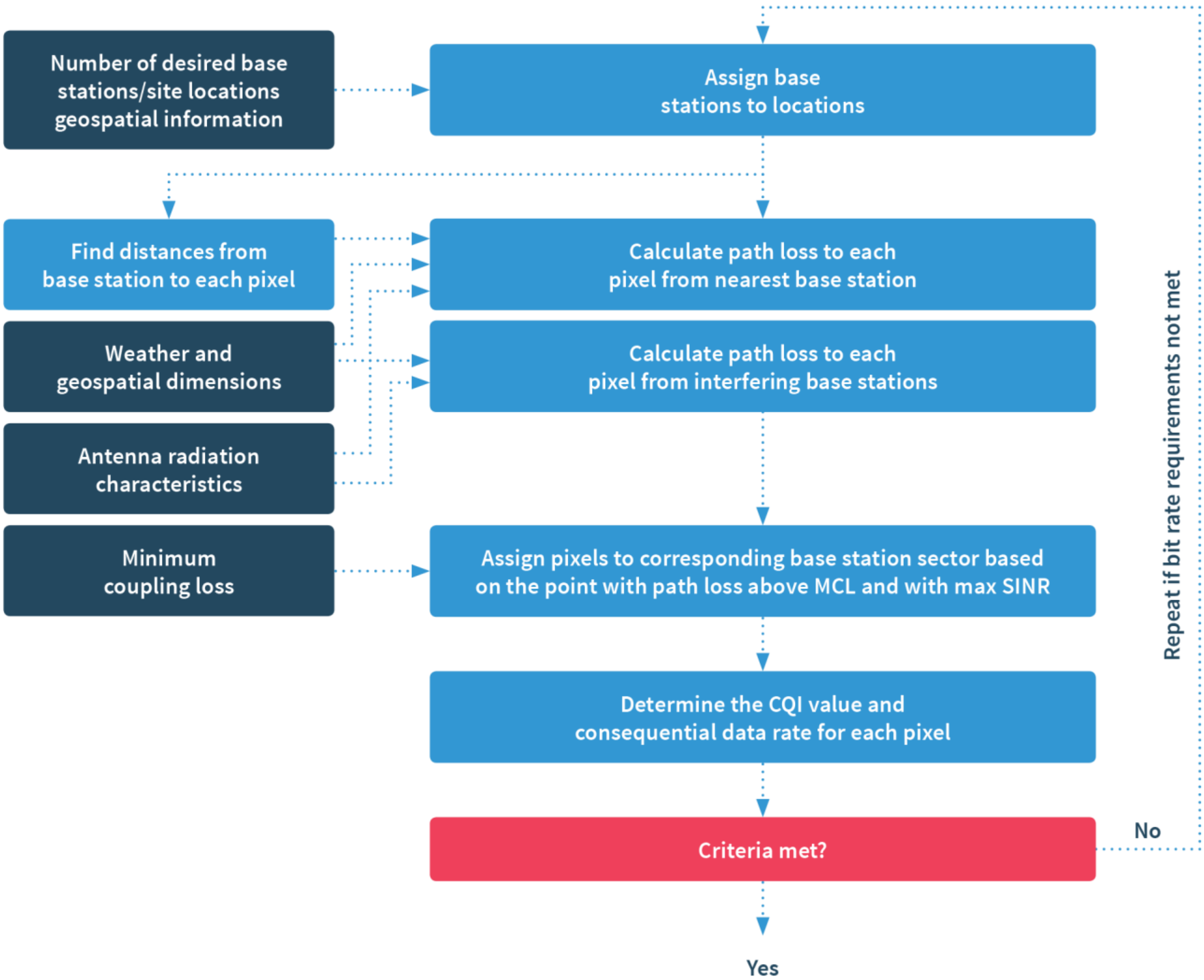

Figure 7-2: Flow diagram of the process for the planning of base station locations

7.6 Coverage map examples

To illustrate the impact of street furniture, frequency and weather, coverage plots have been taken of a rectangular street location 10m wide and 200m in length. The simulation result is first presented in Figure 7-3 at a frequency of 26GHz where two sets of results are shown for the case of no effect from geospatial objects or weather conditions, one for (a) the SINR and another for (b) data rate in gigabits per second (Gb/s). The corresponding colour scale indicator is shown in Figure 7-4. Note that wherever a pixel is red, it has an SINR greater than or equal to 2.69 or a data rate greater than or equal to 1.71Gb/s. At the bottom end of the scale, wherever a pixel is fully blue, then it has an SINR less than or equal to 0.26 or no communication at all since the SINR is too low.

It should first be noted in both Figure 7-3 that black lines are shown in the colour maps. In this instance, the point where the lines intersect on the left and right hand sides of the coverage plot are points where two base stations have been positioned 160m apart. The lines are present in order to show how the sectors are orientated. Therefore in Figure 7-3 it can clearly be seen for the left hand base station that the SINR drops where the edge of the sector is reached because the signal from the sector antenna is weaker at this point while the interference from the corresponding sector on the right hand side is strong. Close to the midpoint between the two base stations, the SINR reaches its weakest level.

One final noteworthy point is that in Figure 7-3a it would normally be expected that Figure 7-3b would have exactly the same corresponding heat map, but the blue region is not present when analysing the data rate. There is a reason for this since the SINR will correspond to a range within which there is a Channel Quality Index (CQI) value and at that CQI value there is a fixed data rate. Therefore, the data rate does not simply increase linearly with SINR, rather the data rate corresponds to the range within which the SINR falls. In the worst case here, the SINR falls to approximately 0.38, which corresponds to a CQI level resulting in a data rate of just 0.32Gb/s.

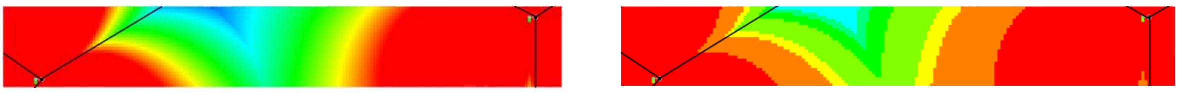

(a) (b)

Figure 7-3: Coverage map on a street with no obstructions for two base stations at each end showing (a) the SINR and (b) data rate degradation at 26GHz with an inter-site distance of 160m

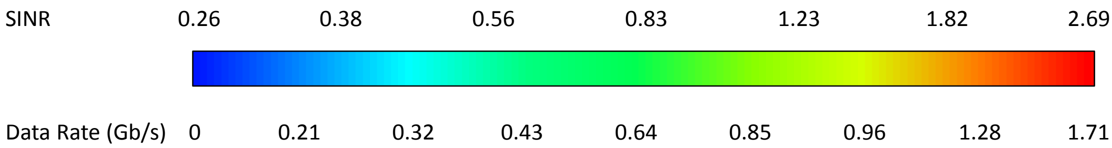

Figure 7-4: Colour scale indicator for both signal to interference and noise ratio as a factor and data rate in gigabits per second (Gb/s) where used in the coverage maps

To show the impact of increasing frequency, Figure 7-6 shows the difference when the frequency is increased from 26GHz to 40GHz. In this instance, the blue region for SINR has clearly widened and at the worst case the SINR has fallen to as low as 0.26Gb/s or less and the corresponding data rate shows that there is a point with no communication and zero data rate.

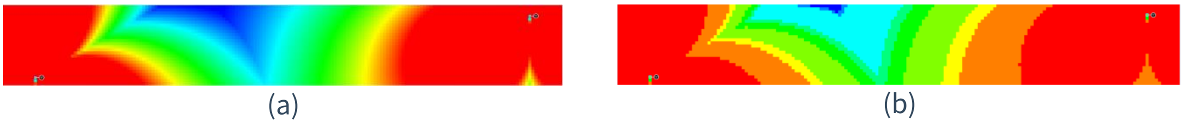

Figure 7-5: Coverage map on a street with no obstructions for two base stations at each end showing (a) the SINR and (b) data rate degradation at 40GHz with an inter-site distance of 160m

Returning back to 26GHz, it is also worth showing how a third base station would be used to fill the region where the data rate is insufficiently low at below 0.5Gb/s. This is shown in Figure 7-6 where a third base station is placed at the top of the rectangle but offset 50m to the left of the centre point between the original two base stations. The sector boundary of the third base station can clearly be seen to be vertical at the point where it is positioned. This means that one of its sectors fills in the original blue spot and now the lowest SINR is greater than 0.45Gb/s. This corresponds to a CQI level with a data rate of at least 0.43Gb/s.

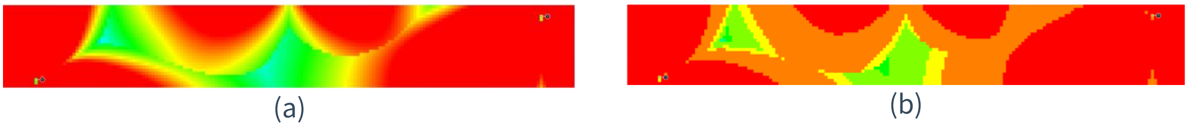

Figure 7-6: Coverage map on a street with no obstructions for two base stations at each end with a third base station in between causing extra interference showing (a) the SINR and (b) data rate degradation at 26GHz with an inter-site distance of 160m – the third base station is offset 50m to the left of the centre point between the original two base stations

Returning back to two base stations at 26GHz, Figure 7-7 illustrates the impact of extreme weather. This is taking a scenario where 50% of the power is lost over a range of 100m. From earlier analysis shown in Figure 5-5, this is an extreme case for 26GHz above the 99th percentile. However, it is chosen as a worst-case scenario and clearly it has shortened the propagation range to the cell edge and introduced a region with no communication when compared with Figure 7-3. This therefore demonstrates an instance where weather has a direct impact on cell range which will be more significant at higher frequencies.

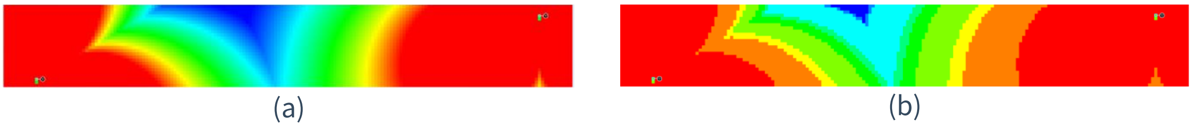

Figure 7-7: Coverage map on a street with no obstructions for two base stations but with the additional loss due to extreme rainfall showing (a) the SINR and (b) data rate degradation at 26GHz with an inter-site distance of 160m

The final and most interesting example is the case where there is an impact of street furniture illustrated in Figure 7-8.

It can be clearly seen that a 2D view is not sufficient to analyse this type of scenario. Therefore, a 3D view is required to perform accurate analysis of the impact of street furniture on cell range as shown in Figure 7-9. Again, the frequency is maintained at 26GHz with the same two base stations as before.

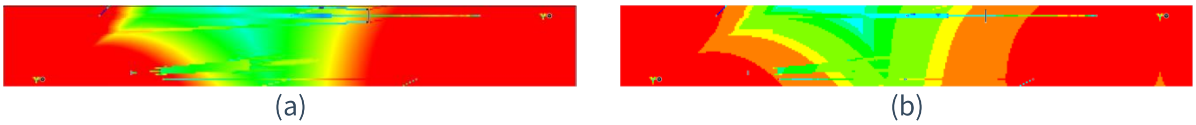

Figure 7-8: Coverage map on a street with street furniture causing obstructions for two base stations at each end showing (a) the SINR and (b) data rate degradation at 26GHz with an inter-site distance of 160m

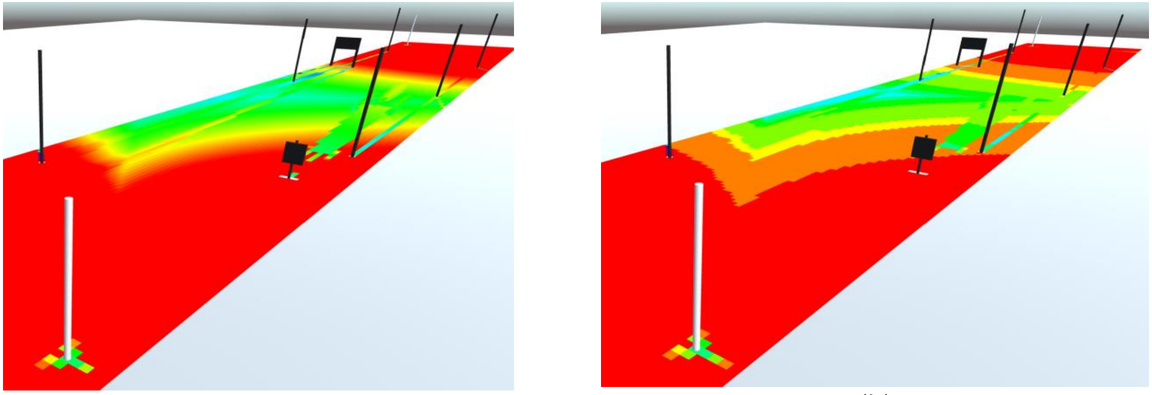

(a) (b)

Figure 7-9: Coverage map on a street with street furniture in 3D causing obstructions for two base stations at each end showing (a) the SINR and (b) data rate degradation at 26GHz with an inter-site distance of 160m

As shown in Figure 7-9, six lamp posts have been inserted and are illustrated in black, while the two poles for the base station are illustrated in white. The lamp posts are all 30cm in diameter which is substantially wider than a typical lamp post but they have been deliberately made wider to show the shield edge diffraction effect. Additionally, two road signs have been inserted, one with a square shape and an edge of 1.6m, while the other is rectangular shaped with dimensions of 1.6x3m.

Clearly, with such significant shadowing objects, the SINR and consequently the data rate drops within the shadow of the object relative to its closest base station. However, this plot does show the importance of evaluating the SINR fully. This is illustrated by observing the square sign and the lamp post to the right of it. The shadow of the square sign shows an SINR of approximately 0.83 corresponding to a data rate of 0.64Gb/s. For the lamp post on the other hand, despite being a slimmer object where the impact would be expected to be lower, the SINR in its shadow falls as low as around 0.45 corresponding to a data rate of only 0.32Gb/s. It should though be noted that the lamp post is closer to the cell edge than the sign and therefore the sign has a higher SINR because more power is coming from the intended base station. Also, it is further away from the interfering base station which consequently reduces the interference and so the SINR increases overall. Even though the lamp post causes less shield edge diffraction loss, the signal is weaker while the interference is stronger resulting in an overall lower SINR.

One other significant point of observation is the middle lamp post of the three lamp posts on the right-hand side of the street. It can be seen that there is a shadow showing an increase in SINR, rather than a decrease when moving towards the furthest base station. This case is therefore providing a shadow to the interference rather than the signal and since the signal is not in a shadow, the SINR increases.

These are useful illustrations of how the tool is sensitive to the impact of geospatial objects not only on the propagation of the signal but also the interference. Clear instances are shown where due to the presence of the shadowing object, the data rate within the shadow can fall below 1Gb/s, whereas if the geospatial object were not present, this would not be the case. This is clearly illustrated in the case of the square sign with a blue region with no communication. For the lamp post in the foreground the SINR drops down below 0.26 in its shadow.

Finally, it can be observed in the foreground base station that the region directly under it is not pure red: a number of pixels there are green. The reason for this is that a device directly under any base station, despite being so close, cannot communicate with it. This is due to the limitations on the beamforming technique applied at the base station which is not capable of directly steering a beam down below. For this reason, any device in such a location has to rely on the next nearest base station, which will obviously yield a lower SINR as is the case here.

7.7 Verification and sensitivity analysis

By presenting the example cases in the previous section, the demonstrator tool shows that it is able to detect the sensitivity of how both a desired and interfering signal can be affected by the landscape whereby its value and corresponding data throughput can change substantially in different pixels. The sensitivity shows the impact of frequency. It not only shortens the propagation range due to more rapid path loss but the geospatial objects become electrically larger in that their size compared to a wavelength at higher frequencies is more substantial resulting in higher losses. The size of objects within 10x10cm pixels are small enough that they can easily scale up to the higher frequencies. The tool also demonstrated its sensitivity to extreme weather conditions, where they are considered in the range over 100m such that the loss over a whole distance is substantial enough to show a measurable impact in terms of substantial reduction in SINR and data rate delivery at a cell edge.

Further considerations beyond the scope of this tool that limit its sensitivity are worth noting. The first of these is antenna orientation at the mobile. On the assumption that the antenna has semi-directional radiation, its orientation will have a significant impact on the propagation. Two clear examples of this are where an antenna is in the shadow of street furniture and the antenna is orientated directly towards it. In such a scenario, the signal is substantially attenuated and the interference will be subject to less attenuation. This will result in a large drop in SINR as a mobile moves past such an object when it is originally in a line of sight link with the base station. However, the SINR would not be affected in such a way if the antenna were orientated in the opposite direction with some opportunity to communicate with another base station. Second, though buildings' façades have not been considered in the examples shown, there will be scenarios where the orientation of a mobile is such that it cannot find a line of sight link with any base station which is typically the case when close to a building, such that it has to rely on a reflection off the building. This will inevitably lead to substantial extra loss as found by measurements in Section 6.6 depending on the roughness of the façade's surface.

Verification of this tool will therefore require the deployment of a measurement trial which will correctly survey the position and size of all diffracting objects as well as having the ability to analyse the change in signal not only due to spatial position but the angular orientation of the mobile antenna at that position. Such physical parameters will substantially change the path loss and also the average path loss will be majorly dependent on orientation. Penetration through enclosures such as bus shelters will require a more exhaustive set of measurements to analyse their losses which can be built in to a model but not only that the frequency dependency will be a key contributor from which the sensitivity to change in frequency can be maintained.

7.8 Summary

Key findings of the demonstrator tool and the methodology have been shown in this chapter and example cases have been highlighted from a 10x200m rectangular area to illustrate the impact of weather, geospatial objects, and frequency on the coverage not only in terms of the signal to interference and noise ratio but also the data rate delivery. It is clear from the illustrations that geospatial objects have a substantial impact both in terms of how they can block a signal and the interference from other cells which significantly impacts on the overall signal to interference and noise ratio. Real street furniture can be modelled from such scenarios through which more important results can be shown.

8

8 Key findings

In this section, we summarise the key findings of this project. We confirm the geospatial and weather data requirements for 5G planning, and discuss the implications for mobile network operators in the absence of these data.

8.1 Confirmation of important geospatial data

The creation of 3D information from the street asset data provided by Bournemouth BC (and depicted in Figure 8-1) was not a simple task; the various datasets were not easy to examine, extrude or integrate without considerable effort. The street asset datasets available from local authorities can be highly variable and may not be suitable or relevant to the 5G infrastructure planning challenge.

Figure 8-1: Classified local authority highways asset data shown on 3D mesh

Point clouds, which can be derived from both aerial and mobile mapping missions, offer a superior and valuable level of granularity. In particular, a point cloud from mobile mapping can clearly reveal individual features at street level. However, point clouds on their own do not carry a rich level of attribution.

The accuracy and specification of data representing street-side assets which can significantly affect high-frequency signals needs to be carefully considered. In Section 6.4 we show that at 26GHz, the lowest of the frequencies of interest, **any street asset with a dimension as small as 10cm is significant** and this figure reduces further at higher frequencies. The precise configuration of street-side assets is also significant, including for instance, the size and position of a road sign on a lamp post, both of which objects will impact signal propagation. If data records about street-side assets are available from a local authority, our experience suggests that they may provide valuable attribution but that they can be geospatially inaccurate and may not contain links to their associated object such as lamp posts. As we have discovered, this makes the task of correctly positioning this type of data extremely time-consuming.

An alternative approach is simply to detect and model street-side objects in geographic space. At the simplest level, we could consider using a basic, unclassified mobile mapping point cloud. However, it is more valuable to be able to identify street assets as objects because these can have key attributes applied to them. We have successfully used software to classify a point cloud and automate the extraction of some types of feature, notably poles and street signs (Figure 8-2). Once extracted, these features have high positional accuracy.

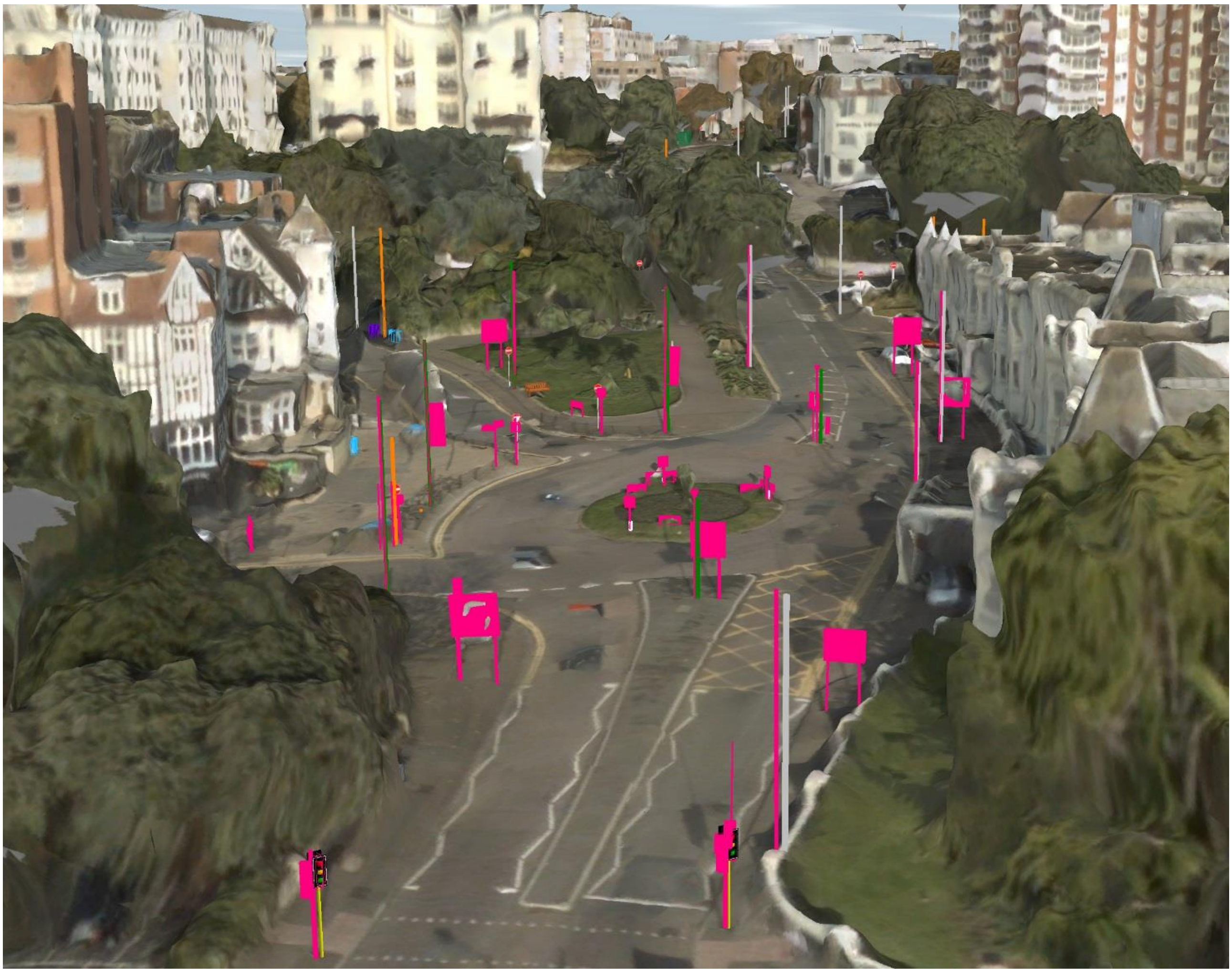

Figure 8-2: Items of street furniture, coloured pink, which were semi-automatically extracted and modelled from a mobile mapping point cloud. Some of these data records were not available from Bournemouth BC data but are likely to represent a block to a 5G signal.

Modelling vegetation from aerial imagery presents many challenges. Although in this project we have applied some automated techniques to extract vegetation, particularly trees, from image-derived point clouds, the resulting objects are sometimes poorly defined, particularly in comparison with the excellent level of detail achieved from a mobile mapping point cloud, shown in the lower part of Figure 8-3.

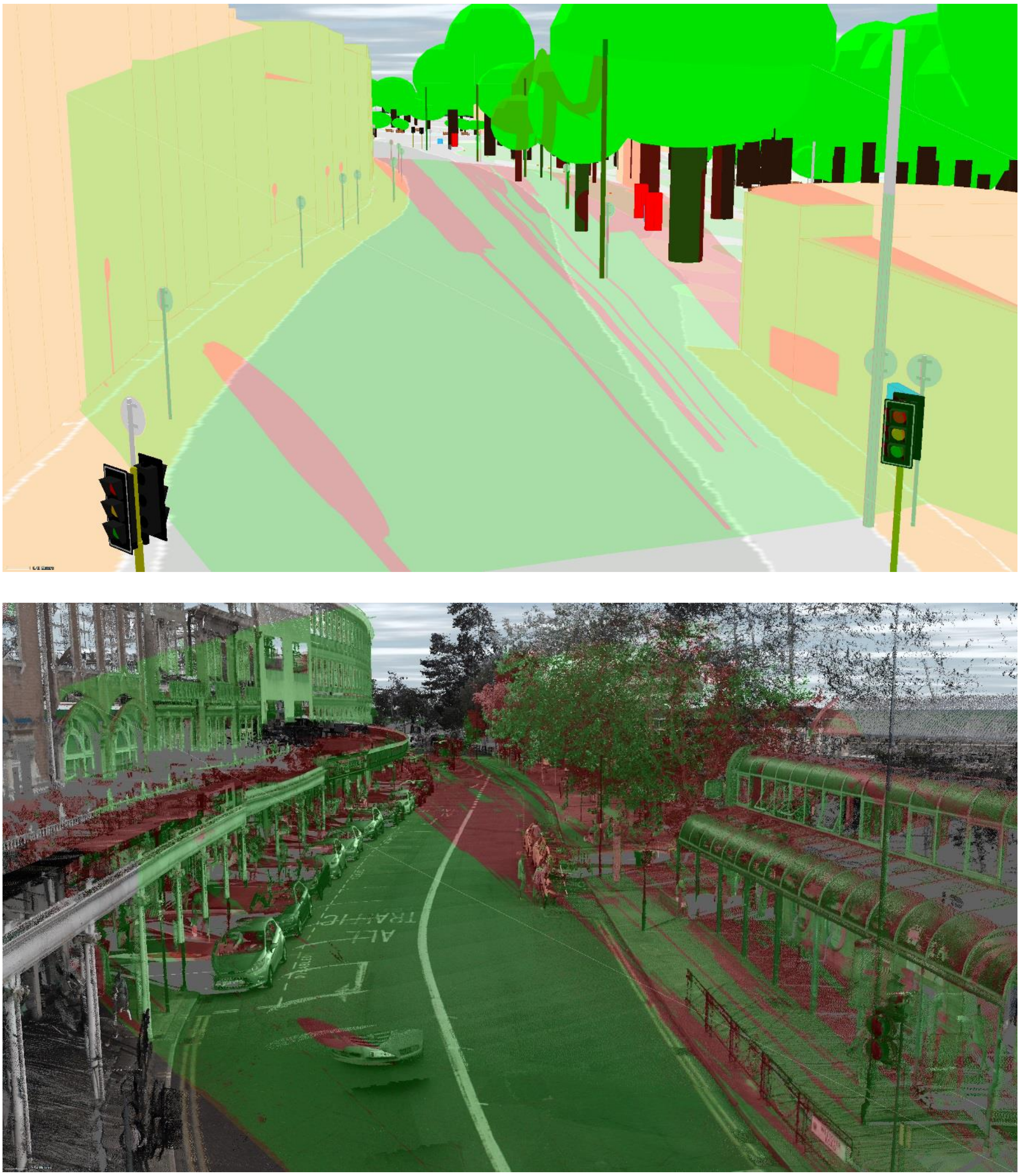

Figure 8-3: Two depictions of the same scene; the top image is largely modelled from pre-existing data sources; the lower image is an example of a mobile mapping-derived point cloud. Both model the effect of urban objects with the point cloud providing a better assessment of line of sight underneath vegetation and building canopies.

The Tree Preservation Order data acquired from Bournemouth BC proved useful as we were able to match them with automatically-derived tree positions, allowing some species to be individually mapped. However, this level of detail is inferior to the outputs from a terrestrial point cloud which can represent a tree's structure, foliage density and dimensions.

It is important to bear in mind that all remote sensing outputs, such as images and point clouds, represent the world as it was detected at a moment in time. Mobile mapping data in particular include transient objects from the time of capture, spanning vehicles, people and vegetation characteristics. Although it is possible to remove any unwanted artefacts from the data, sometimes automatically, there is a good argument not to do so, as the sensed data may be considered as representative of the street scene clutter and therefore of value when assessing placement of 5G network assets.

Of the issues encountered in the use of the mobile mapping data, the main problem was that of the point cloud consistency between driven journeys, termed ‘tracks’. The point cloud positioning was based on an accurate trajectory of the positioning system within the data capture module and is not tied to ground control points (GCPs), and this resulted in data from separate tracks being spatially separated. Overcoming this issue required extensive manual intervention and, as the data were supplied ‘as is’, this was not straightforward. With time and software constraints, some of the mobile mapping data were judged to be below the standard of required positional accuracy and were discarded to prevent systematic data errors being introduced.

Our recommendation is that mobile mapping missions should be engineered to make use of suitable GCPs and that suitable software is available to resolve any data inconsistencies. Automating downstream processing of mobile mapping data becomes more viable once trajectory mismatch issues have been resolved.

Our key conclusions from this analysis are that:

- Data need to be captured at a level of granularity which supports the analysis of 5G signal modelling. To deliver this, **terrestrial mobile mapping technologies provide the most appropriate and cost-effective data source.**
- Remote sensing techniques such as terrestrial mobile mapping can provide basic information about form and function, **but richer object metadata will enable more sophisticated analysis**, for example with respect to planning 5G backhaul.
- **Terrestrial mobile mapping surveys should be carried out in advance of and in coordination with 5G infrastructure deployment.** This will avoid any issues of data temporality and ensure that data can be used as efficiently as possible to extract relevant information.
- Terrestrial mobile mapping data need to relate to a wider 3D geospatial framework and thus should be used in conjunction with topographic mapping and aerial imagery such as nadir and oblique.

8.2 Confirmation of important weather data

Heavy rainfall and sleet have the potential to significantly attenuate 5G signals, even over relatively short distances, reducing the range over which a base station could effectively transmit to a cell edge. We identified two worst-case scenarios for attenuation.

The first case concerned an occurrence of **severe convection in summer time**. The atmospheric energy and humidity of such a scenario enables generation of large numbers of highly attenuating raindrops, which produce significant absorption and scattering. The impact was found to be most severe at the higher frequencies of 71 and 83GHz.

The second case involved **winter time frontal precipitation**. If ground-level temperature conditions rise to just above freezing, falling snow starts to melt. The coating of water can have a scattering and absorption effect comparable to that of larger raindrops. This can cause the overall attenuation to rise significantly, particularly at lower frequencies. **For example, at 26GHz, the attenuation may increase by a factor of six**, making this scenario much more significant than the summer time case.

The severity of these weather effects has a strong geographical dependence. They must be quantified and factored into network design on a region-by-region basis to ensure adequate year-round performance.

This study has demonstrated the possibility of simulating plausible rainfall fields and attenuation values at sufficiently high resolution for application to 5G networks. This is scalable to any frequency band of interest and is suitable for use as a planning tool. While some uncertainty remains around the quantitative relationship between precipitation rate and attenuation, the values passed to the planning tool in this study are likely to represent a reasonable worst-case scenario.

8.3 Implications for the mobile industry without availability of data

The work presented in this study clearly shows the impact of propagation due to geospatial objects including street furniture, vegetation and differing surfaces off building façades and walls. Current cell planning tools for deployments below 6GHz do not require the use of such detailed information. They do not incorporate new propagation modelling techniques including those derived within this work, nor fully operational ray tracing tools, discussed in Section 6.7, which consider the characteristics of geospatial objects with deep granularity.

In the absence of access to an authoritative geospatial database, weather statistics and socio-economic data, the cellular planning process would be substantially more expensive for mobile operators, and moreover link reliability would be compromised after deployment. The costs would be substantially higher because mobile operators would need to carry out their own geospatial surveys and model the position and dimensions of street-side objects to incorporate them into cell planning.

As we have seen, this work is not trivial and relies on considerable specialist expertise if you wish to maximise return on investment for 5G and beyond. Absence of data and expertise would substantially delay the time to complete deployment of a cellular network. This problem is magnified by dealing with change. Operators would need to update their information about local urban landscape and correspondingly alter their 5G network deployment. This is not likely to take place frequently and the need to capture this change is only detected as a result of a network failure.

It is very clear that seasonal changes in an urban environment, such as Christmas decorations, and summer floral arrangements on the lamp posts, building works and temporary buildings such as mobile shopping booths and marquees, will significantly affect 5G coverage. Managing the impact of these changes requires cooperation between local authorities and mobile network operators so that cellular coverage impacts are incorporated into the process of planning temporary changes to the street landscape. The alternative options are to rectify problems after they have occurred or to conduct extensive alpha testing of a deployment.

Footfall data is another vital element that will help both to determine the impact on propagation from people within a given location and also to model the demand for 5G services; otherwise this would need to be determined and tuned retrospectively. It is also, however, important to consider the temporal patterns of footfall which typically vary over daily, weekly and annual cycles and fluctuate heavily when major events, such as music festival or sporting events, take place. Access to advance event information is vital.

If a high-frequency 5G service fails due to the impact of unknown clutter or footfall in an urban location, it should be noted that sub-6GHz deployment will still be operational. However, performance in terms of capacity, speed and latency will be limited and will yield a substantially lower quality of experience, severely limiting advanced multimedia or tactile Internet[13] applications. This represents the worst-case scenario consequences of improper network deployments due to lack of planning data.

[13] Examples of possible tactile Internet applications: 'The Tactile Internet', ITU-T Technology Watch Report, August 2014.

9

9 Conclusions and recommendations

9.1 The scale of the challenge

The volume of new sites required for 5G infrastructure will be significant. The National Infrastructure Commission[14] found that around 40,000 5G access points may be required to serve the City of London with an area of 2.9km^2, whereas a similar number of access points today serve the whole of the UK, with an area of 242,000km^2.

To meet a challenge of this scale the public sector and industry will need to work together to plan and deploy 5G networks quickly and cost-effectively particularly within urban areas. To maximise ROI, use cases beyond 5G should be considered.

9.2 Street infrastructure

Mobile operators will need access to information about street furniture, existing fixed telco infrastructure and access to power. This will require a more collaborative approach between operators, local authorities and central government. There is a role here for cross-sector consortia by providing a platform-as-a-service for all stakeholders and facilitating the flow of the data required for 5G deployment. The key challenge lies in assembling and integrating all the necessary data, including planning permissions, land ownership, fixed telco and street asset data. This, in combination with accurate 3D mapping and signal propagation models, would provide an effective one-stop platform for collaborative 5G deployment.

In Section 6.4 we found that street furniture larger than specified dimensions (10cm at 26GHz, and 5cm at 90GHz) will affect signal propagation. Moreover, this applies not just to street furniture, such as lamp posts, but also attached objects, such as road signs, that exceed these dimensions. **It is therefore important to know precisely what street objects exist where and what other objects are attached to them.** Having attributed information about street furniture will help telco planners work more efficiently and minimise the need for site visits. In consulting with operators we learned that misleading or poorly-captured lamp post information provided by local authorities is a real issue today. Substantiating poor quality information costs operators large amounts of time and money, notably by requiring multiple site surveys.

Having free and unrestricted access to existing street furniture data for small-cell deployment will enable substantial cost savings, and will also help to deploy 5G networks within urban areas much more quickly. Furthermore, we suggest that data relating to public sector buildings should be available to enable mobile operators to install antennae on walls.

[14] 'Connected Future', National Infrastructure Commission Report, 14th December 2016.

The consultation process confirmed that accurate, authoritative, comprehensive, detailed and up-to-date data will significantly reduce costs later in the planning process. For this reason, the datasets that underpin an operational network planning tool should be continuously maintained and upgraded when new types of data become available.

9.3 The planning process

Asset location data need to be available as part of the planning process. Precise size and position has a significant bearing on high-frequency 5G signals. These data should be of sufficient quality and fit for purpose to minimise the risk of inaccurate decision making and preclude the need for expensive ground surveys.

Planning rules require operators to undertake consultations with planning authorities and affected communities. Making adequate information about planning restrictions, public sector buildings, site lease agreements and digging restrictions available at the beginning of the planning process on a common platform would be highly valuable, particularly if this could be viewed and interrogated in the context of a detailed 3D Digital Model such as the one we have developed for Bournemouth.

There are several regulatory and planning constraints relating to mounting equipment on lamp posts or on the sides of buildings[15]. Having insight into these constraints at the local level during the planning process would improve network modelling because initial site assessment would be possible from the desktop without the overhead of applying for constraint information to the local authorities.

In addition, pre-build address data, captured at plot level within proposed planning developments up to two years in advance, are valuable for 5G network planning as they allow mobile network operators to plan to meet future demand.

9.4 5G for road and rail

Thousands of small cells will be required along rail and road networks to provide future 5G coverage. Some cost reductions could be realised by enabling existing private fibre networks along road and rail infrastructure to be part of our future 5G infrastructure. Connecting small cells to fixed networks is the most cost-effective way of providing close to 100% coverage along critical road and railway networks across the country. However, from the planning point of view, the need for access to geospatial data, in this case of underground cables and road/rail infrastructure, remains the same.

Incorporating existing road and rail telco infrastructure into the 5G network will help accelerate the rollout process. Also, site deployment costs can be reduced and disruption to services minimised by using existing above-ground infrastructure such as overhead gantries, road signs and pylons. However, the challenge for future planners is to have access to accurate and current telco and above-ground infrastructure data. Having this information in one place would reduce both planning costs and the time required to gather the information.

Access to sites on the land adjacent to roads and railways is also required to provide backhaul support for small 5G cells. Enhancing the Digital Model with land ownership information and planning application capabilities will reduce administrative costs and give network planners greater flexibility to plan and deploy small cells more precisely and cost-effectively.

---

[15] '5G Infrastructure requirements for the UK - LS Telcom report for the NIC' LS Telecom Report for the National Infrastructure Commission, 12th December 2016.

9.5 Population data

To prioritise small cell deployment, planners need to know where there is demand. Different groups will use 5G networks in many ways, in most cases prioritising data over voice traffic. The applications we can envisage today include outdoor gaming, streaming live sports events in high resolution and connecting to autonomous vehicles. Anywhere that people gather represents a potential demand hot spot.

In Section 4.2.1 we describe population data from Health and Safety Laboratories. Enhancing the Digital Model with measured footfall data will be a valuable future step. Insight into how people move at different times and in different places will help deploy small cells more precisely, providing capacity to meet demand. Crowdsourcing from mobile devices represents a huge opportunity to model and predict demand more precisely, a capability which becomes increasingly important with directional antennae.

9.6 Vegetation and buildings

The results presented in this report demonstrate that vegetation objects (that is, trees and shrubs) with substantial foliage cause disruption to signal propagation above 6GHz. Further development of the 3D model will be required to address this. Specifically, it requires a vegetation model that precisely accounts for the area and type of plant and foliage over an annual cycle wherever small-cell deployment will take place.

Our research has proved that building surface type has an impact on the propagation of high-frequency signals, as variations in surface roughness cause significantly different scattering. Although most common types of building façade have been factored into our propagation model, further work is required to develop a more comprehensive model with additional façade classification and to model different types of building material within the Digital Model environment.

9.7 Weather

Our research into the impact of weather on high-frequency signal propagation concluded that UK rainfall and sleet conditions may limit the maximum separation of 5G access points, in particular in less built-up areas which on their own would encourage larger cell areas. As climate change is already causing unpredictable weather patterns across the globe and an increased likelihood of severe weather in the UK, there needs to be further research in this area and potentially the development of more precise weather models designed specifically for the telecommunication sector.

9.8 5G in context

Network operators told us that an improved planning tool would also help optimise current 3G and 4G networks. 5G will be a heterogeneous network which will function alongside legacy generations of mobile network as well as street Wi-Fi. It is therefore appropriate to consider a planning tool that will serve the needs of multiple communication networks.

9.9 Summary

The huge benefits and costs of deploying 5G represent a major challenge for all stakeholders. Making a success of 5G requires a greater level of collaboration than ever before to deliver new services while minimising timescales and costs.

The Digital Model that we have demonstrated in this study begins to define a vision of the future. Developing this concept into reality will provide reassurance to government, local authorities and regulators that network operators are working with the most up-to-date and accurate representation of the real world thus enabling efficient and effective rollout of a national 5G infrastructure.

A

Annex A: Data preparation and acquisition

Introduction

The objectives of this task were to investigate 3D geospatial data generation and modelling methods and to assess the usability of Ordnance Survey (OS) published data, data specifically collected for this task and third party data, for example Bournemouth Borough Council (Bournemouth BC) asset datasets in a 3D environment.

The research was carried out in late 2016 and early 2017. It aimed to establish how to extract, process and model data for use in a 3D environment with all associated attribution retained. It also considered how this work could be reproduced for future requirements.

Requirements

The 3D model had the following data inputs:

1. Point clouds derived from various sources: NADIR imagery, oblique imagery and mobile mapping;
2. Mesh data generated from oblique imagery, classified, attributed and in a 3DML format;
3. DTM raster data – dataset combined from Environment Agency (EA) data and mobile mapping data;
4. OS orthorectified imagery draped over the DTM;
5. Vector data:
    a. Bournemouth BC data – processed in the previous phase of the analysis;
    b. OSMM data: buildings, roads, bus shelters, bridges, terrainlets;
6. Newly-generated vector data for:
    a) Trees (using point cloud);
    b) Bridges (using non-vegetation classified point cloud and DTM difference in height);
7. 3D solid objects for:
    a) Newly-captured polygon vector data in the central area of the AOI using mobile mapping point cloud. After footprint capture, 3D extrusion was applied for telecoms boxes (telephone boxes, internet fibre boxes, grey boxes and green boxes) and telephone cabinets;
    b) Footprint polygons or point vector data, which were then extruded in 3D:
        - Bournemouth BC point data: lamp posts, sign posts, traffic lights, park benches;
        - OSMM polygon data: bus shelters;
8. Attribution – included in the attribute tables of the vector data and solid objects data.

A variety of GIS applications were used to manually capture and automatically generate data and embedded attribution.

The software that was required for this project stage is listed below:

- SURE (nFrames) – for 2.5D and 3D point cloud data generation;
- QT Reader - for point cloud visualisation;
- DAT/EM Summit Evolution and DAT/EM Landscape – initial test for capture of features on the point cloud;
- Skyline TerraExplorer Pro – to assist with feature data capture (telecoms boxes, street furniture, lamp posts, bus shelters, electricity network) on the terrestrial point cloud and the aerial mesh model;
- Esri ArcMap – manipulating and processing vector and raster data (assigning height, merge, buffer, clip, extrude);
- Esri ArcScene: - viewing data in 3D and carrying 3D operations with the 3D tools (e.g. 3D Editor, Adjust 3D Z); confirming data had been transformed with all available attribution;
- FME Workbench – for data transformation, primarily for creating 3D solid objects;
- FME Data Inspector – for data inspection.

We required software that could attribute and move data, including point clouds, meshes, raster and vector data, within a 3D environment. The software packages we used were capable of this. However, we had significant problems in the early stages with software crashes and data loading due to the very large data volumes.

The tables below summarise the sources of data used in this project.

Imagery datasets	Resolution and image overlap
OS Bournemouth	10cm GSD, 80/60 overlap
OS Bournemouth Oblique	7cm GSD, 70/70 overlap
OS Bournemouth	5cm GSD, 80/60 overlap

Table A-1: Imagery datasets used

Point cloud data sources	Type
OS Bournemouth, GSD: 10cm	Aerial - NADIR
OS Bournemouth Oblique, GSD:7cm	Aerial - oblique
OS Bournemouth, GSD:5cm, 80/60 overlap	Aerial - NADIR
Terrestrial LiDAR	Terrestrial mobile mapping
Leica Pegasus	Terrestrial mobile mapping

Trimble MX-8	Terrestrial mobile mapping

Table A-2: Point clouds data sources

Mesh model data sources	Type
OS Bournemouth Oblique, GSD: 7cm	Aerial - oblique

Table A-3: Mesh model data sources

Vector data	Content used
Bournemouth BC vector data	Geodatabases
OSMM data	• buildings • roads • bus shelters • bridges • terrainlets

Table A-4: Vector data sources

This project stage included the following tasks:

1. Production of aerial point cloud datasets of the entire AOI using both NADIR and oblique imagery;
2. Classification of the aerial point cloud datasets;
3. Re-registration of the mobile mapping data and its classification. This covered the Central AOI ($4km^2$ of central Bournemouth);
4. Capture of new records and validation of the position of existing records for telecoms infrastructure, lamp posts and bus stops within the Central AOI. This was done using mobile mapping point clouds, mesh model and DTM data;
5. Generation of a hybrid DTM from Environment Agency and classified mobile mapping data;
6. Assignment of base heights to all Bournemouth BC data records using the hybrid DTM;
7. Creation of 3D multipatch building objects with embedded attribution;
8. Creation of solid objects using the new/updated features captured from point cloud and mesh data within Skyline TerraExplorer Pro;
9. Assignment of underground height to electricity network data;
10. Assignment of attribution to trees vector data;
11. Cleaning of bridge data using the point cloud, mesh and DTM data. Bridges were cleaned to sit well on the DTM surface.

Figure A-1 illustrates a simplified workflow covering this set of steps.

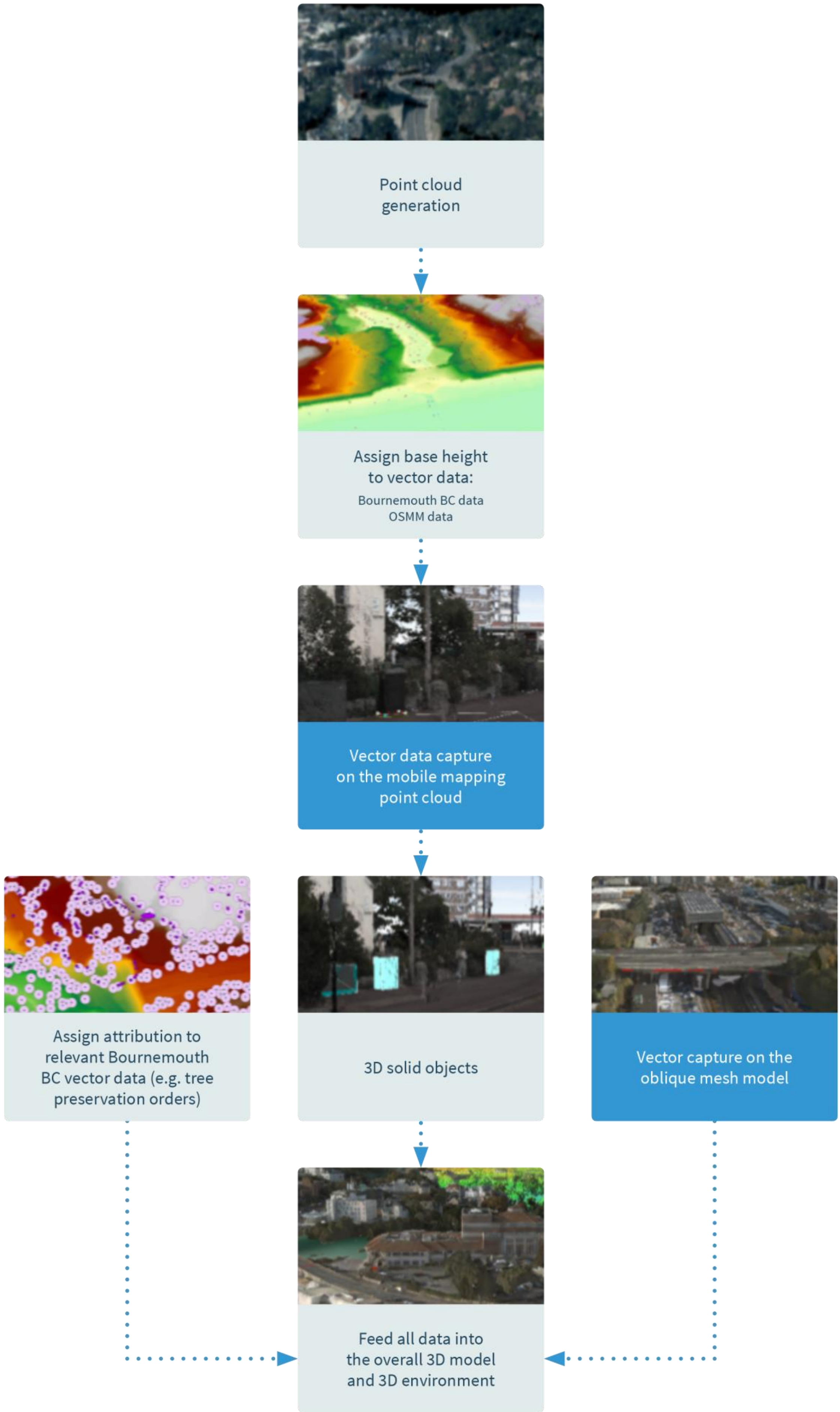

Point cloud generation
Assign base height to vector data:
Bournemouth BC data
OSMM data
Vector data capture on the mobile mapping point cloud
Assign attribution to relevant Bournemouth BC vector data (e.g. tree preservation orders)
3D solid objects
Vector capture on the oblique mesh model
Feed all data into the overall 3D model and 3D environment

Figure A-1: Simplified workflow

Method of data capture and enhancement

Data generation and transformation

GIS applications were used to interrogate the data and learn about the attribution for each dataset, both 2D (vector, raster) or 3D (point clouds), with the aim of automating as much of the workflow as possible.

Automated batch tools were utilised to process multiple files of vector data. The internal parameterisation of the processing pipeline was optimised to output consistent and accurate point cloud data. For this, additional information about the datasets was used for airborne (aerial NADIR or aerial oblique) pre-sets, with the overlap and resolution set to the appropriate values.

An important aspect in all data generation and transformation tasks was to validate the coordinate projection system (British National Grid), 3D representation (absolute or relative to terrain) and attribution of data.

Point cloud generation

Point cloud data were generated for the following imagery datasets:

- NADIR imagery – block flown with Microsoft Vexcel ULTRACAM XP9353 camera - 10cm GSD, 80/60 FOR/AFT overlap;
- Oblique imagery – block from a test flight with Leica RCD30-Penta oblique camera - 7cm GSD, FOR/AFT 70/70 overlap;
- NADIR imagery – block with 5cm GSD, 80/60 overlap.
- We chose SURE, dense image matching software, for point cloud generation. The software has modules for generating:
- Dense point clouds;
- DSMs;
- Meshes;
- True orthophotos.

For this project, the software was only used for dense point cloud generation.

As input data, images and orientation information were required representing the interior and exterior orientation parameters of the camera stations.

Imagery data were input as 1km geotiff format for the entire extent of the Bournemouth imagery block. Orientation data were input as project files created from orientation files.

The alignment between image name and orientation ID was matched and verified automatically.

Internal parameterisation of SURE was used to optimise the dense matching and cloud filtering processes. Specifically for airborne cases, it is strongly recommended to use the Aerial NADIR or Aerial Oblique pre-sets with the overlap set to the appropriate values (e.g. 80/60 or 70/70) because this allows for more object (e.g. buildings, vegetation, street furniture) coverage and information in the imagery, in particular for the sides and occlusions of the objects present in the images.

Point cloud data were outputted as 2.5D and 3D LAS point clouds (.las format). Point cloud filtering was continually improved to obtain precise and noise-free data. We achieved this by working closely with camera software manufacturers to manage issues affecting the imagery (such as sunlight conditions, clouds and flight conditions) which can significantly mask vital features, such as lamp posts, that we wished to capture.

Point cloud cleanliness and accuracy are defined by the level of noise in the data, point densities and vertical (Z) accuracy. These are key factors that influence the classification process.

Vector data

Shapefiles of interest were extracted from the Bournemouth BC geodatabases. These shapefiles were checked and edited for positional accuracy using the mobile mapping point cloud data. The following features were then extracted as individual files:

Bournemouth BC point data:

- lamp posts;
- sign posts;
- traffic lights;
- park benches;

OSMM polygon data:

- bus shelters.

Assigning base height to vector data

Base heights were assigned as follows:

- All Bournemouth BC vector data within geodatabases;
- OSMM vector data: bus shelters and bridges;
- Tree point data extracted from a point cloud from the Bournemouth NADIR aerial imagery.

To batch process these, an automated toolbox was created in ArcMap to iteratively interpolate multiple shapefiles stored either within a geodatabase or in a file folder, as illustrated in Figure A-2. Automation tools of this kind are vital to create efficiently new datasets suitable for 5G infrastructure planning.

The DTM used for assigning base heights to vector data was generated from a combination of EA and mobile mapping point cloud data. The inputs were in raster geotiff (.tif) format.

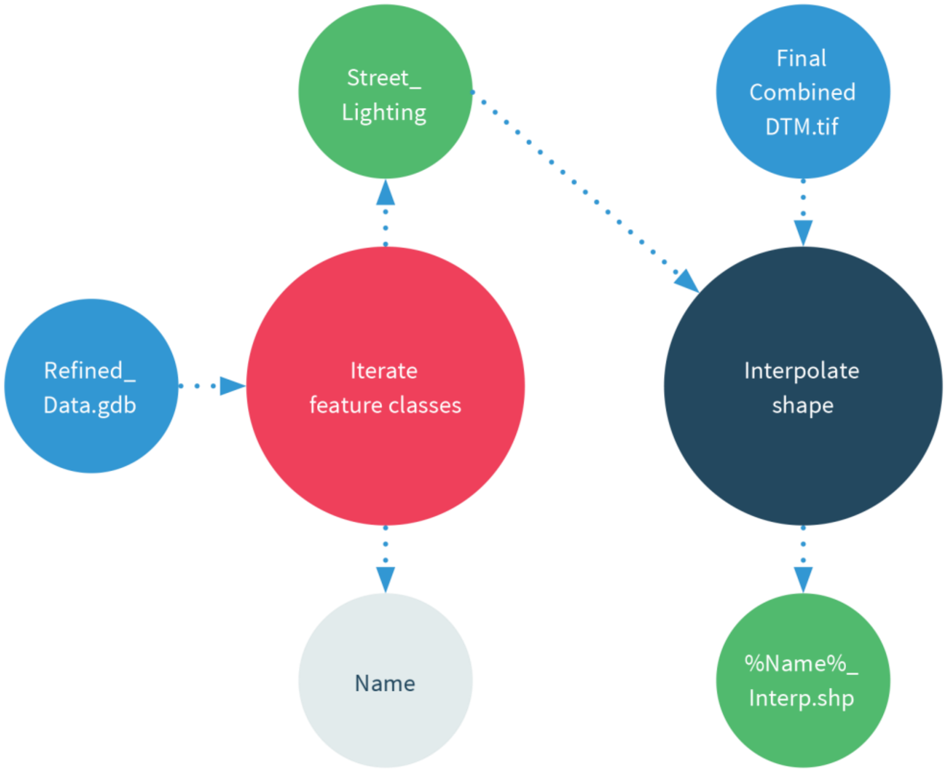

Figure A-2: Automated toolbox created for iteratively interpolating multiple shapefiles in a geodatabase or a computer folder location

Using a point cloud for data capture and enhancement

For this stage, only the Central deep dive area of the AOI was used. The chosen software solution was TerraExplorer Pro from Skyline.

The input data used was from a variety of mobile mapping systems chosen as they are common market technology offerings; unclassified, RGB coloured point clouds from the following sources/sensors and year:

- Terrestrial LiDAR;
- Leica Pegasus 2;
- Trimble MX-8.

Bournemouth BC lamp post data were heighted with the combined DTM. Lamp posts had already been captured as point shapefiles in the previous phases of this project. These shapefiles were interpolated using the combined DTM. Lamp posts are important features for 5G planning as they have a crucial role in enabling the receiving and transmission of 5G signals through the electricity network physically attached to the base of their structure.

The following datasets were used and edited in this stage:

- Street lighting errors repository – some lamp posts could not be captured accurately, even using the stereo imagery, due to overlapping canopies/shadows or unclear coverage. The points in this shapefile represent uncertain lamp posts locations. However, the mobile mapping point cloud allowed us to identify objects under tree canopies and at street level and enabled more accurate and precise feature capture. This is illustrated in Figure A-3.

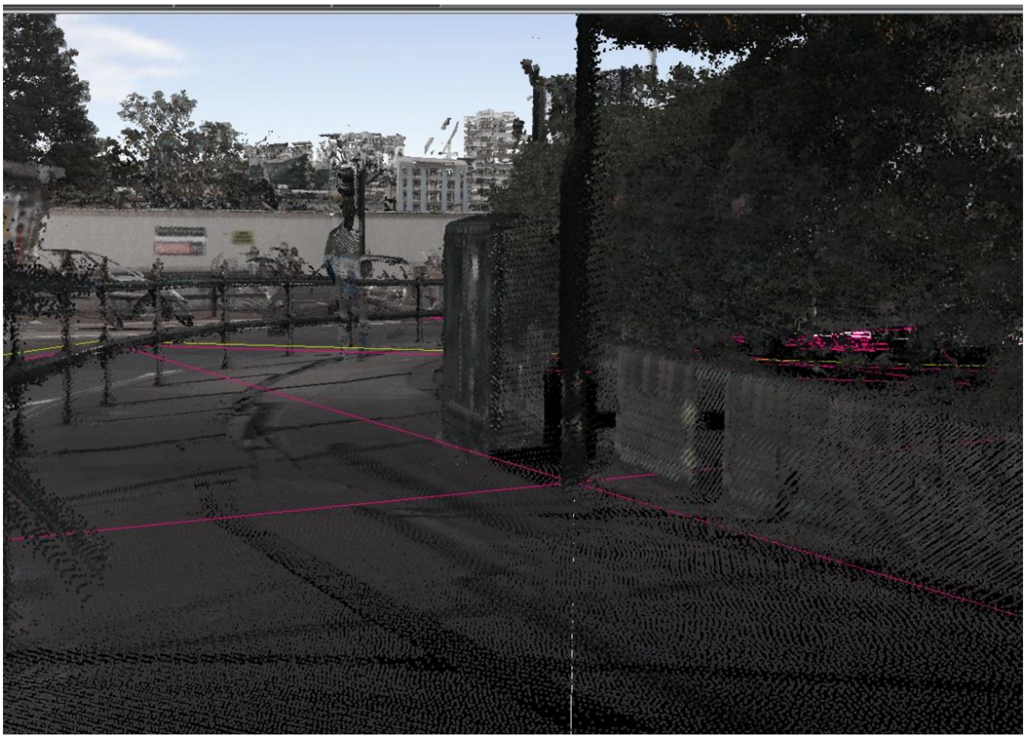

Figure A-3: Mobile mapping point cloud with lamp post errors shown as crossed squares

- Lamp post repository – lamp posts captured in phase 1 and 2 of the project, without positional accuracy issues, using stereo imagery.

New, empty polygon shapefiles (with Z values) were created in ArcMap to capture the following telecoms features:

- telephone boxes;
- internet fibre boxes;
- grey boxes;
- green boxes;
- telephone cabinets.

The 3D shapefiles were then loaded in as layers in ArcMap to start the data capture. Individual layers were turned on and off to avoid overloading the future graphical user interface with excess information.

All vector data were imported into the software aligned OS British National Grid coordinate system. Point data were represented as 'Absolute', whereas polygon data were captured using the 'Relative to Terrain' data positioning. This meant that data were positioned correctly under the OSGB coordinate system with accurate x, y and z values.

Editing

The telecoms objects were captured using vector editing tools in TerraExplorer Pro software, principally using the RGB coloured mobile mapping point cloud data. Lamp post point data were either edited or digitised for data positional accuracy and attribution. Examples of this are shown in the figures below.

Figure A-4: Capturing telephone box footprint on the point cloud

Figure A-5: Capturing fibre box footprint on the point cloud

Figure A-6: Capturing telephone cabinet footprint on the point cloud

Using a mesh and DTM for data capture and enhancement

For this stage, only the Central deep dive area of the AOI was used.

The input data used were:

- Mesh model generated from OS Bournemouth oblique imagery, 7cm GSD, 70/70 overlap;
- Combined DTM generated from EA and mobile mapping datasets;
- Bridge polygon shapefile – created semi-automatically using non-vegetation classified point cloud and DTM difference in height and clipped to an area around the roads.

Digitising and editing of bridge vector data were primarily based on the mesh model and to a lesser extent point cloud and DTM data. The resultant polygons were edited to ensure positional accuracy on the DTM surface. The basic workflow is illustrated in Figure A-7.

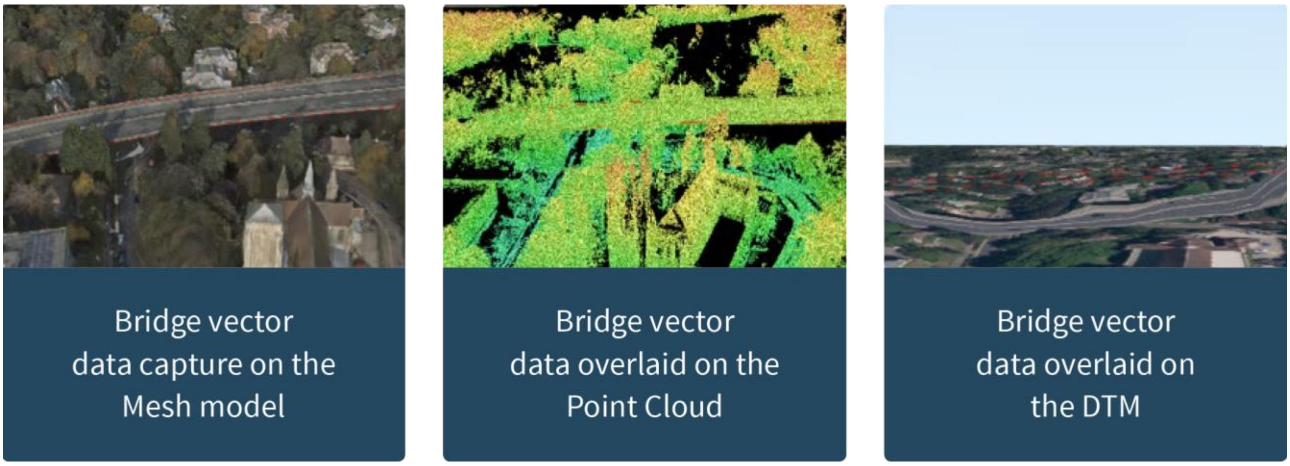

Figure A-7: Simplified workflow for bridge vector data capture

Creating 3D solid objects

This was a necessary step in the project. It provided 3D representations and additional information for features such as telecoms boxes. Having been generated, the solid objects were added to the overall complex 3D model for 5G signal simulation. The following vector data were used as inputs.

Telecoms vector features captured using the mobile mapping point cloud data:

- telephone boxes;
- internet fibre boxes;
- grey boxes;
- green boxes;
- telephone cabinets.

Interpolated Bournemouth BC point data:

- lamp posts;
- sign posts;
- traffic lights;
- park benches.

Interpolated OSMM polygon data:

- bus shelters.

For all input features, the vertical distance was measured using the MX-8 mobile mapping point cloud, as depicted in Figure A-8.

Figure A-8: Bus shelters - measuring vertical distance from a mobile mapping point cloud

These height values were recorded for each input feature and subsequently used to create input values for 3D solid objects.

Two FME workbenches were created for automating the generation of 3D solid objects for:

- extruding polygon vector data (telecoms boxes, telephone cabinets and bus shelters);
- buffering and extruding point vector data.

Assigning underground height values to electricity network data

The input data used for this task were interpolated Bournemouth BC shapefiles containing:

- Electricity ducting;
- Electricity low voltage network;
- Electricity high voltage network;
- Electricity joint nodes.

An underground height of -2m was assigned to these shapefiles using the ‘Adjust Z’ value tool in ArcMap.

Tree data – assigning additional attribution

The input data required for this task were:

- Individual tree point vector data from the classified point cloud using Global Mapper;
- Tree Preservation Orders data from Bournemouth BC with species and location attribution.

The first step was to buffer the tree points in ArcMap with a 5m radius, resulting in a circle polygon shapefile. This was used as an input in the ArcMap Spatial Join tool, together with the Tree Preservation Order polygon shapefile. The attributes were merged in the buffered tree shapefile using the Intersect option in the Spatial Join tool.

The final step was to convert the joined and buffered shapefile from a circle polygon shape format back to a point shape format using ArcMap.

Research findings and results

Point cloud data generation

Both the aerial and oblique point cloud results were very dense and with little or no noise. This high level of output quality is essential for 5G mapping purposes.

The algorithms in SURE software made intensive use of computer resources, especially the CPU. Processing times took up to 4 days to process a 25km^2 area using a computer with the following build:

- 64-bit operating system;
- 128 GB RAM;
- NVidia GeForce GTX 1080 graphics card;
- Intel Xeon E52677W 0 @ 3.10GHz.

We recommend a minimum machine specification of this build for point cloud data processing. Higher specifications would be required for faster processing.

During the project we were in regular communication with nFrames and as a result received updated versions of SURE software which provided higher quality results, notably relating to cloud filtering parameterisation. An example of the point cloud output can be seen in Figure A-9.

The point cloud output generated at this stage was used for classification purposes, that is, to be able to extract features of interest (ground, vegetation, buildings, street furniture etc.). It was therefore important to test the point cloud generation with different parameters so that the results would be as noise-free and accurate as possible to obtain a crisp and clean point cloud.

Figure A-9: Aerial point cloud generated from NADIR Bournemouth imagery

Assigning base heights to 2D vector data

All input vector data were interpolated using the DTM to provide a ground Z value for each feature. Creating and validating an automated toolbox to perform this took less than a day. The processing time of this toolbox was very short; output data were ready in under 10 minutes.

The resulting data were successfully validated in a GIS application to ensure the vector features were positioned accurately on the DTM surface.

New feature data capture from mobile mapping point clouds

The task of capturing telecoms data was hugely time intensive, and took over two weeks for the Central area of the AOI. Faster machines are only of limited help here as the limiting factor is human operator judgement on which features are important and which are not.

The capture process showed that different terrestrial point cloud capture technologies had differing densities, in areas such as occluded street-side areas for example, and positional accuracies. This underlined the need to ensure that capture specifications are well defined before the capture technologies are chosen.

The terrestrial LiDAR data were less utilised because it was a colourised point cloud without RGB colour values embedded into its individual points. This made it inferior in terms of the information it contained. However, it proved to be valuable in places where the other point clouds had gaps.

The editing tools in Skyline are relatively easy for mapping professionals to use and allow for digitising and moving objects or vertices in XYZ axes. Skyline also enables the copy and paste of features which, for example, allows rapid replication of adjacent telephone cabinets.

It was important to check that data were positioned correctly on the ground. Lamp posts were easily identified and captured in the mobile mapping point clouds which are collected through 360° at street level and contain points representing objects under tree canopies, shadows or other occlusions that cannot be identified in stereo imagery.

This innovative data capture method proved to be an effective and swift method of editing features, allowing for greater control when digitising in XYZ and capturing 3D information. Unlike stereo imagery, where z values must be visually judged, with the point cloud, polygon vertices are simply snapped to a chosen point (Figure A-10).

Figure A-10: Digitisation of telecoms vectors on the mobile mapping point cloud

New feature data capture from 3D oblique mesh and DTM

This was another highly resource-intensive task. However, digitising bridge data demonstrated the benefits of data capture using a 3D mesh because snapping vertices to the mesh yields a high level of accuracy.

The XYZ positional accuracy of the bridge polygons was checked using the DTM to match extents; where a bridge ends, the DTM surface should start. This revealed some mismatches in bridge extent coverage since mesh models are derived from an aerial source (top-down or oblique vision) while the DTM was derived from EA LiDAR and MX-8 mobile mapping. An example of a digitised bridge polygon is shown in Figure A-11.

Point cloud data were also used to check positional accuracy and to identify information under tree canopies, under bridges, in shadows and in other unclear areas.

Figure A-11: Digitisation of bridge polygon vectors on the oblique mesh model

3D solid object generation

Creating automated tools in FME proved to be time-intensive. However, once created, the actual processing time was under 10 minutes.

The 3D objects were then assessed for positional accuracy against the mobile mapping point clouds in TerraExplorer. We found that the resultant data are well overlaid in the 3D point cloud as well as in the 3D environment (Figure A-12), precisely keeping their position and attribution.

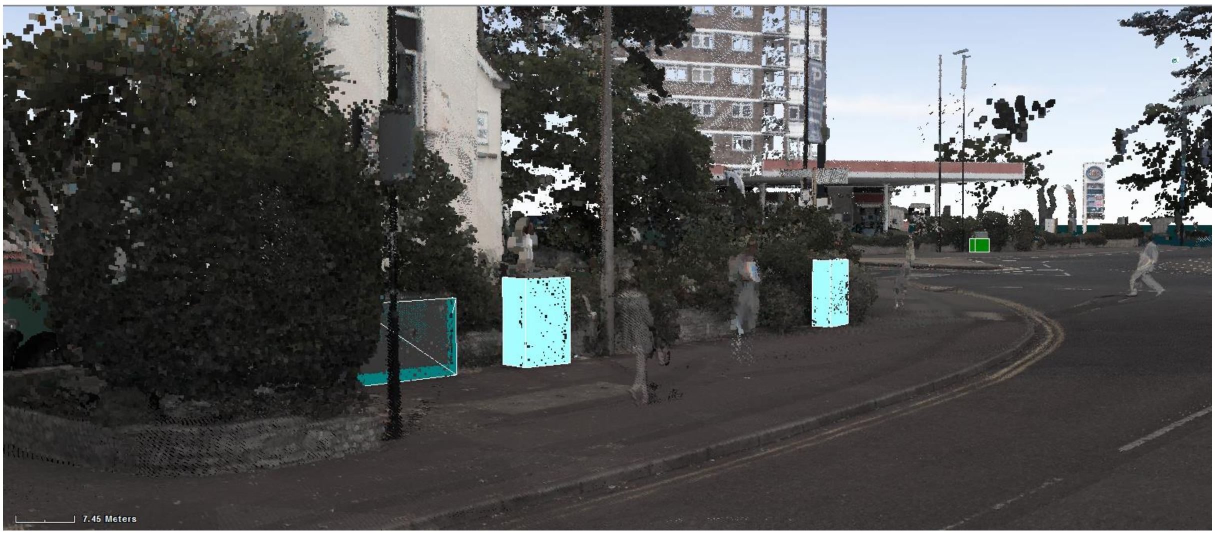

Figure A-12: 3D solid objects overlaid on a mobile mapping point cloud

Assigning underground height to electricity network data

After the electricity network shapefiles were assigned an underground height of -2m, they reflected their position on the ground more accurately. There was no need to create any buffer as symbology solutions can be applied when loaded in the 3D Skyline environment.

Attributed tree point vector data

The tree data output was enriched through intersection of polygon data containing tree position and species information. Attributes were transferred with all the values where the 5m tree buffer intersected a polygon from the Tree Preservation Order (TPO) data. Null values were assigned where the buffer did not intersect the TPO data.

This additional attribution (including species type, canopy geometry and foliage type) is useful for modelling the impact on high-frequency signal propagation. Further refinement of tree data could prove extremely helpful in the context of 5G planning.

Conclusions

This investigation confirmed the importance of highly accurate aerial and mobile mapping data for manual data capture, automated feature extraction and for visualising the urban landscape in different ways.

A range of typical off-the-shelf technologies were adopted and adapted for the project and other options are available. Technology in this area is progressing at a rapid pace and the best-fit technology mix may change in the future. This leads to a need to closely monitor the technology environment.

The data, once captured, must be securely referenced to the correct coordinate projection system and rendered to an appropriate level. Due to the levels of granularity in a very dense mobile mapping point cloud, any error more than 1-2cm makes a very large difference for data capture, and furthermore this has an impact on digitising accurately against point cloud data.

SURE software proved to be effective. It is completely automated for point cloud generation and has advanced parametrisation for cloud filtering processes. Similarly, there is plenty of scope for further development to meet future extraction requirements.

TerraExplorer Pro from Skyline proved to be very efficient for vector data capture in a 3D environment. An example of combined 3D data is shown in Figure A-13.

Both ArcMap and FME software were successfully used to automate iterative and simple operations such as merging, buffering, clipping and extruding data.

The level of detail and information in the 2D and 3D modelled data showed the potential for complex geospatial querying and analysis (such as line of sight and impact simulation analysis) in a 3D environment.

Figure A-13: 3D data in TerraExplorer Pro; point clouds, mesh, polygon vector data and 3D solid objects

Constraints and limitations

An important constraint to consider when dealing with a variety of 2D and 3D datasets is computer and software memory load as well as positional accuracy issues in some areas of the MX-8 mobile mapping point cloud. For this, alternative point cloud reference sources were used: Pegasus mobile mapping data and terrestrial LiDAR data.

Recommendations and next steps

This research showed that there are new and innovative ways of capturing vector data in a 3D environment. Both point cloud and mesh datasets need to have high accuracy values in terms of position and level of point density.

It is important to ensure that the data, on capture, are both securely referenced to the appropriate coordinate projection system and that data are rendered to a suitable level to avoid memory overload.

Imagery is still required at times for checking areas where the mobile mapping point cloud or mesh data lacked coverage. However, data capture using 3D point clouds and meshes has been shown to be an effective and swift method of editing features, allowing for greater control on digitising in XYZ and capturing 3D information about real-world objects. Moreover, these methods showed higher accuracy and efficiency in collecting z information compared to stereo imagery data capture, because data are directly taken from 3D points with RGB colour information embedded in the data, greatly facilitating human interpretation of the data.

The point density of mobile mapping point clouds needs to be very high to ensure data can be captured to the desired level of accuracy.

For the future development of point cloud generation, tools need to be understood and taken into account in data processing workflows. For example, near-infrared point cloud information can now be manipulated within software offering additional capabilities, and capability to use LAS 1.4 format offers additional point cloud classification versatility.

Batch processing of data enhanced the speed and efficiency of workflows, and this is recommended for use when dealing with multiple datasets. However, to work towards creating a fully attributed 3D environment, we were highly dependent on software and hardware resources which we could not fully anticipate at the start of the project. Subsequent work should consider the use of enhanced computer and software resources for a more cost-efficient workflow.

B

Annex B: Point cloud classification and feature extraction

Introduction

Scope

The work was carried out in late 2016 and early 2017 with the following objectives:

1. To output mobile mapping data in a standardised format;
2. To classify mobile mapping data so that their potential for feature extraction could be assessed;
3. To classify a point cloud to enable the extraction of information about vegetation which could potentially block signal propagation;
4. To output useful features for a final 3D model from the enhanced point clouds.

The purpose of this part of the project was to investigate methods of classifying extracting features from point cloud data. A point cloud is a set of data points with location and height values representing an area which can contain added attribution such as colour and classification. The term is not connected to the term ‘cloud’ as normally used by the telecoms community. The investigation aimed to establish the requirements needed to extract features as automatically as possible and to prepare data in a known and consistent format for use in a 3D environment with all relevant attribution maintained from the available data. Consideration was then given to how these methods could be replicated for future programmes.

The data from this part of the investigation were output into Skyline TerraExplorer software for further visualisation and analysis. Skyline TerraExplorer includes tools to create a high-resolution 3D environments for dynamic viewshed analysis.

Outputs from this phase of the project were then created in formats and co-ordinate systems which could be loaded into TerraExplorer.

Various datasets from Bournemouth BC were identified and collated including:

- Mobile mapping surveys;
- Aerial point clouds;
- Environment Agency digital terrain models (DTMs);
- Detailed mapping data from OS MasterMap Topography Layer.

Data preparation workflow

This section outlines the key tasks undertaken to prepare the data for analysis.

Point cloud classification consisting of:

- Converting point clouds from native formats and file structures into an accessible form;

- Evaluating the mobile mapping system point cloud classification using Realworks;
- Assessing how mobile mapping survey data are collected to improve the potential to automatically classify and extract features;
- Creating a combined DTM from mobile mapping data and Environment Agency LiDAR DTM;
- Classifying mobile mapping data to increase the accuracy of the roadside height model;
- Classifying the SURE aerial point cloud created from imagery captured by remote sensing using Global Mapper and FME.

Vegetation vector generation consisting of:

- Using the SURE V2 classified point cloud and FME to create polygons of areas covered by vegetation;
- Using Global Mapper and FME to extract information about individual tree points along with attribution about height and average crown width which was then combined with Bournemouth BC information relating to tree preservation orders.

Adding height values to detailed mapping consisting of:

- Creating Terrainlets – area polygons heighted using the combined DTM;
- Creating Multipatch building objects – 3D buildings from height data and building polygons.

Heighting road network data consisting of:

- Creating point clouds of individual bridge features in one of the ‘deep dive’ extents (the central area) of the AOI to create 3D meshes;
- Investigating automatically detecting and modelling of bridges using a variety of data and software techniques;
- Adding height values to road networks, considering bridges ‘over’ and ‘under’ each segment of the network. This was done to assist in the understanding of relationships between communication networks and help with the placement of street furniture.

Figure B-1 summarises the overall workflow used to prepare data for analysis.

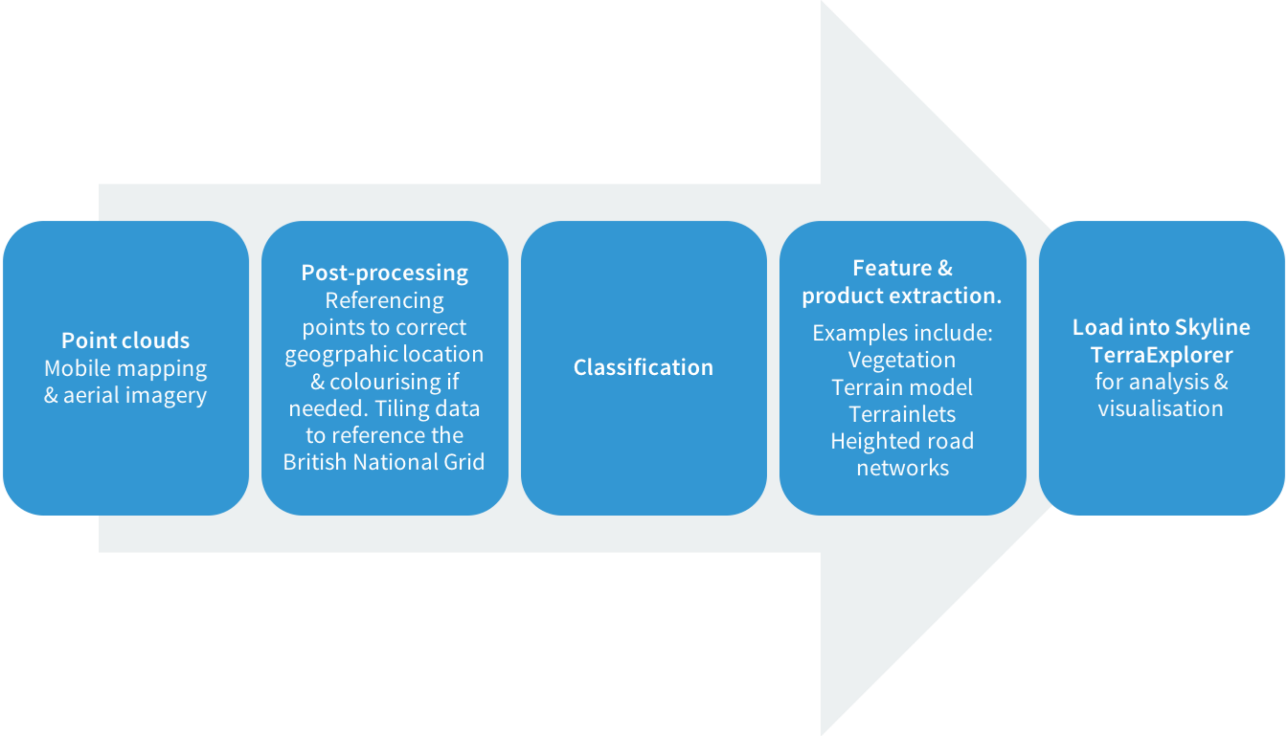

Figure B-1: Simplified workflow

Research methods

Software requirements

We were heavily dependent on a suitable software and hardware configuration to create a fully attributed 3D environment for the project. The software used, and the primary functions used, are listed below.

Trimble Trident

- Used for accessing the MX-8 mobile mapping data from its native format, georeferencing it, colourising it and converting it into LAS 1.2, the most widely used format for storing 3D point cloud data. The 1.2 version of LAS includes information about point colour, position and options for classification;
- The feature extraction tools in Trident were not used for this project.
- Trident is designed to process data from systems created by Trimble and stored in native Trimble databases.

Trimble Realworks

- Used for the classification of the mobile mapping point clouds;
- Data were imported in LAS format.

Global Mapper 18.0

- Used for classification of the aerial point cloud to assist in feature extraction;
- It is capable of automatic feature extraction from a classified aerial point cloud.

FME Workbench 2016.1

- Used for tiling final outputs into 1km tiles;
- Also used for enhancing the aerial point cloud classification;
- Used as a generic tool for point cloud and vector manipulation.

ArcMap 10.2.2

- Used for visualisation and analysis.

ArcPro 1.4

- Used for the creation of the building Multipatch objects.

Point cloud data available

The project used huge amounts of new and historic data from surveys collected from trials in the last 10 years. This has helped to investigate the utility of the systems and get a better understanding of the key aspects to focus on when conducting a mobile mapping survey.

Data were used from three surveys, the details of which are below in Table B-1. This provided a range of inputs of typical industry offerings. The different sensors (measuring devices) from different mobile mapping systems provide slightly different outputs. The configuration of the system and the way in which the survey is conducted result in different levels of relative and absolute accuracy. Depending on the type of sensor, they may come with cameras which capture imagery and can be used to add colour (RGB values) to the point cloud. This can be helpful for data capture and visualisation.

Sensor	Format	RGB Available
Pegasus 2 (Leica)	LAS 1.2	Yes
StreetMapper (3DLM)	LAS 1.2	No
MX-8 (Trimble)	LA20 *	Yes

Table B-1: Summary of mobile mapping data sources (*LA20 is a Trimble internal format)

An aerial point cloud was also provided using software called SURE from nFrames covering the entire AOI. The creation of data, using imagery collected and flown by Ordnance Survey, is discussed in Annex A.

Point cloud conversion

Key tasks

The key point cloud conversion tasks are listed below according to the sensor used for data capture.

MX-8

- Extract data from Trimble internal format were output as a colourised point cloud which could be viewed and analysed in other software;
- Classify the point cloud;
- Assess potential for automatic feature extraction;
- Tile into 1km tiles in relation to the National Grid to standardise and easily locate data for visualisation and analysis.

StreetMapper

- Classify the point cloud;
- Assess the potential for automatic feature extraction;
- Tile into 1km tiles;
- Use ground classification to assist in creating a DTM of the area.

Pegasus 2

- Classify the point cloud;
- Assess the potential for automatic feature extraction;
- Tile into 1km tiles;
- Use for visualisation and data collection in Skyline Software.

Street mapper survey process

The StreetMapper sensor system contains a 3D laser scanner and no associated imagery was captured. Permission was gained to capture data in some pedestrian areas of Bournemouth, for instance within the Lower Gardens, which was not covered in other surveys. The output data had been processed previously with Ground Control Points (GCPs) added in locations such as car parks to securely reference the data. These data were output as a non-colourised point cloud.

Pegasus 2 survey process

Pegasus 2 is a system produced by Leica. It is a single laser scanning instrument mounted on a vehicle with six cameras which combine to form a 360° view. This survey only followed three streets within the central area of Bournemouth. The data had been previously processed and output as a colourised point cloud, as illustrated in Figure B-2.

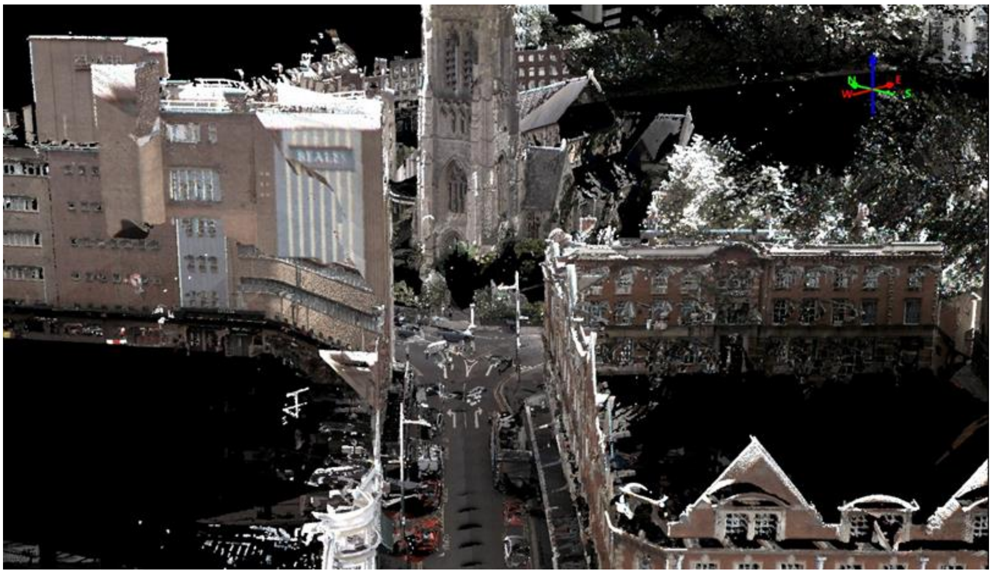

Figure B-2: Pegasus 2 point cloud

MX-8 survey process

The MX-8 survey data in Bournemouth was captured as part of mobile mapping trials investigating the manual capture of street-side assets. The collection and post-processing of the data were undertaken by Korec. The system consisted of seven cameras and two LiDAR scanners mounted in a pod on a specifically converted van. Three cameras faced forward, three cameras backward and one downward at the rear and well as a 360° panoramic camera mounted at the front of the vehicle. The survey itself was divided into the different roads. GCPs were not used in the post-processing phase for referencing the points to each other; the internal IMU/GNSS were deemed accurate.

The data were delivered in a Trimble database consisting of separate point clouds and images. An initial process was undertaken to extract the individual laser scans as a colourised point cloud in a format which could be opened in other software.

Colourising the point cloud

The ‘RGB Laser Colorizer’ within Trident (mobile mapping processing software from Trimble) colourises the laser points using the RGB colour values from the images in the camera system. The data had to be georeferenced with all the correct files present so that the software could recognise the corresponding images for each part of the scan.

To reduce the amount of the mobile mapping system visible in the colourised point cloud, two methods were available within Trident:

- Select front or rear facing cameras as preference for colourising the point cloud. For this system, the front facing cameras were found to be preferable as the laser scanner was mounted on the van behind the camera, dramatically reducing visibility from the rear-facing images;
- Create a ‘masking template’ to remove areas from the images that are not wanted for colourising the point cloud, for example the car in Figure B-3. A template image can be export and loaded into an image editing software, in this case GNU Image Manipulation Program (GIMP), where the area covered by the mobile mapping system is coloured in black (RGB values 0, 0, 0). These points could easily be filtered out if desired.

The final output of this process is shown in Figure B-4.

Figure B-3: Example of masking template for images. Areas not used for colourising the point cloud are coloured in black. This is automatically applied to all images in the scan.

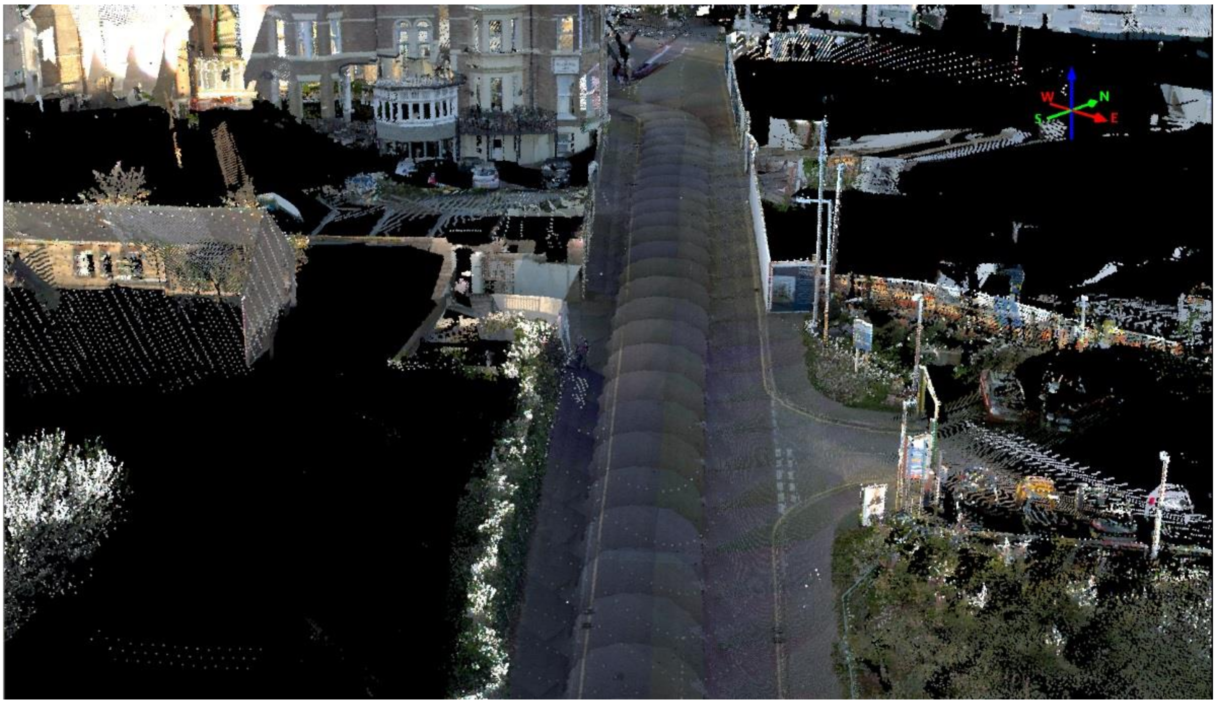

Figure B-4: Same location after the masking template has been applied

Registering and georeferencing scans

When the different scans were merged in 1km tiles we noted that in some cases there was an offset which could be present along the x, y or z axis to varying degrees, although usually less than 30cm (see Figure B-5 and Figure B-6 for examples). The process to match these scans together was explored within Trident with the following issues identified:

- When attempting to run the processing, repeated errors occurred suggesting certain key calibration and GPS files were missing from the database, preventing the process from running;
- It was difficult to identify how the data were processed and why these files had been missing as a third party had processed it.

Figure B-5: Z shift between scans in the MX-8 data, black lines indicate the ground level in the two different scans. The difference at this location is around 30cm.

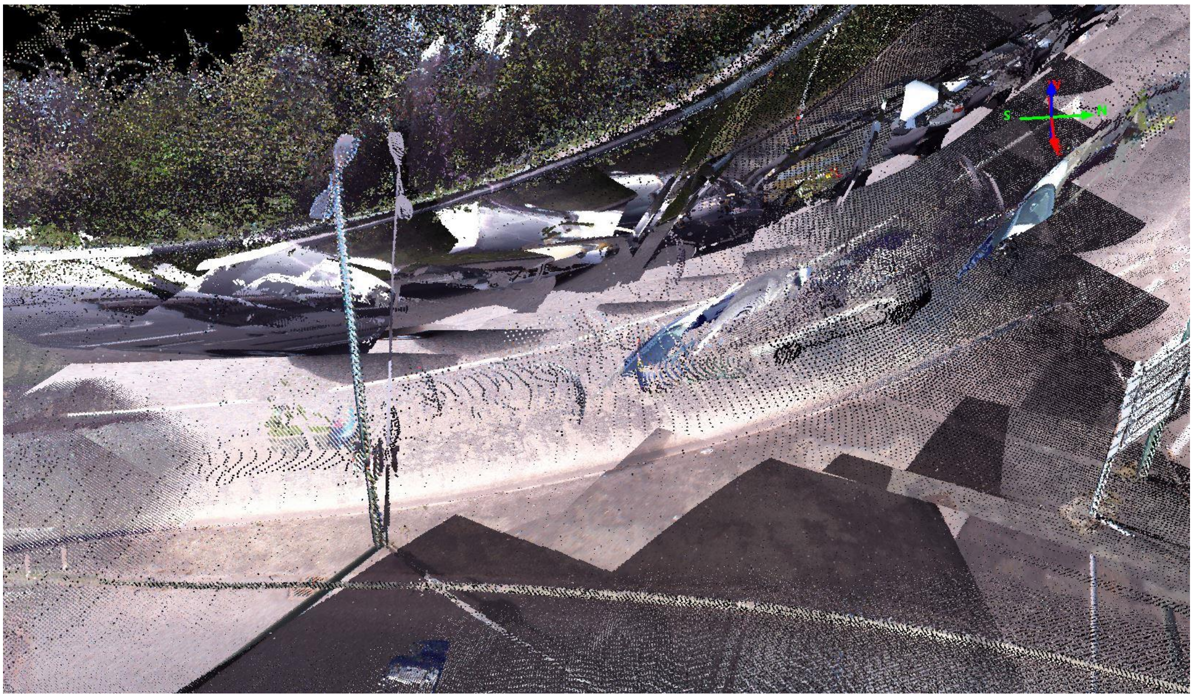

Figure B-6: Horizontal warping between scans causing ‘double lamp post’ effect

As this offset was unable to be resolved in the initial processing in Trident, the capability of Realworks Georeferencing tools were investigated. This software has two capabilities:

- Referencing data to another point cloud;
- Referencing data to a set of GCPs.

It was also noted at this point that some of the scans, although exported from Trident, were unusable because of gross errors in the GPS files as displayed in Figure B- 7.

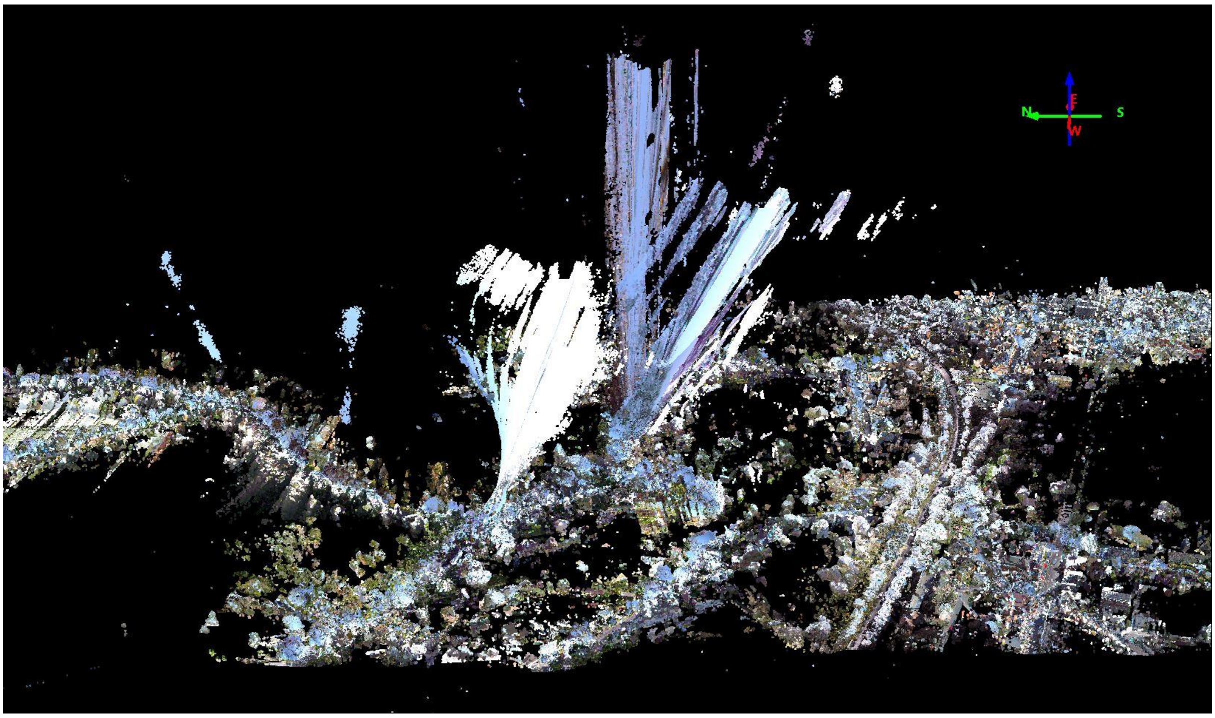

Figure B- 7: Example of large errors in GPS rendering scans unusable

Exporting colourised point clouds

The colourised point clouds were then exported to LAS 1.2 format using the 'Laser Point Cloud Export / Re-compute Module'.

Point cloud classification

Mobile Mapping – RealWorks

The mobile mapping datasets were loaded into Trimble Realworks to be classified automatically. Realworks has the capability of classifying point clouds into:

- Pole – individual features identified;
- Building – individual features identified;
- High vegetation;
- Unclassified (all other features);
- Ground.

The classification process is fully automatic - there are no parameters to alter. The process can be re-run iteratively to improve the classification, reducing the number of features left unclassified. These were then exported as LAS point clouds.

Subsets of data representing the individual bridge extents in the Central Area were clipped manually from the MX-8 data (Figure B-8). The bridge features were output as individual E57 point clouds to enable meshes of the individual structures to be created. These were then loaded into Skyline and used for visualisation and analysis.

Figure B-8: Individual point clouds of bridges exported to be converted into 3D meshes for display and analysis in Skyline

Classification process in Global Mapper

Global Mapper works by classifying points based on their planar relationships to each other.

The main steps of classification are:

1. Classify noise points – that is, extremely high and low points outside expected elevations;
2. Classify ground points – that is, points representing the ground surface;
3. Classify non-ground points – that is, everything else, including trees and buildings;
4. Extract vector features.

Each of these processes has several parameters which were adjusted to consider the nature of the point cloud.

Global Mapper classifies points into five classes:

- Building;
- Vegetation;
- Ground;
- Unclassified;
- Noise.

There is also a capability to manually assign points to these classes as well as to Water, Low and Medium Vegetation. There is functionality to semi-automatically extract overhead powerlines but a very dense point cloud is needed and it was not tested in this project as there were a limited number of overhead lines in the Bournemouth area.

Prior to using Global Mapper for the Bournemouth 5G project, the software was tested for its capability using subsets of different point clouds produced from several different systems in the Bournemouth area. This assisted in getting a better understanding of the classification process in Global Mapper as well as its strengths and weaknesses. There were some key parameters that had to be set. These could be adjusted each time depending on the point cloud being processed.

Important methodology points which were carried through from the original testing:

- Features are classified in Global Mapper based on their 'texture' over a certain distance. It is therefore important not to have too much smoothing within the point cloud. This makes it difficult for the software to differentiate between non-ground features;
- Global Mapper needs an unclassified point cloud as input;
- Global Mapper appears to be less effective for classifying mobile mapping data than aerial data;
- The size of point clouds Global Mapper could process was limited by the memory available. We recommend a minimum specification of RAM equal to 1.25 the size of the point cloud data file.

The newly created SURE aerial point clouds were classified in Global Mapper. These were divided into three projects due to the limiting factor of computer memory.

Enhancing Global Mapper classification process

The initial outputs from Global Mapper were found not to be refined enough for the process of feature extraction. The ground classification was suitable. However, there was still some misclassification (mainly around the edges of buildings and within vegetation). FME was used to enhance the classification using other input sources, namely:

- 1m resolution NDVI raster created from the 4-Band orthorectified images of Bournemouth to assist in identifying areas of vegetation;
- Ordnance Survey building polygon data representing the geographic extent of building footprints;
- The combined DTM created from the mobile mapping data and Environment Agency LiDAR.

Once these data had been reprocessed, they were fed back into Global Mapper to be used for automatic vector feature extraction. This is the process whereby the operator automatically extracts features such as building footprints and points representing individual trees. A final process of enhancement was conducted after vector feature extraction using the building polygons created in Global Mapper. The point cloud was input into FME and the vector features were used to clip and reclassify the final smaller areas of vegetation still misclassified on certain buildings.

Feature extraction

Several products needed to be output using point cloud data for analysis in the final model as well as for use in later stages of processing. These were:

- Individual tree points with height and crown attribution;
- Combined DTM;
- Heighted road networks – to assist in identifying different heights within the data and provide additional attribution;
- Locations of bridges;
- Multipatch building objects.

Combined DTM

Environment Agency's 50cm raster DTM, created from LiDAR data, was selected for its high resolution and its full coverage across the AOI. The raster was converted into a TIN surface and heighted shapefile points with 0.2 thinning using ArcGIS.

The ground (bare earth) classification was used to enhance the DTM along the road surfaces and in some pedestrianised zones within the central area of Bournemouth; the coverage extent can be seen in Figure B-9. The mobile mapping data were thinned slightly and output as shapefile points to reduce data sizes. We recommend the use of 0.03m thinning based on our experience to retain roadside detail, such as kerb lines, in the final output.

Figure B-9: StreetMapper data extents

The points were removed from the Environment Agency DTM in the area covered by the mobile mapping point cloud. These were then replaced by the higher resolution points from the mobile mapping data. The combined points were converted into a TIN and the 'Outlier Analysis' tool was run on the data in ArcGIS which removed wells and spikes. The TIN was then visually inspected for errors. Some breaklines were added around the edges of bridges to help define changes of slope within the data. The final output was exported as a 0.5m resolution Geotiff file for input into Skyline. This was also used as a basis for adding height values to the feature data collected manually and acquired from Bournemouth BC to provide consistency across all data sets. The result is illustrated in Figure B-10.

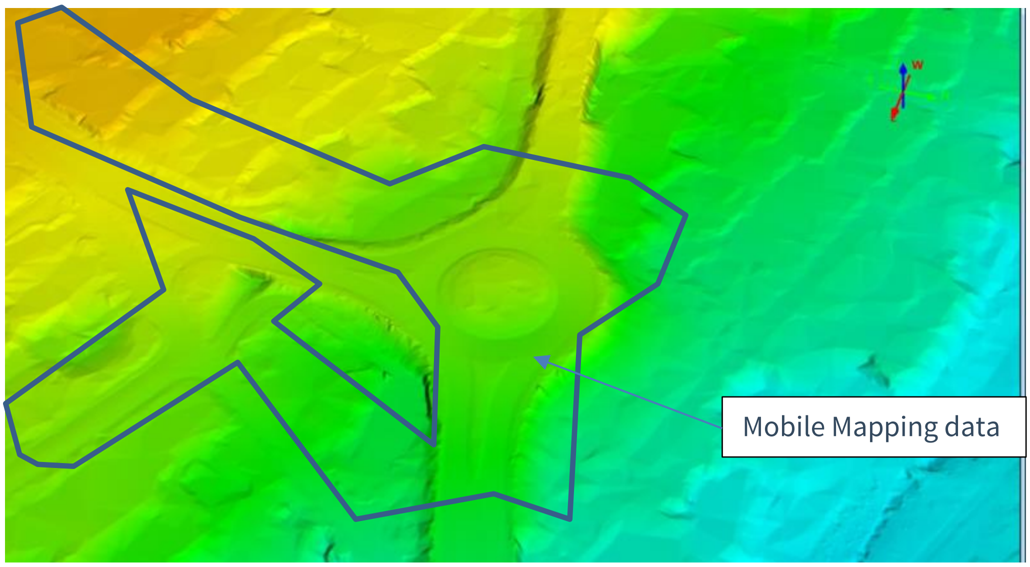

Figure B-10: Combined DTM (mobile mapping and Environment Agency aerial LiDAR). The mobile mapping adds extra definition around the road surfaces such as kerb lines and a smoother road carriageway. This can be used for more accurate heighting of other features for use within the Skyline environment.

Terrainlets

These were created in ArcGIS using mapping polygons which were heighted using the Combined DTM to create Multipatch objects retaining the mapping attribution. These were used for visualisation and viewshed analysis in Skyline to provide an accurate heighted representation of the mapping data for use in a 3D environment.

Attributed Tree Points and Areas

Points representing individual trees within the area of interest were created using the 'Extract Vector Features' tool operated on the classified SURE aerial point cloud. This tool creates points at the calculated tree top location. Each point is then attributed with height, average crown size and maximum crown size. Whilst the height attribute values seemed valid, and the individual tree points appeared to be situated at valid locations, the crown widths appeared to be the same for every tree. Moreover, some trees were incorrectly classified by the software and positioned within some of the buildings due to some misclassified points not removed in the classification refining process. Areas representing the building footprints were extracted automatically using Global Mapper and used to remove any tree points which fell within them.

To create better approximate tree crown measurements, FME was used to create polygon features of the tree coverage as defined by the classified aerial point cloud. These were filtered only to extract areas of vegetation over $4m^2$ to remove poorly classified points such as areas in the centres of buildings, and some smoothing was applied. These polygons were then segmented up by point and an average tree crown calculated from the polygon extent. An example of this can be seen in Figure B-11.

Figure B-11: Tree polygons segmented to assist in calculating average crown width

This was then used to attribute the points which were loaded into Skyline with a 3D model template created in Blender software. The 3D model had to be simple enough for Skyline to be able to load it, but with enough detail to be effective for 3D analysis (Figure B 12).

The tree polygons were tiled into 1km tiles and used to attribute mesh models in Skyline City Builder, a tool which merges feature layers and mesh layers together into a format optimised for visualisation and analysis in Skyline TerraExplorer. This generates interactive mesh models where features can be selected by the user, switched on and off, attribution displayed and queried. It is an effective way of combining 2D mapping with 3D real-world visualisations in an intuitive way.

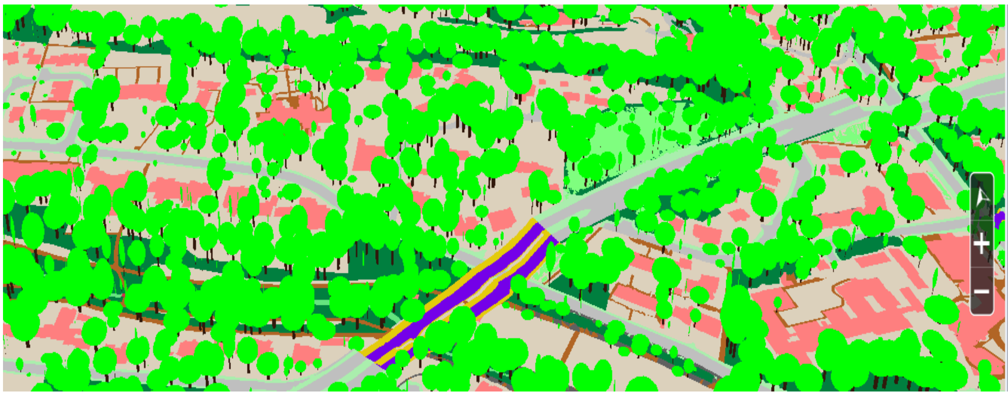

Figure B 12: Simple 3D tree models displayed on the terrainlet data in Skyline

Bridges and heighted integrated transport network

Bridge polygons were created semi-automatically using the classified point cloud with the vegetation points removed using an FME workbench. Other features used to identify the classification were the Combined DTM and mapped road and building polygons. The final output was visually inspected for any remaining false positives, wrongly indicating the presence of a bridge.

The areas representing bridge extents were used to clip and height the road network data to model them in a 3D environment while retaining associated attribution. If a DTM only was used, any links passing over bridges or in tunnels would be incorrectly heighted. The road network link identified to be on the bridge had a higher 'grading' which was attributed on capture for the purposes of network planning. An attribution of 1 represents a road on a bridge over another road, and 0 for a road beneath a bridge beneath another road.

Attribution from OSMM polygons was queried at the point of road network intersections to identify which type of feature, such as a railway, crosses a road and whether it lies over or under the road in question (see Figure B-13).

Figure B-13: Example of railway and road networks in relation to OSMM

All features were heighted using the combined DTM except for those on bridges which were heighted using the classified aerial point cloud with vegetation removed. The only situation where this did not work was where a road went underground into a small tunnel. The heighting of the data was achieved using ArcMap 10.2.2. The final result can be seen in Figure B-14.

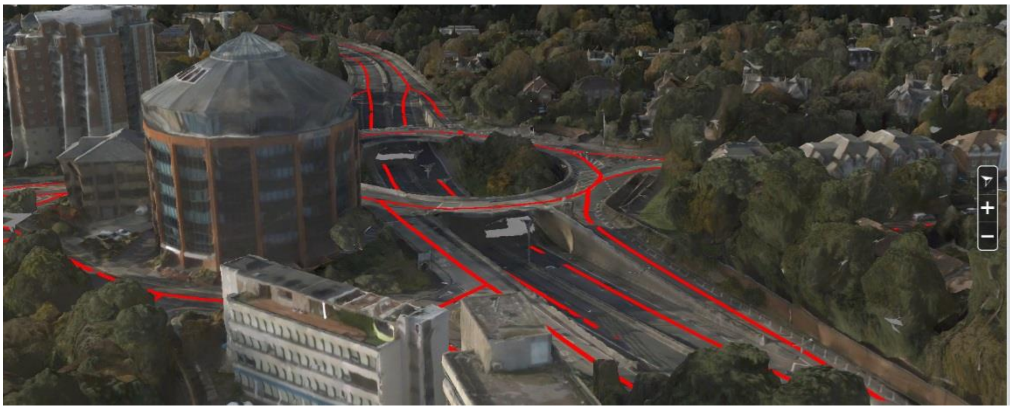

Figure B-14: Heighted road network over mesh created from oblique imagery and displayed in Skyline TerraExplorer

The bridge polygons were generalised and extruded to create 3D objects, but the output was considered to be too rough to be of value in a 3D environment. This is illustrated in Figure B-15 where areas have been cut out of the bridge due to the encroachment of overhanging vegetation on the bridge surface. These polygons were therefore used as a guide for manual capture.

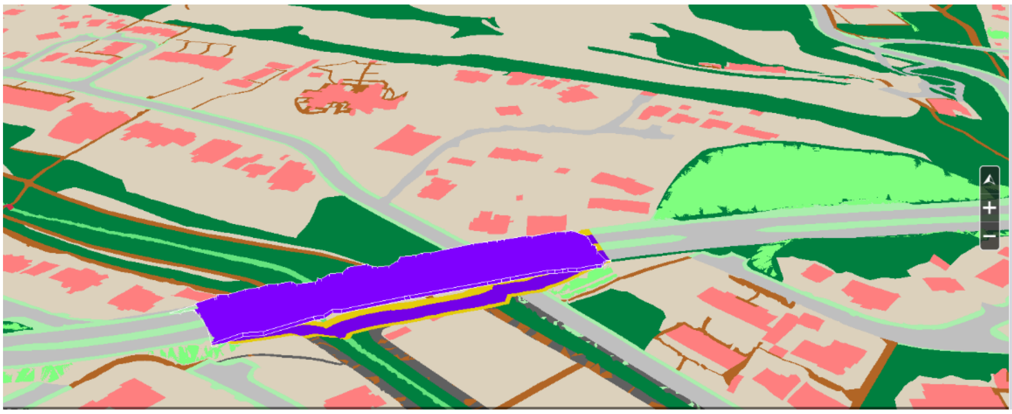

Figure B-15: Automatically generated 3D bridge displayed in Skyline over the terrainlet data

Multipatch building objects

With the new release of ArcPro 1.4, a new tool became available called 'LAS Building Multipatch'. This directly used a classified point cloud, building footprints and the combined DTM to create 3D building models. The classified aerial point cloud was thinned in FME to improve processing speed. The points classified as buildings (using building area polygons) were used to height the roofs, and the combined DTM to provide base heights. Due to the data volumes, buildings were output as a feature class in a geodatabase format as they exceeded the limits of shapefiles.

However, loading large volumes of complex features such as these created problems and options were investigated to simplify the data further or tile it into smaller files, and we found that simplifying the data further produced the best results.

Research findings & results

Mobile mapping outputs

The ‘offsets’ between some scans were usually less than 30cm. For automatic feature extraction these levels of accuracy proved insufficient. Some surveys were also not usable due to errors in the GPS which we believe occurred because the positional accuracy could be affected by satellite drop out caused by trees, vegetation and high buildings obscuring the data (see Figure B-16).

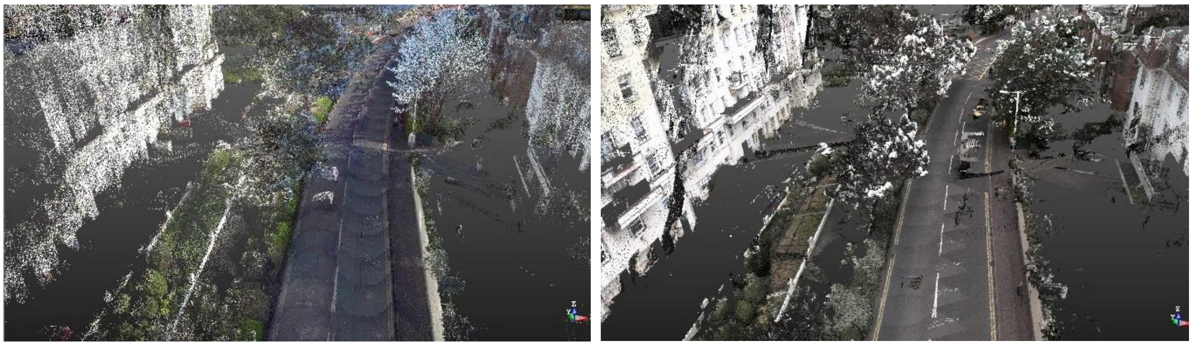

Figure B-16: Left: colourised point cloud output from MX-8 system; right: colourised output from Pegasus 2 system

The output produced from the different systems produced different quality results. However, the non-ground feature classification appeared to be mixed as can be seen in Figure B-17-Figure B-19. In general, across all data sets, the software does not seem to be suitable for extracting non-ground features automatically.

Compared to aerial sources, the mobile mapping systems provided greater visibility beneath vegetation (see Figure B-20). This was, therefore, the most suitable dataset to be used as the basis of manual capture and repositioning of street-side furniture. However, the other datasets could be used to augment this in areas for which they were available.

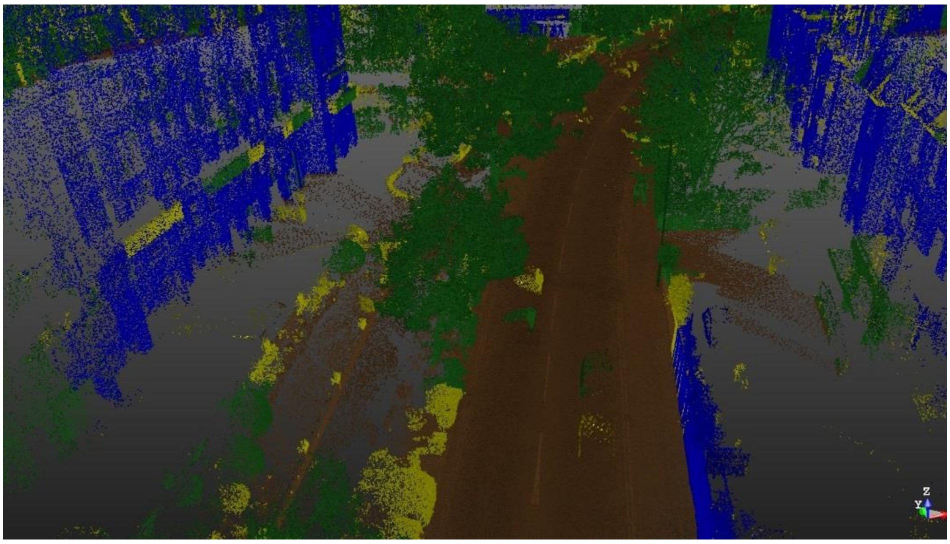

Figure B-17: MX-8 data classified in Realworks. Brown - ground, blue - building, green - high vegetation (trees)

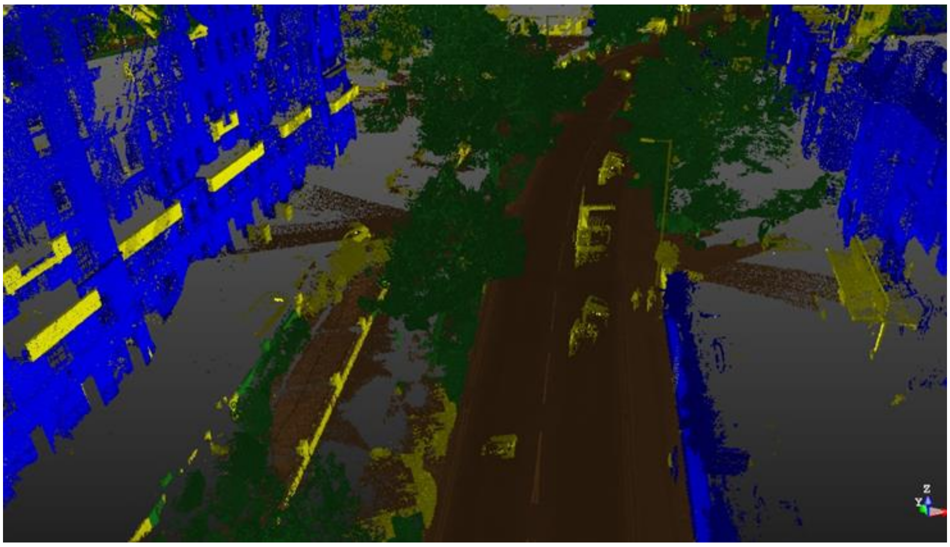

Figure B-18: Pegasus 2 data classified in Realworks. Brown - ground, blue - building, green - high vegetation (trees)

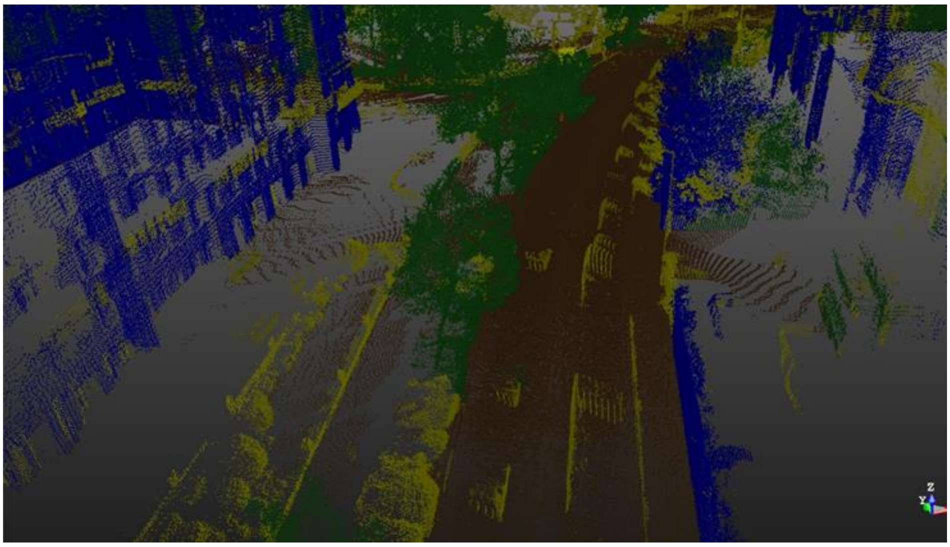

Figure B-19: StreetMapper data classified in Realworks. Brown - ground, blue - building, green - high vegetation (trees)

Figure B-20: Example of output colourised MX-8 point cloud.

Aerial point cloud outputs

The outputs from the classification can be seen in Figure B-21. There are some consistent errors from this output:

- Large buildings have their outside edges classified as building, but are otherwise classified as ground;
- Edges of buildings, chimney pots and other changes in surface in a building roof were misclassified as vegetation (Figure B-22);
- For the data to be classified as vegetation, the point cloud needs to have a rough texture. This is how the software differentiates between building and vegetation. As a result, smooth areas within areas of vegetation are classified as building. (Figure B-23).

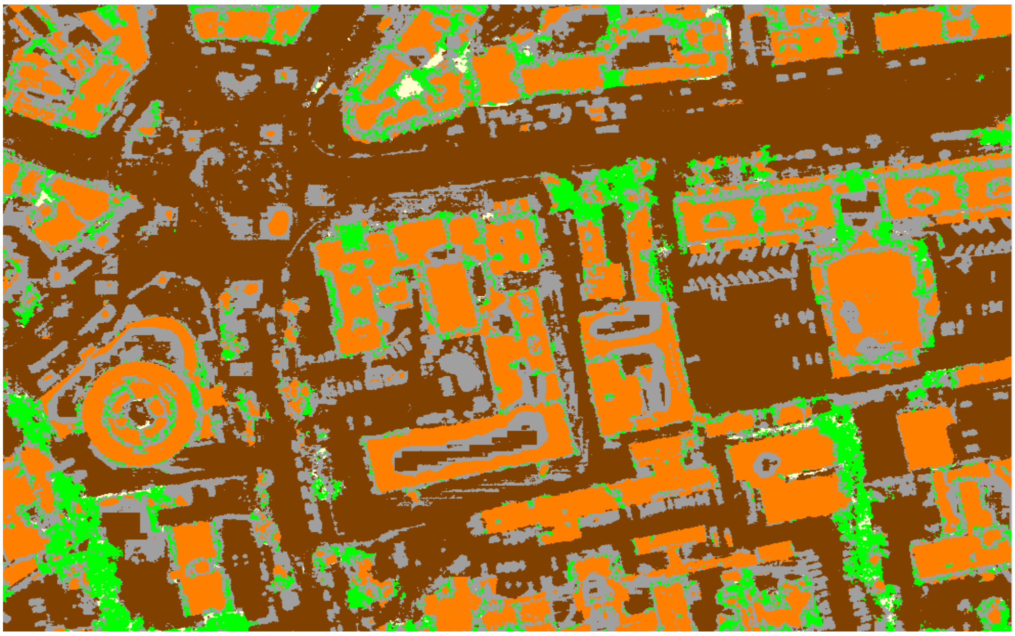

Figure B-21: Output from Global Mapper classification, no additional processing

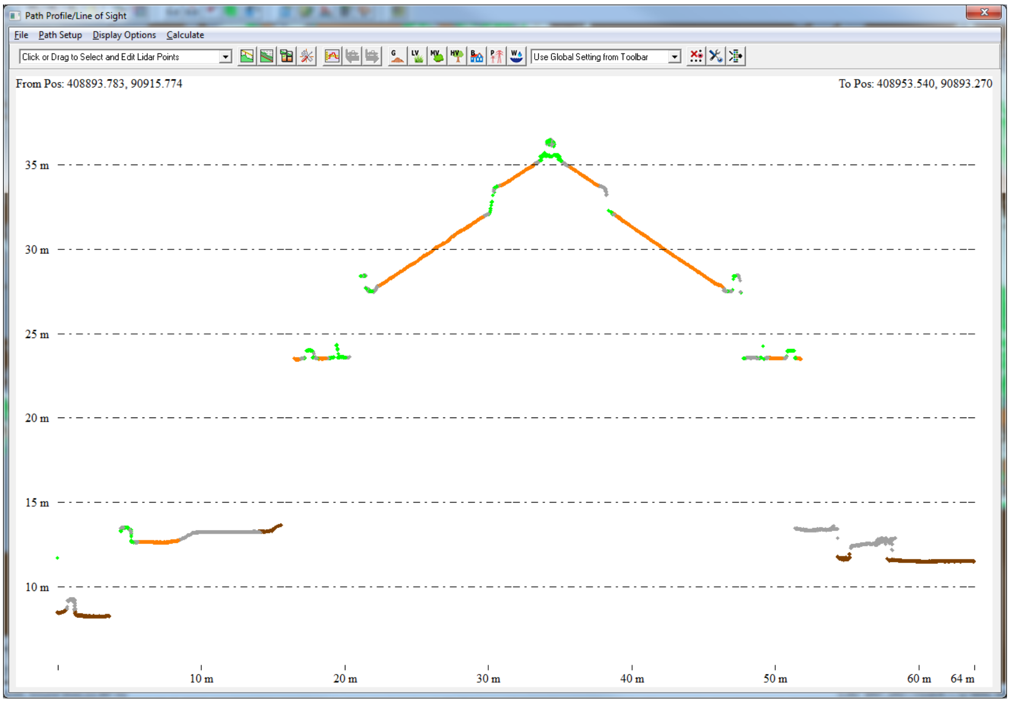

Figure B-22: Edges of buildings classified as vegetation in Global Mapper. Orange - building, green - high vegetation, brown - ground, grey - unclassified

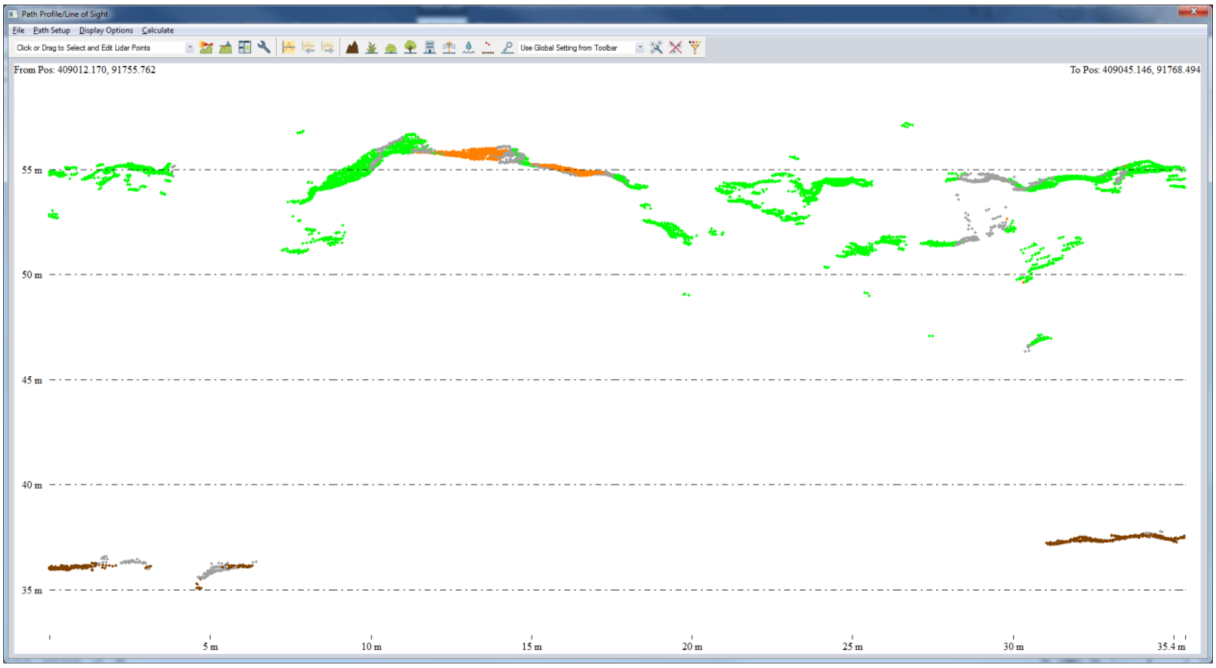

Figure B-23: Profile of area of trees displaying the effect of smoothing in the point cloud causing misclassification of vegetation. Orange – building, green - high vegetation, brown - ground, grey - unclassified.

After processing the data in the FME workbench, the output is much clearer (Figure B-24). There were still some errors, mainly small areas of vegetation points on roof areas. However, the point cloud proved suitable at this point for feature extraction from Global Mapper of trees and building polygons without too many false positives.

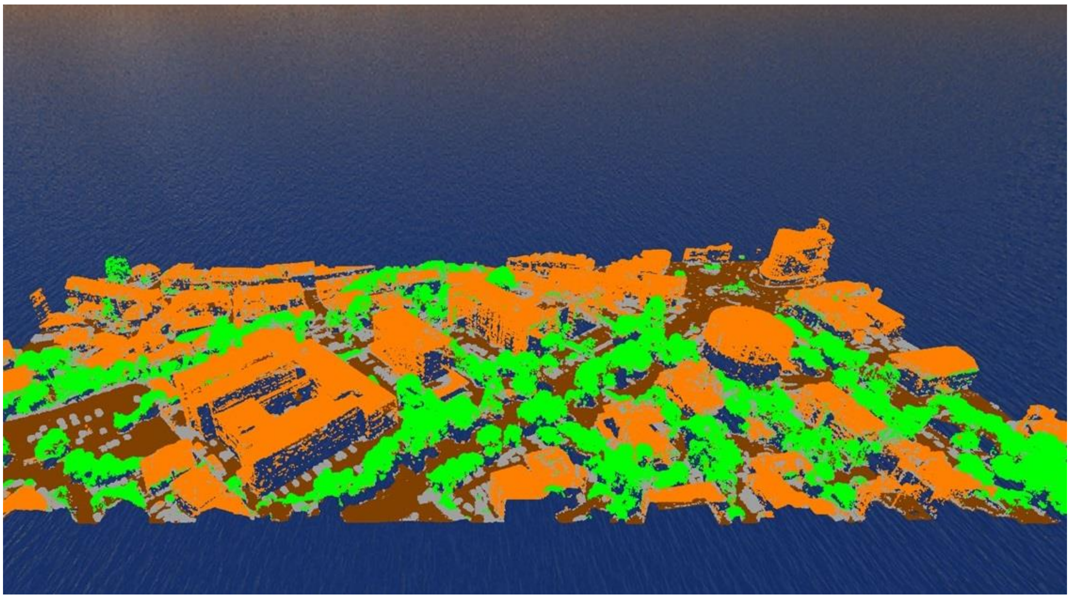

Figure B-24: Final output of SURE Point cloud classification after processed in Global Mapper and FME

Conclusions and recommendations

This project has highlighted the value of high-accuracy terrestrial mobile mapping data for more automated methods of feature extraction. There is a need to ensure that the data being captured are fully georeferenced to real world GCPs and to other scans. Due to the levels of detail involved in a high density mobile mapping point cloud, any positional error of more than 1-2cm makes a very large difference. It is difficult to reference more than a couple of scans together after the fact.

Typical data collection and processing technologies were used in this project and this technology mix may change going forward to give the optimum result.

To improve the classification and usefulness for feature extraction, a point cloud with this sort of error would be preferable.

It is possible to combine the ground classification from terrestrial and aerial LiDAR to produce an effective DTM for heighting data within a 3D environment. This provides highly accurate information to add height data at the street level, where analysis for signal propagation for 5G is most important, and provides a consistent base for all datasets.

Recommendations:

- When mobile mapping data are collected, they need to be very securely georeferenced for the highest levels of accuracy for future use;
- Ground control points for the mobile mapping data should be collected in areas where multiple scans overlap;
- Maintain detailed documentation or continuing in-house expertise on any data collected, to maximise its future utility / remain aware of its limitations;
- Whilst the aim is to reduce the amount of manual classification, this is still required today.

Next steps:

- Trial other automatic classification and feature extraction software that is commercially available;
- Engage with software vendors to support the development of improved automated classification software solutions to increase data collection speeds and reduce costs for creating data for a 3D environment;
- Investigate semi-automated approaches to feature extraction which could speed up data capture where fully automated classification is not possible.

C

Annex C: Lifecycle of a 5G coverage plan

Derived from consultation with the mobile industry.

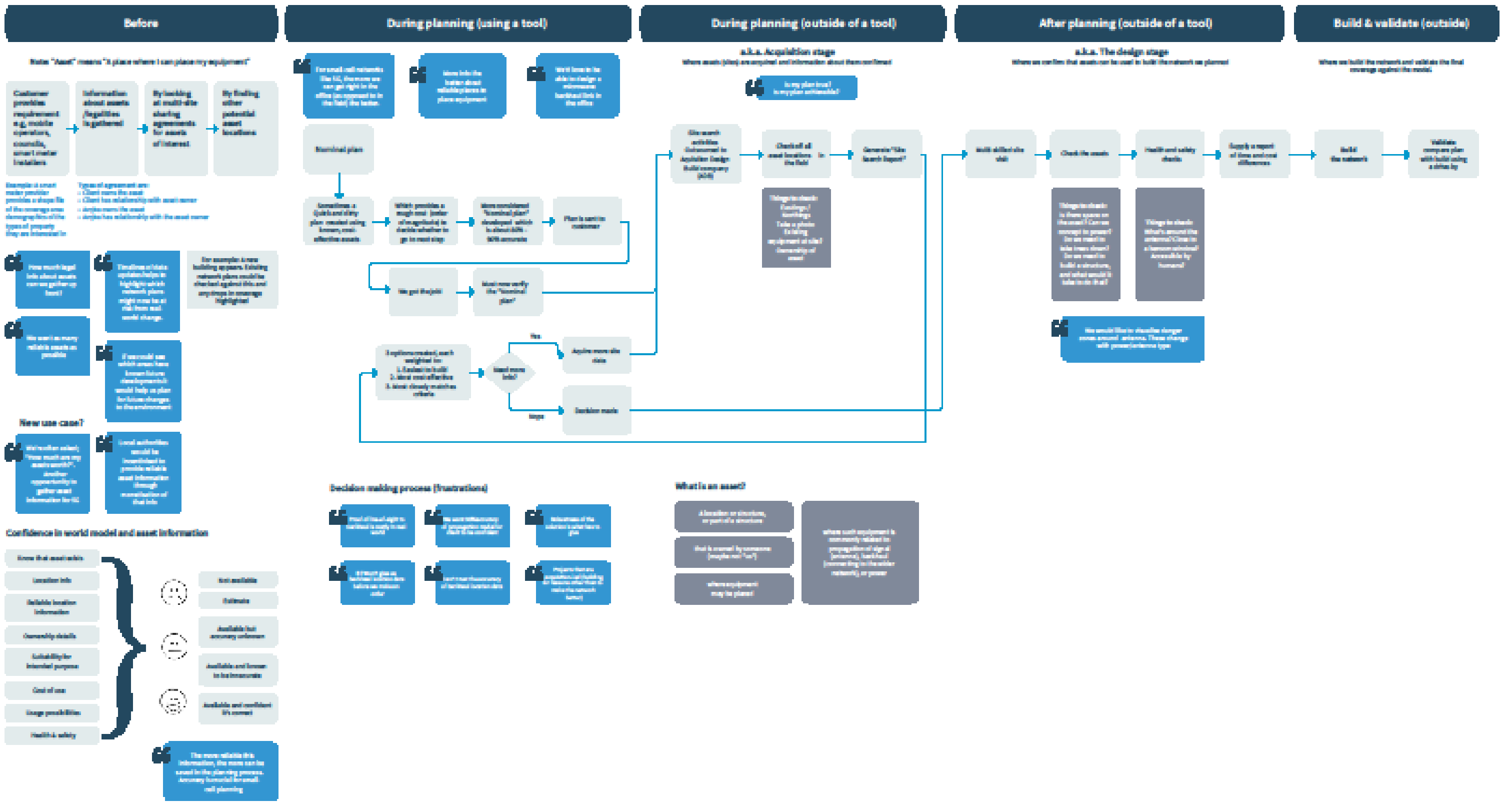

D

Annex D: Glossary

Term	Definition
2.5D	Two and a half dimensions, also termed three-quarter perspective and pseudo-3D a term used to describe 2D graphical projections and similar techniques used to cause images or scenes to simulate the appearance of being three-dimensional (3D) when in fact they are not. 2.5D data contains only one Z value per XY. Overhangs cannot be modelled.
3DML	3D Mesh Layer format for TerraExplorer software from Skyline.
Accuracy	The statistical error of the position of a ground point, specified in ground coordinates. Absolute accuracy is the error related to 'ground truth' (latitude/longitude/elevation). Relative accuracy is the error with respect to another ground point.
AOI	Area of Interest.
ArcGIS/ArcMap	GIS software from Esri Inc.
ASCII	American Standard Code for Information Interchange.
AT	Aerial triangulation.
Attribute	Non-spatial information about a geographic feature, usually stored in a table and linked to the feature by a unique identifier. For example, attributes of a river might include its name, length, and sediment load at a gauging station.
Attribution	The process of assigning attributes to features.

Term	Definition
Backhaul	A backhaul network is a packet link between the core network, or backbone network and the small subnetworks at the 'edge' of the entire hierarchical network.
Base height	In 3D analysis, the height at which a surface, raster or feature is drawn in a scene. Base height for features and rasters can be set from a surface, such as a DTM, or by using a constant value or expression. Features with height (z) values stored in their geometry can have their base height set using z-values. Setting the base heights from a surface is also called draping.
Base station	A base station is a wireless communications station installed at a fixed location and used to communicate as part of a cellular telephone system.
Colourise	To add colour values to a laser-scanned point cloud from images.
Dark fibre	A privately-operated fibre optic network that is run directly by its operator over dark fibre leased or purchased from another supplier.
Data capture	Any procedure that creates data in computer-readable form. Geospatial data can be captured from sources such as remote sensing or GPS, or they can be digitised, scanned or keyed in manually from paper maps or photographs.
DEM	Digital Elevation Model (generic term for DSM/DTM) - a 3D representation of a surface.
DSM	Digital Surface Model - 3D representation of the earth's surface including all objects, such as vegetation and buildings, that sit on it.
DTM	Digital Terrain Model - In contrast to a DSM, this represents the bare ground surface without any objects such as vegetation and buildings.
E57	File format for storing 3D point clouds and images from 3D imaging systems.
EA	Environment Agency.

Term	Definition
Feature	A physical object located on the surface of the earth, such as a river, road, building, fence or lake.
Feature class	A feature class is a homogeneous collection of common features, each having the same geometry type and spatial representation, and a common set of attribute columns. The most commonly used feature classes in GIS software are points, lines, polygons and annotation (the geodatabase name for map text).
Feature extraction	The process of graphically delineating and attributing features from a source dataset such as an image, and storing them in a database.
FME	Feature Manipulation Engine software – used for transforming and manipulating geographic data.
Geodatabase	A native data structure for ArcGIS; the primary data format used for editing and data management. It is optimised to store and query GIS data representing simple geometric objects such as points, lines and polygons. Some geodatabases handle more complex structures such as 3D objects, topological coverages, linear networks and TINs.
Georeference	Alignment of geospatial data into the correct location and coordinate system.
Global Mapper	Software from Blue Marble for viewing and managing geographic data. It also contains tools for analysis and classification of LiDAR data.
Grid	Raster-based dataset with values spaced at regular intervals.
Ground points	Term that includes control points, tie points and check points.
Ground control point (GCP)	An accurately measured reference point created using GPS or survey instrumentation, used to ensure that geospatial data is correctly positioned.
GNSS	Global Navigation Satellite System – an overarching term for satellite systems (e.g. GPS) used to pin-point a receiver's location.

Term	Definition
IMU	Inertial Measurement Unit – a device to measure the pitch, roll and yaw of a vehicle to position a point correctly. For example, it considers if the vehicle is on a slope or has a wheel on a kerb.
Interpolation	Interpolation is a procedure used to estimate unknown surface values of cells or unsampled points based on known surface values of neighbouring points. It is based on the principles of spatial autocorrelation which measures the level of spatial relationship or dependence between near and distant objects.
LAS	Format to hold point cloud data.
LAZ	Compressed LAS file.
LiDAR	Light Detection and Ranging – a remote sensing technology to collect accurate measurements using a laser signal from a remote sensing platform.
Mesh model	Connected vertices, edges and faces describing the shape of a 3D surface.
Metadata	Information (data) about other data.
Mobile mapping	Collecting geospatial data from a vehicle.
Multipatch	3D file format used by ESRI representing 3D geometry.
NADIR aerial imagery	Downward-facing imagery; a NADIR is the point on the ground directly in line with the remote sensing system and the centre of the earth.
NDVI	Normalised Difference Vegetation Index – a measure of green vegetation.
Oblique imagery	Aerial imagery captured with the axis of the camera held at an angle between the horizontal plane of the ground and the vertical plane perpendicular to the ground.

Term	Definition
Oblique mesh	A high-resolution 3D surface representation of the real-world environment generated from oblique aerial imagery.
Orthorectified imagery	Imagery that has been processed to take account of terrain displacements so that it is true to National Grid coordinates.
OS	Ordnance Survey – the national mapping agency for Great Britain.
OS MasterMap Topography Layer, OSMM	OS MasterMap Topography Layer – detailed, intelligent mapping data from Ordnance Survey representing objects in the natural and built environment of Great Britain.
Planar	In the form of a flat surface.
Physical memory load	Amount of memory being consumed by computation tasks.
Point cloud	A set of data points in a three-dimensional coordinate space that can include extra information (such as colour, intensity and classification). The points represent the external surface of the ground and landscape features. Point clouds are generated using laser scanning or image matching algorithms.
Point cloud filtering	Thinning the density of point cloud data.
Polygon	On a map, a closed shape defined by a connected sequence of x, y coordinate pairs.
Raster data	Any data which may be stored or represented as a 2-dimensional array of data points as opposed to vector data. Terrain grids and imagery are both examples of raster data.
Realworks	Software from Trimble designed for point cloud processing and analysis.

Term	Definition
RGB	A colour model that uses red, green and blue, the primary additive colours used to display images on a monitor. RGB colours are produced by emitting light, rather than by absorbing it as is the case with ink on paper. Adding 100% of all three colours results in white light.
Semi-automatic	Requiring some manual input.
Shapefile	Vector GIS data format developed by Esri.
Software stability	The software capability to run consistently without functioning failures such as software crashing.
Solid object	A three-dimensional (3D) modelled real-world object.
Stereo aerial imagery	Imagery taken from a flying object (airplane, kite, balloon etc.). Most professional aerial stereo images are taken from specially built planes that are equipped with cameras at the bottom pointing straight down to the earth.
SURE	A software solution produced by nFrames for dense image matching designed for professional production environments. It contains modules for generating dense point clouds, DSMs and true orthophotos.
Terrainlet	A polygon feature heighted against a digital terrain model.
Terrestrial LiDAR	Data from a land-based laser scanner which, combined with a highly accurate differential GPS, enables us to produce point clouds and other 3D modelled data.
Telecoms features	Fixed or mobile telecommunications infrastructure assets.
TerraExplorer Pro, Skyline	3D GIS desktop viewer and creator software from Skyline.
Tile	A rectangular patch of geospatial data.

Term	Definition
Tiling	Splitting a large input dataset into a series of gridded tiles.
TIN	Triangulated Irregular Network – a vector-based representation of a surface based on irregularly distributed nodes and lines with three-dimensional coordinates arranged in a network of non-overlapping triangles.
Triangulation	The process of orientating and registering images to the ground.
Vector data	Coordinate-based data that represent geographic features as points, lines and polygons.
Viewshed	The geographical area that is visible from a location. It includes all surrounding points that can be seen and excludes points that are beyond the horizon or obstructed by terrain and other features such as buildings and trees.
WGS84	World Geodetic System 1984 – a global geographic co-ordinate system.

Contact us

Ordnance Survey, Explorer House,
Adanac Drive, Southampton SO16 0AS

+44 (0)345 605 0505
os.uk/5G